Evaluation of water matrix effect on degradation of pharmaceuticals and determination of degradation mechanism

Samzadeh, Amin

UNIVERSITY OF ZAGREB

FACULTY OF CHEMICAL ENGINEERING AND TECHNOLOGY

Amin Samzadeh

EVALUATION OF WATER MATRIX EFFECT ON DEGRADATION OF PHARMACEUTICALS AND DETERMINATION OF DEGRADATION MECHANISM

MASTER'S THESIS

Zagreb, June 2021

UNIVERSITY OF ZAGREB

FACULTY OF CHEMICAL ENGINEERING AND TECHNOLOGY

Amin Samzadeh

EVALUATION OF WATER MATRIX EFFECT ON DEGRADATION OF PHARMACEUTICALS AND DETERMINATION OF DEGRADATION MECHANISM

MASTER'S THESIS

Supervisor :

Tomislav Bolanča, Ph.D., Full professor

Committee of the thesis exam :

Tomislav Bolanča, Ph.D., Full professor

Ana Lončarić Božić, Ph.D., Full professor

Hrvoje Kušić, Ph.D., Associate professor

Zagreb, June 2021

Acknowledgments

First of all, I would like to express my deepest and sincere gratitude to prof. dr. sc. Tomislav Bolanča and prof. dr. sc. Hrvoje Kušić for giving me the opportunity to study Chemical Engineering and Technology master program that was co-financed by the European Social Fund.

I would like to express my sincere gratitude to my supervisor, prof. dr. sc. Tomislav Bolanča, for giving me the chance to join their team.

I am very grateful to my co-supervisor, dr. sc. Matija Cvetnić, for his insight and kind support, as well as his guiding of my work and helpful recommendations and comments on my thesis.

I am very thankful to my second co-supervisor, dr. sc. Marija Sigurnjak Bureš, who put a lot of effort into helping me with starting the project and giving helpful recommendations and monitoring my progress step by step.

Finally, my deep and sincere gratitude to my family for their continuous and unparalleled love, help and support. I am grateful to my sister for always being there for me as a friend. I am forever indebted to my parents for giving me the opportunities and experiences that have made me who I am.

Abstract

According to the 3rd EU Watch List under the Water Framework Directive, a list of substances was suggested as good candidates for the next watchlist. In this study two pharmaceuticals from this list were chosen, Carbamazepine (CBZ) and Ibuprofen (IBP), two important and widely used recalcitrant pharmaceuticals found in water. The aim of this study is to evaluate the influence of several water matrix factors on the degradation of CBZ and IBP, with three different advanced oxidation processes (AOPs). To the best of our knowledge so far, there has been no research comparing UV-C, ultrasound (US) and microwave (MW) based processes under different operational parameters (oxidant dosage, pH, humic acid, nitrite ion, nitrate ion, chloride ion, phosphate ion and sulfate ion). Each of these factors depend on the degradation process had synergistic or inhibitory effect on degradation rate of studied pharmaceuticals. The used Taguchi method had great and significant results and indicated the effect of studied factors on degradation processes that, in most cases, were in agreement with previous literature findings, as well as required fewer experiments, time, and costs. Water matrix constituents had a significant impact on the degradation efficiency. Furthermore, the biodegradability of CBZ and IBP and degradation products of CBZ through UV-C based processes were investigated.

Keywords: UV-C-based processes, Ultrasound-based processes, Microwave-based processes, Carbamazepine, Ibuprofen, Water matrix

Table of contents

1. Introduction

Water is a natural resource, scarce, and indispensable for human life that also allows the sustainability of the environment. It is an essential part of any ecosystem, both qualitatively and quantitatively. However, water is unevenly distributed in different regions of the world, and its quality is not the same in all of them. For example, more than one-half of the world's major rivers are severely depleted or polluted, so they degrade contaminated ecosystems and threaten the health of living beings. According to WHO and UNICEF data, 780 million people do not have access to drinking water, of which 185 million use surface water to meet their daily needs [1].

Pharmaceutical compounds constitute one of the largest groups of organic micropollutants that are present in the aquatic environment [2]. Municipal effluents into which these compounds are transported along with waste products from people taking them, inappropriately utilized expired or unused medication, as well as surface effluents from farming areas on which they are applied, are considered their main source [3, 4]. It is estimated that the pharmaceutical market of the European Union comprises approximately 3000 different substances [5], and this number keeps increasing. Wastewater treatment plants that apply conventional wastewater treatment methods based mainly on activated sludge methods that enable them to decrease the concentration of high molecular organic compounds and biogenic compounds do not guarantee a complete elimination of pharmaceutical micropollutants [6] classified as barely biodegradable substances [7].

Currently, there is great interest in advanced oxidation processes due to their potential capacity to degrade a broad range of trace organic contaminants (TrOCs) such as pharmaceuticals (e.g., carbamazepine, ibuprofen), personal care products (e.g., benzophenone and triclosan), and industrial chemicals (e.g., bisphenol A) [8, 9]. TrOCs that are toxic and recalcitrant in nature and are resistant to biological or physicochemical treatments have been reported to be well degraded by AOPs [10]. AOPs, namely, photolysis, photocatalysis, ozonation, Fenton process, wet air oxidation, sonolysis, and anodic oxidation, involve the generation of hydroxyl radicals that unselectively attack different types of contaminants and degrade them [10].

Inorganic anions are ubiquitous in water bodies. Similar to experimental parameters, inorganic anions also have an important influence on the performance of AOPs. A significant research gap has been noticed in terms of studies on the effect of different co-occurring organic and inorganic species on the removal of pharmaceuticals. AOP efficiency can either increase or decrease in the presence of different organic or inorganic species. These chemical species form active radicals that help in degradation or they show a radical scavenging effect and retard pharmaceutical degradation [11, 12].

The aim of this study is to compare the kinetic degradation of two widely used recalcitrant pharmaceuticals found in water, Carbamazepine and Ibuprofen, by three AOPs (UV-C, ultrasound and microwave) utilizing two common oxidants (hydrogen peroxide and persulfate) in a synthetic water matrix including humic acid (HA) as natural organic matter (NOM) and five important inorganic ions (nitrate, nitrite, chloride, phosphate and sulfate). The Taguchi method was used to determine the effect of each of the eight employed factors (pH, oxidant concentration, humic acid, and inorganic ions) on the kinetic degradation of the studied pharmaceuticals. Furthermore, the biodegradability of CBZ and IBP and degradation products of CBZ through UV-C based processes were investigated.

2. General part

2.1. Pharmaceutical

The consumption and manufacturing process of pharmaceutical products (e.g. medicines, personal care products) is prevalent in today's society. While bringing many benefits, these products leave a trace after usage. After consumption, drugs are ingested and undergo metabolic reactions. However, a considerable fraction of the original products remains unchanged and leave the living organisms (humans and animals) along with an amount of their metabolites via excretion and enter the sewage. Chemicals discharged from pharmaceutical manufacturing, hospital services, animal husbandry and agricultural activities also find their way into the sewage system [13]. These factors result in the presence of pharmaceutical traces in the raw influent of the wastewater treatment plants (WWTPs). Small doses of these chemicals continue to remain in the effluent after the treatment process and are discharged into the environment [14].

Over the last years, the occurrence of pharmaceuticals in water bodies has attracted more attention from environmental administrative authorities as potential dangerous pollutants to the environment as well as to the living entities [15]. They are found to be present in all types of water bodies: surface water, ground water, tap/drinking water, sewage, wastewater treatment plants (WWTPs) influent/effluent, animal manure and agricultural soil with low concentration (ng/L to μg/L range). These substances are usually water soluble, biologically active compounds but do not biodegrade easily [16]. They can remain in water bodies and accumulate until reaching a critical dose, which can pose a harmful effect on both the ecosystem and human health [17]. With population continues to age and living quality raising every year, pharmaceutical consumption and discharge quantity might be set to increase in future years.

Typical types of pharmaceutical pollutants found in the sewage and water environment are [18]:

- Analgesics/anti-inflammatories: painkillers and drugs that reduce inflammation.
- Antibiotics: antimicrobial medicine applied in the treatment of bacterial infections.
- Antidiabetic: drugs used in diabetes treatment.

- Antifungal: medication used to treat and prevent mycoses (fungal infections).
- Anti-hypertensives: drugs prescribed for curing hypertension (high blood pressure) and their complications.
- Beta-blockers: pharmaceuticals used to treat abnormal heart rhythms, hypertension, heart attacks and their complications.
- Diuretics: drugs that promote diuresis, i.e. increased production of urine and excretion of water from body.
- Lipid regulators: cholesterol-reducing drugs used in treatment of high fat (lipids) levels in the blood.
- Psychiatric drugs: medications for mental illnesses.
- Receptor antagonists: drugs that dampen or completely block the neurotransmitter-mediated response to another chemical substance.
- Synthetic Hormones/Estrogens: artificial female human hormones used in treatment of menopausal symptoms.
- Antiseptic: chemicals applied to living skin tissue to destroy bacteria to treat and prevent infection.
- Contrast agent (or contrast medium): compounds used to improve the contrast of structures or fluids in medical imaging.

2.1.1. Occurrence

The presence of pharmaceutical residues has been shown to be global [13]. Figure 2.1 shows that every single continent on the planet has records on detection of pharmaceuticals in the aquatic system. Within Europe and North America, painkillers, cardiovascular drugs, and antibiotics are the most popular form of pharmaceutical residues. The heavy occurrence is obviously apparent in developed countries since it is a known fact that the application of pharmaceuticals in medical treatment, agriculture, research is copious in nowadays modern

era. However, developing regions of the world, such as Africa and South America also find their water contaminated with these chemicals. Carbamazepine, sulfamethoxazole, ibuprofen, trimethoprim, and paracetamol are presented most abundantly in Africa, while very high concentrations of synthetic hormones such as estrone, estradiol, and ethinylestradiol were commonly found in South America. Asian water especially has very high concentration of antibiotics (ciprofloxacin, erythromycin, norfloxacin, and ofloxacin) which can be attributed to the heavy consumption and production of these drugs. While limited severe cases of adverse effect have been reported, the Earth's water source should be kept clean and free of unwanted leftovers for our present and future generations. Table 2.1. depicts the quantity of Carbamazepine and Ibuprofen detected in aquatic systems and their recorded concentrations from all over the globe.

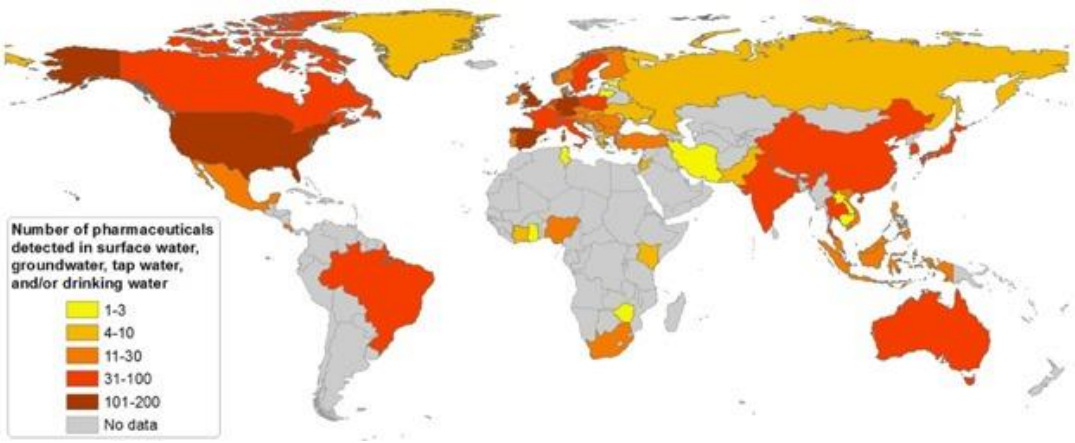

Figure 2.1. Occurrence of pharmaceuticals in surface water, ground water and drinking water in the world [13].

Table 2.1. Depicts the quantity Carbamazepine and Ibuprofen detected in aquatic systems and their recorded concentrations from all over the globe [13].

Pharmaceutical	Average concentration (µg/L)	Maximum concentration (µg/L)
Carbamazepine	0.187	8.05
Ibuprofen	0.108	303.0

2.1.2. Pathway

Pharmaceutical residues can enter the environment through multiple complex routes. Figure 2.2 presents some of the most common exposure pathways of pharmaceutical products from manufacturing source to wastewater then into living bodies.

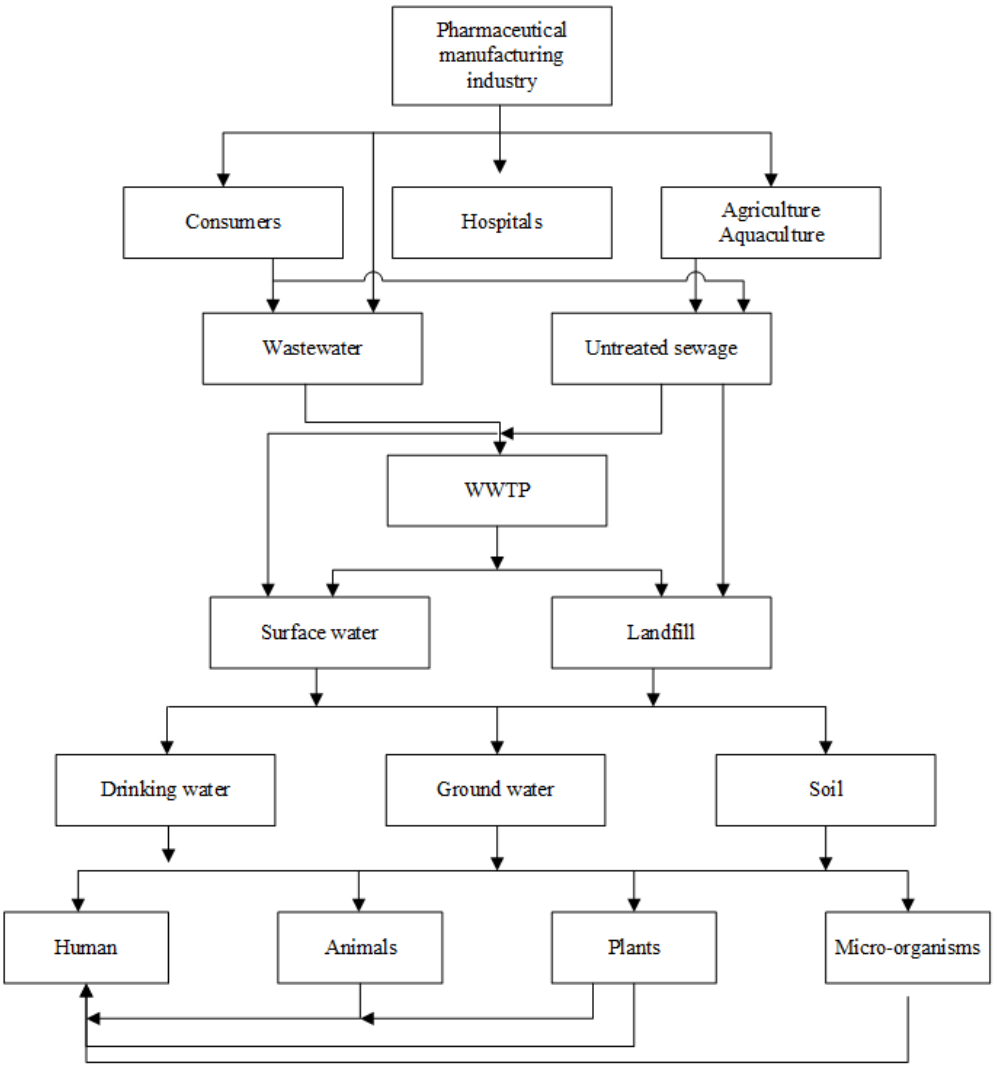

Figure 2.2. Exposure pathways of pharmaceutical products.

Pharmaceuticals can enter into wastewater as early as during the production process. It has been found that effluent from pharmaceutical production site contains a large amount of chemicals which arises from the manufacturing process [19]. After the production phase, pharmaceutical products are delivered to pharmacies, health facilities then to the consumers. Most of the pharmaceuticals are consumed by hospitals, healthcare facilities, private

consumers and agriculture (with farming, animal husbandry being the most notable) to treat and prevent diseases. When consumed by humans or animals, pharmaceutical products are metabolized to a range of degrees. Their discharged metabolites and parent (original) compounds can be found in urine or feces which go to the sewage system. After that, the biological, chemical and physical processes within WWTPs and the receiving water bodies can further alter these substances' structure [20, 21]. Pharmaceutical residues in animal excretion from agriculture activities through surface runoff can be further exposed to upper soil layer and surface water. They may continue accumulating in the soil layer or penetrating into the groundwater system through leaching [22]. Hospitals are another source of pharmaceutical discharge. As hospitals do not usually accommodate a sewage water treatment unit to immediately treat their effluent after discharge, a large amount of chemicals resulted from healthcare services are discharged directly into the urban wastewater [13]. High concentration of various drugs has been found in hospitals' sewage effluent [23].

In general, municipal wastewater treatment plants (WWTPs), even with activated sludge process, are not well equipped to remove all complex pharmaceutical residues since most of them were built with the main goal of removing biodegradable carbon, nitrogen, phosphorus and microorganisms. The removal rates are from less than 20 % up to more than 80 % for most chemicals [24]. However, it is not complete removal; therefore, pharmaceuticals find their way into the receiving water bodies after the effluent has been discharged from the WWTPs. From there, they can be moved along to accumulate in water bodies, soil, groundwater then drinking water and eventually living organisms.

2.1.3. Eco-toxicology

So far research has revealed that although the acute toxicity of pharmaceuticals within water bodies is insignificant due to very low concentration (ng/L level), their chronic toxicity may pose a threat to non-target aquatic species in the future [25]. Pharmaceutical residues, difficult to biodegrade in the environment, can accumulate and be exposed to aquatic beings throughout a long period of time (sometimes their whole life cycle), which may cause undesirable side effects on the ecosystem function [15]. Presently, some compounds have already reached the concentration level of displaying chronic/acute toxicity effects, such as diclofenac, propranolol and fluoxetine [26]. Antibiotic resistance is another concern

regarding pharmaceuticals in aquatic environment. Antibiotics after consumed by humans and animals can lead to the development of bacteria which are resistant to those drugs in the gut. These bacteria can be released into the environment through excretion. Antimicrobial resistant genes can also be promoted in the aquatic system when antibiotic traces are available. Afterwards, these genes can be passed on to pathogenic bacteria, making them more potent as they may become more resistant to current treatment [15].

2.2. Studied pharmaceuticals

According to the 3rd EU Watch List under the Water Framework Directive, a list of substances was suggested as good candidates for the next watchlist. In this study, two pharmaceuticals from this list were chosen, Carbamazepine and Ibuprofen, two important and highly consumed pharmaceuticals found in water [27].

2.2.1. Carbamazepine

Carbamazepine is an antiepileptic drug commonly used for treatment of schizophrenia as well as bipolar disorder. Due to the chronic administration in high dosages (100–2000 mg daily), the annual production is typically very high [28]. Approximately 3% of the dosed CBZ is excreted in unaltered form, along with the pharmacologically active 10,11 epoxy-carbamazepine and further hydrolyzed dihydroxy derivatives. Carbamazepine, which is detected ubiquitously in sewage-impacted water, is highly persistent in nature due to the presence of electron-withdrawing groups (amine group) in its structure, thus often showing poor removal by different AOPs [29-31].

As CBZ is highly stable, it allows long-term transportation within the aquatic environment [32]. Studies have demonstrated that the removal efficiency of CBZ by conventional wastewater treatment plants is very low (< 10%) [33], which results in presence of CBZ in bio-solids and treated water discharges. Considering these aspects, CBZ can get accumulated in root tissues of plants and also translocated into other parts including beans. CBZ has been reported to have significant effect on the embryonic cell growth [34]. The chromic exposure of fish to CBZ has been demonstrated to yield reduction in fish steroid

hormone which influences the reproduction ability of fish population. Also, low concentration exposure of CBZ to the fish caused an adverse effect on histology of kidney and liver, hampering fish development [35]. Thus, it has become imperative to develop an efficient method which will ensure complete removal of CBZ from effluents.

2.2.2. Ibuprofen

Ibuprofen is propanoic acid, a non-steroidal anti-inflammatory drug (NSAID), which is one of the most widely used over-the-counter drugs and consumed by humans and used in domestic animal practices or farming etc. [36-38]. After exertion, approximately 15% of IBP leaves the body as the unaltered parent compound, while 26% as metabolized hydroxyl-ibuprofen and 43% as carboxy-ibuprofen of applied therapeutic dose [39]. The untreated municipal wastewater and medical waste such as the hospital or industrial production waste may contain the non-metabolized and metabolized form of IBP [40]. In one study, it is reported that in influents of WWTPs, IBP was present at concentrations of up to 3 μg/L [41]. IBP influences the cyclooxygenase pathway, which could affect the regulators of reproduction in both vertebrates and invertebrates [42]. It could also present a potential hazard for aquatic ecosystems and human health through coexistence with other drugs [43]. With the accumulation of IBP, an irreversible harmful effect was observed in frog embryos [44]. IBP can accumulate in the plasma of channel catfish [45]. It is also reported that the IBP can also induce liver injury in an adolescent athlete [46]. Furthermore, the IBP may have synergistic ecotoxicological effects when present in the mixture with other non-steroidal anti-inflammatory drugs [47]. Due to the toxic effects of IBP, the most important requirement is the removal of the ibuprofen drug residue from wastewater [48]. Table 2.2 shows the characteristics and physicochemical properties of CBZ and IBP.

Table 2.2. Characteristics of CBZ and IBP.

Pharmaceutical	Carbamazepine	Ibuprofen
Abbreviation	CBZ	IBP
CAS number	298-46-4	15687-27-1
Chemical formula	$C_{15}H_{12}N_2O$	$C_{13}H_{18}O_2$
Purity %	99	98
Molecular weight (g/mol)	236.27	206.29
Water solubility (mg/L), 25˚C	17.7	21
pK_a	13.9	4.91
log K_{ow}	2.45	3.97
K_d	25.52	453.79
log K_{OC}	3588	2596
Henry's Law Constant (atm.m^3.mol^{-1}), 25˚	1.08×10^{-10}	1.5×10^{-7}
Half-life ($t_{1/2}$)	25-65 hr	1.8-2 hr
Φ_{254} (10^{-2}) mol/Einstein	0.06	19.2
ε_{254} (10^3) L/mol/cm	6.07	0.25
$k_{HO^{\cdot}}$ (10^9), M^{-1} s^{-1}	8.02	5.57
$k_{SO_4^{\cdot-}}$ (10^9), M^{-1} s^{-1}	1.92	1.32
Chemical structure	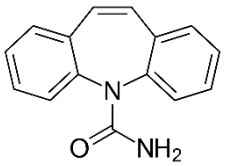	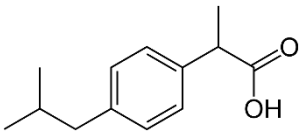

2.3. Taguchi design

The Taguchi method is a robust statistical design method developed by Genichi Taguchi to improve the quality of manufactured goods. It is also applied in environmental engineering, especially in wastewater treatment, to increase the efficiency of the removal of COD (chemical oxygen demand), TOC (total organic carbon), and other contaminants. The TM has been used for the optimization of Fenton process for the removal of amoxicillin from the aqueous phase [49], chemical coagulation [50], flux parameters in water containing nitrate, nitrite, phosphate, and sulfite [51], synthetic textile wastewater [52], the electrochemical oxidation of Acid Red 18 [53], and many other processes.

The successful applications of Taguchi methods by both engineers and statisticians within British industry have led to the formation of UK Taguchi Club [54]. Taguchi's approach is totally based on statistical design of experiments [55]. This can economically satisfy the needs of problem solving and product/process design optimization. By applying this technique one can significantly reduce the time required for experimental investigation. This is important in investigating the effects of multiple factors on performance as well as studying the influence of individual factors to determine which factor has more influence, which has less [56].

Taguchi approach developed rules to carry out the experiments, which further simplify and standardize the experiment design. In the Taguchi method, the results of experiments are analyzed to achieve the following objectives: (i) to find the best or the optimal condition for the product or the process, (ii) to identify the contribution of individual factors and (iii) to estimate the response under the optimal conditions. A commonly applied statistical treatment, analysis of variance (ANOVA), was also used to analyze the results of experiments and to determine how much variation each factor contributes. By studying the main effects of each factor, the general trends of the influencing factors can be characterized. Main effects plots show how each factor affects the response characteristic (means of degradation rates). A main effect exists when different levels of a factor affect the characteristic differently. For a factor with two levels, we may discover that one level increases the mean compared to the other level. This difference (delta) is the main effect. The sign and magnitude of the main effect would tell us the following [57]:

- The sign of a main effect tells us of the direction of the effect, i.e. if the average response value increases or decreases.

- The magnitude tells us of the strength of the effect.

One can use the response tables to select the best level for each factor, the delta and rank values to identify the factors that have the largest effect on each response characteristic. Then, determine which levels of these factors meet the objectives.

2.4. Water matrix

AOPs have been widely studied for the degradation of different types of pharmaceuticals. Most studies on pharmaceutical degradation by AOPs have used ultrapure water spiked with model pharmaceuticals. Although such experimental design is important to reveal the kinetics of pharmaceutical degradation, these studies do not provide information on the interactions between pharmaceuticals and different co-occurring chemical species and often fail to reveal the true potential of a particular AOP on large scale.

Actual water matrix contains a large amount of various inorganic ions and organic compound. Therefore, we studied the effects on degradation of CBZ and IBP by adding five different inorganic anions (nitrite, nitrate, chloride, phosphate and sulfate) and organic compound (humic acid) in environmentally relevant concentrations to the reaction system.

These organic and inorganic species can have neutral, promoting or retarding effect on the degradation of pharmaceuticals in different AOPs depending on their concentration in the mixture and other reaction conditions [58].

2.5. Biodegradability

COD (chemical oxygen demand) is defined as the amount of dissolved oxygen to oxidize and stabilize a sample when organic or inorganic matter of sample solution is responsive by a strong chemical oxidant. The COD value indicates the mass of oxygen consumed per liter of solution and expressed in milligrams per liter (mg/L). The higher the chemical oxygen demand, the higher the amount of pollution in the water sample. However,

COD is considered one of the important quality control parameter of an effluent in wastewater treatment facility [59]. Colorimetric measurement of COD is considered faster and easier to perform than titrimetric analysis. The sample is digested in an ampule, culture tube or vial under closed reflux conditions [60]. A spectrophotometer is needed to make a standard calibration curve by measuring concentration of dichromate and their absorbance. Normally, COD vials are commercially available for COD measurement and potassium hydrogen phthalate (KHP) is used as a reference standard for colorimetric analysis [61].

BOD (biochemical oxygen demand) is defined as the amount of oxygen required by microorganism to stabilize decomposable organic matter at a particular time and temperature. If a small amount of biomass (primarily bacteria) seed is mixed in wastewater (containing of organic matter such as carbohydrates, proteins and fats) and added nutrients for biomass growth, biodegrading of organic matter will be increased and dissolved oxygen will be decreased [62]. The organic matter is the growth substrate (carbon and energy source) for the generation of new biomass. Biomass is considered as the catalyst for the reaction where oxygen is consumed. Theoretically infinite time is required for complete biological oxidation of organic matter of domestic sewage. But for all practical purposes, the difference between the initial amount of oxygen and the remaining amount of oxygen after 5 days of water sample yields the ”biochemical oxygen demand after 5 days” or the BOD_5 value [63].

The biodegradability of the solution prior to and during the treatments was expressed as the BOD_5/COD ratio. It is commonly accepted that wastewater with $BOD_5/COD < 0.3$ are not biodegradable; those with $0.3 < BOD_5/COD < 0.4$ are partially biodegradable; and those with $BOD_5/COD > 0.4$ are biodegradable [64].

2.6. Degradation processes

Advanced chemical oxidation as a technology in water and wastewater treatment is based on the generation of highly reactive and non-selective radical species, mostly the hydroxyl radical, that is known as one of the most powerful oxidants [65] (Table 2.3). Intensive studies on hydroxyl radicals demonstrated their ability to oxidise a wide range of organic compounds at a very high rate with reaction rate constants in order of 10^8-10^{10} L/mol.s [65].

Table 2.3. Relative oxidation power of some oxidants.

Oxidizing agent Potential	(V)
h^+ (TiO_2)	+ 3.50
Fluorine	+ 3.03
Hydroxyl radical	+ 2.80
Sulphate radical	+ 2.60
Persulphate anion	+ 2.10
Hydrogen peroxide	+ 1.78
Perhydroxyl radical	+ 1.70
Oxygen (atomic)	+ 2.42
Ozone	+ 2.08
Chlorine	+ 1.36
Chlorine dioxide	+ 1.57
Oxygen (molecular)	+ 1.23
Potassium permanganate	+ 1.68
Hypochlorous acid	+ 1.49

However, some species present in water matrix may terminate the radical chain reaction by reacting with hydroxyl radical. Such species are called hydroxyl radical scavengers as they are able to obstruct the attack of free radicals on the target compound. Thus, hydroxyl radicals are consumed by competitive reactions with carbonate, bicarbonate ions and some organic species. The presence of radical scavengers in water matrix may cut down the total efficacy of advanced oxidation processes in many cases.

The term “advanced oxidation processes” was first introduced by Glaze et al. [66] who defined it as “the oxidation processes, which generate hydroxyl radicals in sufficient quantity to affect water treatment at ambient temperature and pressure”. Later on, this technology application was expanded to contaminants removal from soil and polluted air; some other than hydroxyl radical reactive species have been introduced and successfully tested; currently the range of advanced oxidation technologies (AOTs) is not limited by ambient temperature and pressure applications only.

Broad number of chemical oxidation processes are currently qualified under AOT definition: hydrogen peroxide photolysis; photocatalysis; ozonation at elevated pH or combined with UV, hydrogen peroxide, catalysts and activated carbon; the Fenton reaction based processes; ultrasound including processes; microwave; wet air oxidation; persulphate oxidation, etc.

AOPs involve two steps, namely, generation of radical species and oxidation of pharmaceuticals by the radicals [10]. Radical formation in AOPs depends on various reaction conditions as well as water chemistry and the nature of the contaminant. Pharmaceuticals contain different types of functional groups in their structures, which influence their reactivity towards a particular AOP [67]. Functional groups can be categorized as electron-donating groups (EDGs) or electron-withdrawing groups (EWGs). A few examples of EDGs are $-NH_2$, -OH, -R, $-NR_2$ etc., while examples of EWGs include -X, -CN, $-CF_3$, - COH, -COR, etc. [68].

Currently, persulfate and hydrogen peroxide are considered as the two major oxidants for generating $SO_4^{-\bullet}$ and $HO^{\bullet}$, respectively. However, both PS and H_2O_2, by themselves, can only generate radicals at an extremely slow rate in wastewater treatment conditions. Therefore, in most practical applications additional measures, such as energy input (microwave irradiation, ultraviolet irradiation, and ultrasonication) and transition metals, etc., are necessary to activate these two oxidants to generate radicals rapidly.

In this study, three AOPs were applied: UV-C based processes, ultrasound based processes and microwave based processes.

2.6.1. UV-C based processes

2.6.1.1. UV-C direct photolysis

A ground state molecule (RX) under the UV-C irradiation can be promoted to its electronically excited state (RX^*). When the molecules contain a chromophore group with carbon-halogen (C-X) bond, homolysis of the C-X bond proceeds to form a carbon centered radical and halogen atom (Eq. 2.1). Subsequently, the carbon centered radical formed can be efficiently trapped by molecular oxygen present in the reaction medium to generate peroxyl radical that will be further transformed to its photoproducts (Eq. 2.2). Other mechanisms for direct photolysis of the organic pollutant in water include the electron transfer from the electronically excited state (RX^*) to the molecular oxygen present in the reaction medium, which leads to the formation of substrate radical cation and superoxide radical. A series of subsequent reactions such as recombination of the radical ions or hydrolysis of the radical cation occurs to produce the corresponding photoproducts (Eq. 2.3). Additionally, the RX^* formed can be deactivated by a quencher via energy transfer, electron transfer, or chemical reaction etc. For example, RX^* may be quenched by molecular oxygen to generate singlet molecular oxygen (Eq. 2.4) [69].

$$RX \xrightarrow{h\nu} RX^* \rightarrow R^\bullet + X^\bullet \quad (2.1)$$

$$R^\bullet + O_2 \rightarrow RO_2^\bullet \rightarrow \text{photoproduct} \quad (2.2)$$

$$RX^* + O_2 \rightarrow O_2^{-\bullet} + RX^{+\bullet} \rightarrow \text{photoproduct} \quad (2.3)$$

$$RX^* + O_2 \rightarrow RX + {}^1O_2 \quad (2.4)$$

The direct photolysis rate of the organic pollutant depends on the UV-C absorbance of the organic pollutant at the wavelength in question, quantum yield of the whole photochemical processes, and the photon flux emitted by UV-C lamp at that wavelength [70].

2.6.1.2. UV-C indirect photolysis

2.6.1.2.1. Fundamentals of the UV-C/H_2O_2 process

The UV-C/H_2O_2 process is a traditional AOP that generates $HO^{\bullet}$ with high redox potential (1.8–2.7 V) through the UV photolysis of the -O-O- peroxidic bond in H_2O_2 (Eq. 2.5) [70]:

$$H_2O_2 \xrightarrow{h\nu} 2HO^{\bullet} \quad (2.5)$$

The formation rate of $HO^{\bullet}$ in the UV-C/H_2O_2 process depends on the quantum yield and the absorbance coefficient of H_2O_2 at the specific wavelength [71]. In the UV-C/H_2O_2 process, the quantum yield is reported to be 0.5 for the production of $HO^{\bullet}$ at relatively high UV-C light intensity at 254 nm and low peroxide concentrations [72]. H_2O_2 has a maximum absorbance at 210-230 nm, and its UV-C absorbance coefficient at 254 nm is 19.6 M^{-1} cm^{-1} [72, 73]. Meanwhile, the generated $HO^{\bullet}$ is affected via propagation (Eqs. 2.6 – 2.8) and termination (Eqs. 2.9 – 2.11) [74].

$$HO^{\bullet} + H_2O_2 \rightarrow HO_2^{\bullet} + H_2O \qquad k = 2.7 \times 10^7\ M^{-1}s^{-1} \quad (2.6)$$

$$HO_2^{\bullet} + H_2O_2 \rightarrow HO^{\bullet} + H_2O + O_2 \qquad k = 3.0\ M^{-1}s^{-1} \quad (2.7)$$

$$HO^{\bullet} + HO_2^{-} \rightarrow HO_2^{\bullet} + OH^{-} \qquad k = 7.5 \times 10^9\ M^{-1}s^{-1} \quad (2.8)$$

$$HO_2^{\bullet} + HO_2^{\bullet} \rightarrow H_2O_2 + O_2 \qquad k = 8.3 \times 10^9\ M^{-1}s^{-1} \quad (2.9)$$

$$HO^{\bullet} + HO^{\bullet} \rightarrow H_2O_2 \qquad k = 5.5 \times 10^9\ M^{-1}s^{-1} \quad (2.10)$$

$$HO^{\bullet} + HO_2^{\bullet} \rightarrow H_2O + O_2 \qquad k = 7.1 \times 10^9\ M^{-1}s^{-1} \quad (2.11)$$

The concentration of $HO^{\bullet}$ in UV-C/H_2O_2 depends on its production and consumption. The concentration of $HO^{\bullet}$ increases with increasing H_2O_2 dosage during the UV-C/H_2O_2 process when the concentration of H_2O_2 is low (mM) because of the enhanced formation of $HO^{\bullet}$ [75]. However, this enhancement becomes limited at high concentrations of H_2O_2 (~mM) [76], resulting from the important scavenging effect of H_2O_2 on $HO^{\bullet}$ at

2.7×10^7 M^{-1} s^{-1}. Thus, the concentration of $HO^{\bullet}$ in the UV-C/H_2O_2 process is in the range of 10^{-12}-10^{-13} M in pure water [75].

2.6.1.2.2. Fundamentals of the UV-C/$S_2O_8^{2-}$ process

The UV-C/persulfate (UV-C/PS) process has received increasing attention in recent years because of its high capability and adaptability for the degradation of emerging contaminants and the convenient transportation of persulfate. There are two types of persulfates: persulfate (PDS, $S_2O_8^{2-}$) and peroxymonosulfate (PMS, HSO_5^-).

UV-C light can activate PDS to form sulfate radicals ($SO_4^{-\bullet}$) which are strong oxidants with redox potentials from 2.5-3.1 V [77]. The activated process involves different mechanisms based on the UV-C wavelength. The first mechanism is the fission of the O-O bond [78]. In UV-C/PS, $SO_4^{\bullet-}$ is generated primarily via the photolysis of PDS (Eq. 2.12), and $HO^{\bullet}$ is the secondary radical formed during the UV-C/PS process via the reaction between $SO_4^{-\bullet}$ and H_2O/OH^- (Eqs. 2.13 and 2.14) [79].

$$S_2O_8^{2-} \xrightarrow{h\nu} 2SO_4^{-\bullet} \qquad (2.12)$$

$$SO_4^{-\bullet} + H_2O \rightarrow HO^{\bullet} + SO_4^{2-} + H^+ \qquad k = 6.6\times10^2\ s^{-1} \qquad (2.13)$$

$$SO_4^{-\bullet} + OH^- \rightarrow HO^{\bullet} + SO_4^{2-} \qquad k = 6.5\times10^7\ M^{-1}s^{-1} \qquad (2.14)$$

The readical scavenger reactions in UV-C/PS process is as following (Eqs. 2.15 and 2.16).

$$SO_4^{-\bullet} + S_2O_8^{2-} \rightarrow SO_4^{2-} + S_2O_8^{-\bullet} \qquad k = 6.6\times10^5\ M^{-1}s^{-1} \qquad (2.15)$$

$$SO_4^{-\bullet} + SO_4^{-\bullet} \rightarrow S_2O_8^{2-} \qquad k = 3.1\times10^8\ M^{-1}s^{-1} \qquad (2.16)$$

2.6.1.2.3. Oxidation mechanism of hydroxyl and sulfate radical

$HO^{\bullet}$ can primarily react with the organic pollutant through 2 oxidation mechanisms: (i) by electrophilic addition to a double bond or an aromatic ring; (ii) by hydrogen abstraction from a carbon atom [71].

$SO_4^{-\bullet}$ oxidation of the organic pollutant occurs primarily through 3 oxidation mechanisms: (i) by electrophilic addition to a double bond; (ii) by abstracting a hydrogen atom from a saturated carbon; (iii) by electron transfer from a carboxyl group and from certain neutral molecules [80, 81].

Compared to $HO^{\bullet}$, $SO_4^{-\bullet}$ reacts more slowly with organic pollutants through hydrogen abstraction and addition. On the other hand, $SO_4^{-\bullet}$ oxidizes some organic pollutants with higher rate constants through electron transfer oxidation. For example, most aliphatic acids can be degraded effectively by $SO_4^{-\bullet}$ through electron transfer oxidation of carboxyl group, while their reactions with $HO^{\bullet}$ led to little decarboxylation [82].

2.6.2. Ultrasound based processes

The US process has been reported as a very efficient AOP for the degradation of emerging contaminants (ECs) present in water. Additionally, it can overcome the limitations ascribed to the use of other AOPs commonly used for water treatment. It is noteworthy to mention that, by using the US process, mass transfer within the reaction medium is improved, as well as the EC degradation reaction rates [83].

Aqueous medium sonolysis involves the production of waves through sound at a specific frequency, with compression and expansion cycles, leading to the formation of cavitation bubbles. These bubbles grow by the diffusion of vapor or gas from the liquid medium, reaching an unstable size that provokes their violent implosion, which in turn generates very high temperatures and pressures, approximately 5000 K and 500 bar [68], producing the so-called “hot spots” that allow the decomposition of the water molecule to generate $HO^{\bullet}$ [84], which is capable of oxidizing recalcitrant pollutants such as pharmaceuticals with its high oxidation potential, leading to the degradation of the toxic

compounds and producing innocuous products, such as H_2O, carbon dioxide (CO_2) and inorganic ions (Fig. 2.3) [85].

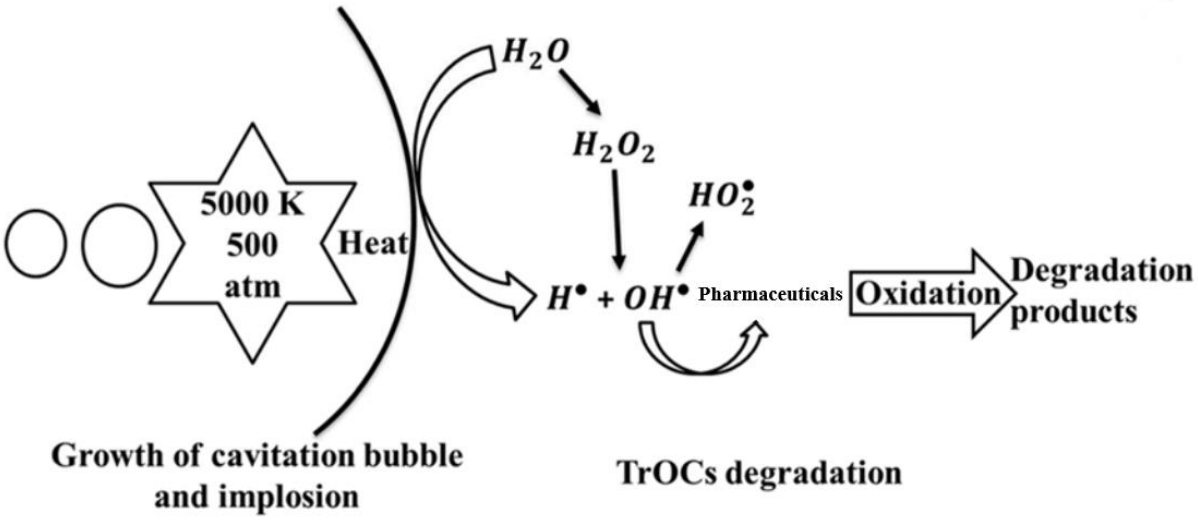

Figure 2.3. Reaction mechanisms for the removal of pharmaceutical by sonolysis (taken from [86]).

Equations (2.17)–(2.20) show the decomposition of water and other molecules commonly dissolved in water by sonochemical waves [84, 87], being the $HO^{\bullet}$, as well as the hydroperoxyl radicals ($HO_2^{\bullet}$), the main species that oxidizes the organic compounds present in the aqueous medium. When oxidants such as hydrogen peroxide and persulfate are added, ultrasound can activate oxidants to produce hydroxyl radicals and sulfate radicals by energy transfer (Fig. 2.4).

$$H_2O \xrightarrow{)))} H^{\bullet} + HO^{\bullet} \quad (2.17)$$

$$O_2 \xrightarrow{)))} 2O^{\bullet} \quad (2.18)$$

$$N_2 \xrightarrow{)))} 2N^{\bullet} \quad (2.19)$$

$$H^{\bullet} + O_2 \xrightarrow{)))} HO_2^{\bullet} \quad (2.20)$$

The cavitation bubbles are produced in two ways, symmetrically and asymmetrically. The difference between these is the support provided by a rigid surface (for instance, the surface of the reactor) for the bubbles to be formed. This difference has a direct influence on the way in which the bubbles implode, and thus on the release of pressure and temperature

into the medium, resulting in the rupture of the water molecule and the formation of HO• [84]. The symmetrical bubbles release energy in all directions around their surface, while the asymmetrical ones generate an eruption of the liquid, mainly on the parts of the bubbles that are far away from the surfaces, forming long-range "micro-jets" that go to the solid surfaces [85].

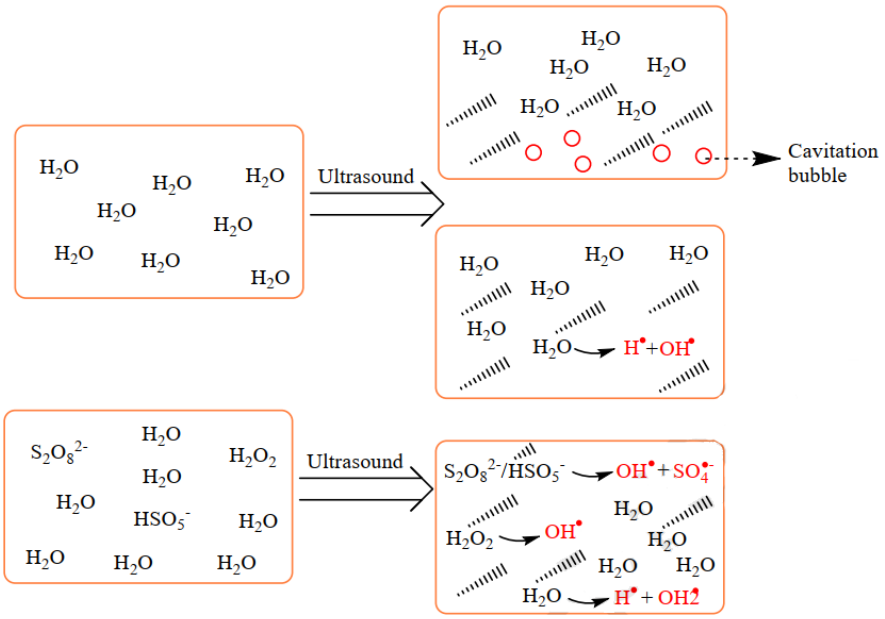

Figure 2.4. Reactive species produced during the process of ultrasound (taken from [88]).

There are three reaction zones in the solution during the ultrasonic treatment process: (a) inside the cavitation bubble, (b) the bubble/water interface and (c) within the bulk solution [85, 89, 90]. In each of these zones, different reactions occur that favor the decomposition of pollutants. Hydrophobic, non-polar and/or volatile compounds react inside the cavitation bubbles and at the bubble/water interface, while hydrophilic and/or non-volatile pollutants react within the bulk solution [85, 91-93].

Inside the cavitation bubbles, the reaction of the pollutant can occur in two ways: pyrolysis of the highly volatile compounds, or chemical reaction with the free HO• formed. At the bubble/water interface, the reaction occurs by pyrolysis and, fundamentally, by a reaction with the HO• that are formed from implosion and tend to diffuse throughout the solution medium, reacting with the compounds that are present at the interface. Within the solution, decomposition occurs only by reaction with HO•, which are released into the aqueous medium through implosion of the cavitation bubbles [84].

When free radicals reach the aqueous solution, they can recombine, as expressed in Eqs. (2.21)–(2.23), or react with hydroxyl ions (HO^-) (Eq. (2.24)), resulting in a decrease of the system oxidation potential.

$$HO_2^{\bullet} + HO_2^{\bullet} \rightarrow H_2O_2 + O_2 \qquad k = 8.3 \times 10^5\ M^{-1}s^{-1} \qquad (2.21)$$

$$HO^{\bullet} + HO^{\bullet} \rightarrow H_2O \qquad k = 5.5 \times 10^9\ M^{-1}s^{-1} \qquad (2.22)$$

$$HO^{\bullet} + HO_2^{\bullet} \rightarrow H_2O + O_2 \qquad k = 7.1 \times 10^9\ M^{-1}s^{-1} \qquad (2.23)$$

$$HO_2^{\bullet} + HO^- \rightarrow H_2O + O_2^{-\bullet} \qquad k = 10^{10}\ M^{-1}s^{-1} \qquad (2.24)$$

However, from Eq. (2.24), superoxide radicals ($O_2^{-\bullet}$) are formed, as well as from the decomposition of $HO_2^{\bullet}$, as described by Eq. (2.25), which also contribute to the degradation of emerging organic compounds, although in a smaller proportion than by $HO^{\bullet}$ [94]. Additionally, in acidic medium, $O_2^{-\bullet}$ can react with protons (H^+) to form $HO_2^{\bullet}$ (Eq. (2.26)). Both of the free radicals can recombine, as represented in Eq. (2.27), resulting in the production of HO_2^-, which in turn can be involved in $HO^{\bullet}$ quenching (Eq. (2.28)).

$$HO_2^{\bullet} \rightarrow H^+ + O_2^{-\bullet} \qquad k = 7.5 \times 10^6\ M^{-1}s^{-1} \qquad (2.25)$$

$$H^+ + O_2^{-\bullet} \rightarrow HO_2^{\bullet} \qquad k = 5.1 \times 10^{10}\ M^{-1}s^{-1} \qquad (2.26)$$

$$HO_2^{\bullet} + O_2^{-\bullet} \rightarrow HO_2^- + O_2 \qquad k = 9.7 \times 10^7\ M^{-1}s^{-1} \qquad (2.27)$$

$$HO^{\bullet} + HO_2^- \rightarrow HO_2^{\bullet} + HO^- \qquad k = 7.5 \times 10^9\ M^{-1}s^{-1} \qquad (2.28)$$

Hydrogen peroxide (H_2O_2) can also be formed in the US process, as described in Eq. (2.21). In spite of the fact that H_2O_2 can scavenge $HO^{\bullet}$ or be decomposed (Equations (2.29)–(2.31), respectively), it can be involved in the oxidation of ECs, as well as on the production of a higher amount of $HO^{\bullet}$, when US process is combined with UV radiation.

$$HO^{\bullet} + H_2O_2 \rightarrow H_2O + HO_2^{\bullet} \qquad k = 3 \times 10^7\ M^{-1}s^{-1} \qquad (2.29)$$

$$H_2O_2 \rightarrow HO_2^- + H^+ \qquad k = 2 \times 10^{-2}\ M^{-1}s^{-1} \qquad (2.30)$$

$$HO_2^- + H^+ \rightarrow H_2O_2 \qquad k = 10^{10}\ M^{-1}s^{-1} \qquad (2.31)$$

The reaction rate constants for the reactions expressed in Equations (2.21)–(2.31) were taken from Pavlovna et al. [95], demonstrating that, in general terms and according to the values of the reaction rate constants, the free radicals are easily formed through the US waves. As mentioned previously, these free radicals can react with the target pollutant; however, they can also recombine or be quenched by other compounds found in water such as the natural constituents of the matrix, making the reaction of the hydrophilic compounds within the solution less efficient and slower [96]. In this regard, in order to avoid side reactions of the US oxidation system, the optimization of the operating parameters or factors influencing the most the oxidation potential of the system must be conducted. This would subsequently allow the reduction of the economic costs associated with the studied advanced oxidation process for a more efficient degradation of the ECs of interest [83]. The US process must consider the control and variation of the different operating parameters, including the ultrasonic frequency, the electrical power and the pH and temperature of the solution [97, 98], in order to be optimized with the subsequent reduction in the costs associated with the process performance. The nature of the contaminant of interest and the constituents of the water matrix must also be considered during the US-assisted AOP optimization procedure since they are involved in the efficiency of the process. In addition to these factors, the type and the geometry of the sonochemical reactor must be considered.

The frequency with which ultrasonic waves are produced can range from 20 to 10,000 kHz, and the US process is divided into three regions: low, high and very high frequency [99]. In Table 2.4, the frequency ranges used in the ultrasonic oxidation process are listed.

Table 2.4. Frequency ranges used in the ultrasonic process.

Name	Ultrasound range (kHz)
Very high	5000-10000
High	200-1000
Low	20-100

Ultrasonic frequency is a fundamental parameter in the performance of US process, since the size and duration of the cavitation bubble, the violence of the implosion and, therefore, the production of HO• depend considerably on it [84].

The number of cavitation bubbles and bubble collapses increases with rising frequency. However, it is important to note that the bubbles generated at high frequencies are small, and release less energy than low frequency bubbles generated by a single pulse [100-102]. In addition, the escape of more HO• is inferred, before recombining, when faster collapses occur [84, 103]. In this sense, the optimal frequency is determined by the integral efficiency of the energy discharge, which depends on the quantity, size and lifetime of the bubbles. It is noteworthy to mention that the optimal frequency varies according to the different compound to be treated [104, 105].

Rao et al. [84] chose two frequency values (200 and 400 kHz) to determine the optimal one for the degradation of CBZ. The first of these values was more effective for the degradation of the target compound. This result was ascribed to the differences in calorimetric powers obtained for both frequencies under the same electrical power (100 W), resulting in a higher calorimetric power for the 200 kHz frequency. This can be attributed to what was previously explained, i.e., each EC requires an optimal frequency at which its degradation will be favored, which depends on its physicochemical properties. This optimal frequency will also be influenced by the geometry of the reactor since, as mentioned above, it will depend on the formation of symmetrical or asymmetrical cavitation bubbles.

2.6.3. Microwave based process

Microwaves (frequencies of 0.3–300 GHz and wavelengths of 1 m to 1 mm) lie between radio wave frequencies and infrared frequencies in the electromagnetic spectrum. Domestic and industrial microwave ovens generally operate at a frequency of 2.45 GHz corresponding to a wavelength of 12.2 cm and energy of 1.02×10^{-5} eV [106].

Microwave irradiation has been tested to determine its efficacy for degrading pollutants because of its short reaction time, high efficiency and lack of secondary pollutant generation [107, 108]. Additionally, the heating that occurs with microwave irradiation

accelerates the reaction rates more than conventional heating, thereby saving energy and shortening the treatment process time [109]. For instance, the thermal effect of microwave treatment could efficiently remove volatile and semi-volatile pollutants [110]. However, microwave irradiation alone cannot degrade certain organic pollutants such as azo dyes, pharmaceuticals and pesticides [110-112]. Consequently, microwave irradiation has been combined with oxidants, e.g., persulfate, hydrogen peroxide, or catalysts to enhance degradation of the target pollutant [112-115].

MW produces homogeneous and quick thermal reactions due to the molecular-level heating. MW has been used in various environmental remediation processes, especially in wastewater treatment [116, 117]. The installation and operational costs of MW system are expensive; therefore, optimization of maximum power utilization and recovering part of the process heat through heat exchangers is advisable to minimize the overall cost. However, MW can reduce the treatment time required and can also produce high treatment efficiency for selective compounds, for instance, ammonia. On the other hand, a complete treatment of more complex wastewater with multiple pollutants or the removal/degradation of highly bio-refractory pollutant like pentachlorophenol (PCP) is highly difficult with MW alone. Therefore, many researchers combined MW with oxidants, catalysts or AOPs [112].

Microwave energy can be transformed into heat when a dielectric substance, having permanent or induced dipoles, is exposed to microwave radiation of a certain band of frequency. The literature reveals that microwave heating occurs by two mechanisms, which are dipolar polarization, and ionic conduction whereas another called interfacial polarization is a combination of the two. Dipolar polarization is by which heat is produced in polar molecules like water. Dipoles align themselves by rotating with the electric field associated with waves. To achieve the thermal effect the frequency of microwave is so adjusted that in an alternating electric field, the phase difference between rotating the dipoles and orienting the field causes molecular friction and collisions that give rise to dielectric heating [118].

The main advantage of combining MW with oxidants is the stimulation of free radical generation from the oxidants and rapid polarization of the pollutant molecule [119]. When combining MW and oxidants, higher reaction temperature could be reached within a shorter time frame compared to the traditional thermal or catalytic oxidation method. This assists in the faster degradation of pollutants. The two most common oxidants used along with MW are

hydrogen peroxide and persulfate. The dipolar polarization mechanism is responsible for enhancing the degradation of various pollutants in the systems combining MW and oxidants. This mechanism creates elevated temperature within a shorter span as compared to conventional heating methods, which provokes the increased decomposition of H_2O_2 into $HO^{\bullet}$ as shown in Eq. (2.32) [120]. Subsequently, the $HO^{\bullet}$ generated in the system undergoes adduction reaction with the target pollutants and the resulting intermediates. As a result, rapid and improved degradation rates are observed [121]. On the other hand, H_2O_2 can act as $HO^{\bullet}$ quencher at high concentrations as shown in Eqs. (2.33)–(2.35), consequently lowering the $HO^{\bullet}$ concentration which decreases the degradation rates. Therefore, the optimum dosage of H_2O_2 must be determined to maintain a higher degradation rate as well as to minimize the cost of overall treatment.

$$H_2O_2 \xrightarrow{\text{microwave}} 2HO^{\bullet} \quad (2.32)$$

$$HO^{\bullet} + H_2O_2 \rightarrow HO_2^{\bullet} + H_2O \quad (2.33)$$

$$2HO_2^{\bullet} \rightarrow H_2O_2 + O_2 \quad (2.34)$$

$$HO^{\bullet} + HO_2^{\bullet} \rightarrow H_2O + O_2 \quad (2.35)$$

Persulfate is also capable of absorbing MW for the generation of active free radicals and heat point as shown in Eq. (2.36). Several researchers reported that MW with persulfate oxidation has produced better degradation efficiency [119, 122]. Temperature plays a major role in MW-assisted degradation process with persulfate because at extremely high temperature the radical itself could act as a scavenger (Eqs. (2.37) and (2.38)). Therefore, identifying the optimum MW temperature is an important step in MW-assisted systems with persulfate.

$$S_2O_8^{2-} \xrightarrow{\text{microwave}} 2SO_4^{-\bullet} \quad (2.36)$$

$$SO_4^{-\bullet} + SO_4^{-\bullet} \rightarrow S_2O_8^{2-} \quad (2.37)$$

$$SO_4^{-\bullet} + S_2O_8^{2-} \rightarrow SO_4^{2-} + S_2O_8^{-\bullet} \quad (2.38)$$

Moreover, the ratio of oxidant and pollutant concentration plays a major role in the efficiency of MW with oxidant systems. Since H_2O_2 is more effective under acidic pH levels, combining MW with persulfate could be a wise option for water treatment around neutral pH.

Several factors can influence the pollutant degradation and mineralization efficiency of MW system including MW power, irradiation time and treatment temperature. Generally, the efficiency of MW system increases gradually with increase in MW power and irradiation time [119]. This could be attributed to the generation of additional heat, which favors the impetuous and rapid molecular motion. On the other hand, the degradation rates of dimethoate and pentachlorophenol (PCP) were enhanced by increasing the MW power [119, 123]. MW energy causes the polarization of molecules leading to electronic vibration, which results in the generation of heat. Therefore, the increase in the MW power input rises proportionately the reaction temperature [123, 124]. The treatment time required for removing a target compound could be shortened by increasing the MW power input. In some cases, the efficiency of MW system was found to decrease under very high temperatures; thus, it is mandatory to identify the optimum MW power and reaction temperature for the degradation of particular target pollutant.

It is interestingly to mention that, most of the general literature indicates that water containing ions is more efficiently heated by microwaves in comparison to pure (deionized) water [118].

3. Experimental part

3.1. Materials

- Pharmaceuticals:
    - Carbamazepine, 99%, Sigma-Aldrich, USA
    - Ibuprofen, 98%, Sigma-Aldrich, USA
- Oxidants:
    - Hydrogen peroxide, 30%, Gram-mol, Croatia
    - Sodium persulfate, Sigma-Aldrich, USA
- pH adjustment:
    - Sulfuric acid (H_2SO_4), 0.05M, Kemika, Croatia
    - Sodium hydroxide (NaOH), 0.02M, Kemika, Croatia
- Water matrix:
    - Sodium nitrite ($NaNO_2$), Kemika, Croatia
    - Sodium nitrate ($NaNO_3$), Kemika, Croatia
    - Sodium chloride (NaCl), Gram-mol, Croatia
    - Sodium phosphate ($Na_3PO_4 \times 12H_2O$), Kemika, Croatia
    - Sodium sulfate (Na_2SO_4), Merck, Germany
    - Humic acid sodium salt (technical grade, (H16752) Sigma-Aldrich, USA)
- Other:
    - Ethanol 96%-tni, Gram-mol, Croatia
    - Acetone, Gram-mol, Croatia

- HPLC mobile phases:
    - Acetonitrile (C_2H_3N), HPLC grade, JT Baker, USA
    - Methanol (CH_3OH), HPLC grade, JT Baker, USA
    - Formic acid (CH_2O_2), 96%, Sigma-Aldrich, USA
    - Ammonium acetate ($C_2H_7NO_2$), 98%, Sigma-Aldrich, USA
    - Ultra-pure water (Millipore Direct-Q UV 3 system, Merck, USA

- COD and BOD test:
    - COD test vial LCK 1414, HACH, USA
    - BOD test vial LCK 554, HACH, USA
    - BioKit for BOD_5 cuvette test (inoculation material) (HACH, USA)

3.2. Instruments

- HPLC (Series 20, Shimadzu, Japan) equipped with pump LC-20AD XR × 2 units, autosampler SIL-20AC XR, detector SPD-20AV, column oven CTO-20AC and LCMS-2020, Shimadzu, Japan
- Column Waters XBridge C18 3.5 µm, 4.6×150 mm, P/N: 186003034
- UV lamp Pen-Ray P/N 90-0012-01, 254nm, UVP, Cambridge, UK
- Pen-Ray power supply PS-11, 0.21 Amps, 230v, UVP, Cambridge, UK
- Ultrasound Bandelin sonopuls (25Hz)
- Microwave laboratory system Milestone ETHOS 1600
- pH meter, pH 50+ DHS XS instruments
- Ultrasonic bath Rocker model SONER 210 (50Hz)
- UV spectrophotometer DR3900, HACH Co., USA
- Milli Q water maker TKA-GenPure
- Analytical balance Sartorius
- Magnetic stirrer MSH-300 bioSan

3.3. HPLC method development

The concentration of CBZ and IBP was determined with HPLC (Series 20) (Fig. 3.1) and column Waters XBridge C18 3.5 µm, 4.6×150 mm. For CBZ the mobile phase was 35% acetonitrile and 65 % formic acid 0.1%, and the detector wavelengths were 220 nm and 285 nm. The analysis was performed under isocratic conditions at a flow rate of 1 mL/min; with an injection volume of 10 µL; and oven temperature of 40 ºC. For IBP the mobile phase was 70% methanol and 30 % ammonium acetate 10mM, and the detector wavelengths were 220 nm and 222 nm. The analysis was performed under isocratic conditions at a flow rate of 1 mL/min; with an injection volume of 20 µL; and oven temperature of 40 ºC. HPLC method development and MS condition for CBZ and IBP are summarized in Table 3.1.

Table 3.1. HPLC method development and MS condition for CBZ and IBP.

Pharmaceutical	CBZ	IBP
Mobile phase A	35% acetonitrile	70% methanol
Mobile phase B	65% formic acid 0.1%	30 % ammonium acetate 10mM
Total flow	1.00 mL/min	1.00 mL/min
Mode	Isocratic flow	Isocratic flow
Oven temperature	40 ºC	40 ºC
Injection volume	10 µL	20 µL
Detector wavelength	220 nm, 285 nm	220 nm, 222 nm
Retention time	10 min	10 min
Detection time	between 5 and 6 min	between 3 and 4 min
ESI mode	Positive	Negative
Start m/z	100	50
End m/z	500	400
Scan speed (u/sec)	406	358

Figure 3.1. HPLC series 20.

3.4. Design of Experiment (DOE)

As DOE, we used the Taguchi design with 8 factors and 2 levels (L12 (2^8)). The DOE matrix in Table 3.2 shows that we had 12 experiments for each process. In Table 3.3 factors and their levels are specified.

Minitab version 20.2 and Design Expert version 13.0 were used for design of experiment and further analysis.

Table 3.2. Experimental layout using an L12 orthogonal array.

Experiment no.	pH	Oxidant	HA	NO_2^-	NO_3^-	Cl^-	PO_4^{3-}	SO_4^{2-}
1	1	2	1	2	2	1	2	2
2	2	1	1	2	2	2	1	2
3	1	2	2	1	2	2	1	2
4	2	2	1	2	1	2	1	1
5	2	2	1	1	2	1	2	1
6	1	1	1	1	1	2	2	2
7	2	2	2	1	1	1	1	2
8	2	1	2	1	2	2	2	1
9	1	1	1	1	1	1	1	1
10	1	2	2	2	1	2	2	1
11	2	1	2	2	1	1	2	2
12	1	1	2	2	2	1	1	1

Table 3.3. Factors and their levels.

Factor	Level 1 (low)	Level 2 (high)	Unit
pH	4	10	-
Oxidant	0.05	10	mM
HA	2	10	mg/L
NO_2^-	0.1	10	mg/L
NO_3^-	1	70	mg/L
Cl^-	10	250	mg/L
PO_4^{3-}	0.08	0.5	mg/L
SO_4^{2-}	20	600	mg/L

3.5. Pharmaceutical aqueous solution preparation

Separately, aqueous solutions of studied pharmaceuticals were prepared by dissolving respective quantities in ultra-pure Milli-Q water with a concentration of 50 µM . The quantity of CBZ and IBP prepared in a 2L flask was 0.0236 gr and 0.0206 gr respectively. After one day of stirring with a magnetic stirrer, the aqueous solutions of studied pharmaceuticals were stored in plastic bottles in a 4ºC refrigerator.

3.6. Water matrix solution preparation

We used related salts to prepare various inorganic ions that were used as factors in the Taguchi design. The concentration and quantity of each factor of the synthetic water matrix are shown in the Table 3.4. The solutions were prepared by dissolving respective quantities of salts in ultra-pure Milli-Q water and stored in plastic bottles in a room temperature.

Table 3.4. Factors' characteristics and used concentration.

Factor	Molar mass (g/mol)	Concentration	Quantity (for 1L flask)
NO_2^- ($NaNO_2$)	69	1000 ppm	1 gr
NO_3^- ($NaNO_3$)	84.99	10000 ppm	10 gr
Cl^- (NaCl)	58.44	10000 ppm	10 gr
PO_4^{3-} ($Na_3PO_4 \times 12H_2O$)	380.12	1000 ppm	1 gr
SO_4^{2-} (Na_2SO_4)	142.04	100000 ppm	100 gr
HA	-	400 ppm	-

The quantity of used factors for making synthetic water matrix that are presented as minimum and maximum levels in the Taguchi design are shown in the Table 3.5.

Table 3.5. Factors' quantity for level 1 and 2.

Factor	Level 1	Level 2
NO_2^-	8 µL	800 µL
NO_3^-	8 µL	560 µL
Cl^-	80 µL	2000 µL
PO_4^{3-}	6.4 µL	40 µL
SO_4^{2-}	16 µL	480 µL
HA	400 µL	2000 µL

3.7. Oxidants

In this study, two oxidants were used: hydrogen peroxide and sodium persulfate. The oxidants used had concentrations of 0.5 mM and 10 mM. The amount of oxidant used is seen in the Table 3.6.

Table 3.6. Oxidants' quantity for level 1 and 2.

Oxidant	Molar mass (g/mol)	Level 1	Level 2
H_2O_2	34.01	4.1 µL	82 µL
$Na_2S_2O_8$	238.03	0.0095 gr	0.1904 gr

3.8. UV-C based processes

As can be seen in Figure 3.2, all experiments were performed in a glass water-jacketed batch photoreactor (total volume, V_T=0.1 L, solution volume, V_S=0.08 L, and T=25.0 ± 0.2 °C). The photoreactor was equipped with UV-C lamp providing circum monochromatic light at 254 nm, with incident photon flux (P_0) of 1.04×10^{-6} Einstein s^{-1}, which was placed in the middle (irradiation path L=1 cm), and magnetic stirrer in order to provide effective mixing of reaction solution (mixing speed was 550 rpms). The procedure began after the warmed-up UV-C lamp was placed into a quartz cuvette. The power supply of the UV lamp was 48.3 W with frequency of 50-60 Hz.

Every degradation process had 12 experiments, according to the Taguchi design table. An experiment was completed in 60 seconds, with samples taken every 10 seconds. 7 samples were taken from each experiment and overall, for three studied UV-C based processes we had 252 samples in HPLC vials. To quench the radicals in the hydrogen peroxide reactions, 100 µL methanol was applied to each sample.

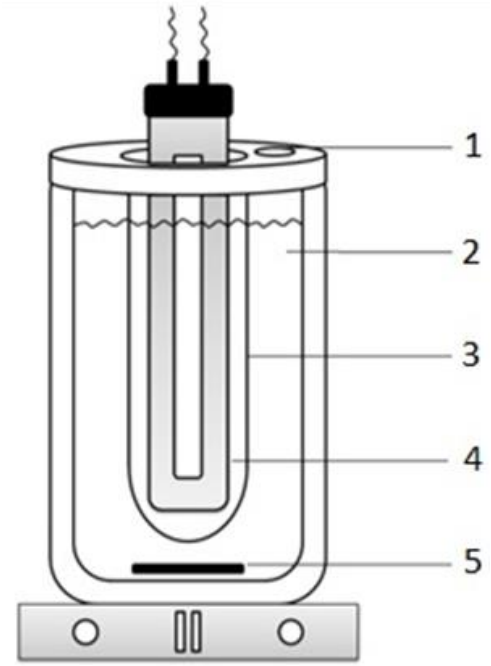

1. Inlet of the syringe for sampling
2. Sample solution
3. Quartz cuvette
4. UV lamp
5. Magnet

Figure 3.2. UV-C reactor.

After analyzing the samples by HPLC, kinetics degradation of each process and effect of factors on each degradation process were obtained.

The mineralization was carried out in accordance with the optimum conditions of each process. In total, we conducted six mineralization experiments using UV-C based methods. All processes were conducted for 90 min; samples were collected at 0, 15, 30, 60 and 90 min. 7.5 mL was the volume of each sampling (1 mL for TOC, 6 mL for BOD, 2 mL for COD and 0.5 mL for HPLC analyzing). The samples contained H_2O_2, quenched with sodium thiosulfate.

Overall, 30 samples were collected and stored in a freezer (-20ºC) to stop the radicals' activities. It should be noted that in processes containing persulfate oxidant, we didn't adjust the pH and the reactions were held in pH-free conditions because pH was not influential factor in UV-C/$S_2O_8^{2-}$ processes.

3.9. Ultrasound based processes

As can be seen in Figure 3.3, all experiments were performed in a glass water-jacketed batch reactor (total volume, V_T=0.1 L, solution volume, V_S=0.08 L). The probe of ultrasound was located at the middle of the reactor. For controlling the temperature of the reaction, the reactor placed in a cool water bath. The temperature of the reactor from the beginning of the reaction was 23 ºC and in 2 hours of the process, it raised continuously to 35 ºC. All processes were conducted for 120 min; samples were collected at 0, 5, 10, 15, 30, 60, 90 and 120 min. The power of the ultrasound set on 70 W and the frequency of the instrument was 25 kHz.

The preliminary tests revealed that the ultrasound process with hydrogen peroxide was more efficient than the sodium persulfate process in both studied pharmaceuticals, and due to the time-consuming process, we decided to only do the processes with hydrogen peroxide.

Overall, for CBZ and IBP degradation by US/H_2O_2 processes, 192 samples in HPLC vials were collected and quenched with 100 µL methanol and analyzed with HPLC.

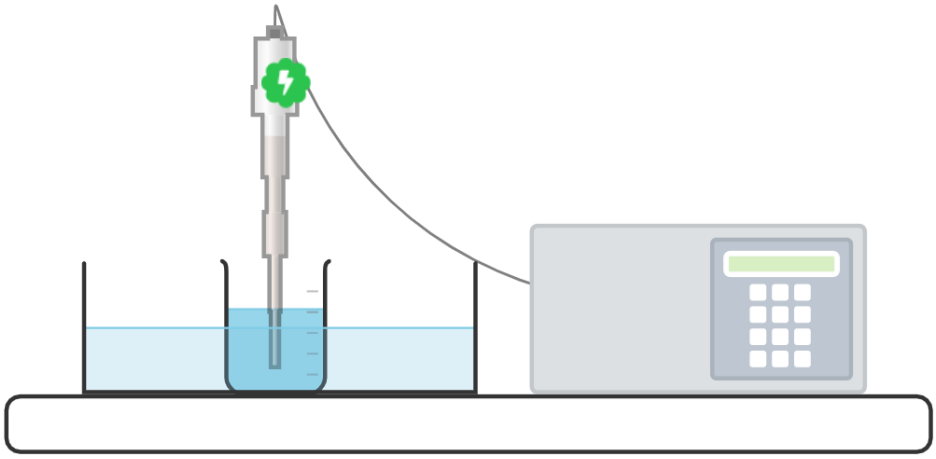

Figure 3.3. Setup experiment of ultrasound based processes.

3.10. Microwave based processes

Microwave laboratory system Milestone ETHOS 1600 was used for all performed experiments. The microwave instrument is shown in Figure 3.4. The microwave contains of 10 reactors. After preparation of sample solution in 80 mL volume, 60 mL of that was measured and poured in reactor because the volume of the reactor was 70 mL. All experiment were performed at power of 700 W (70 W for each reactor). It should be noted that preliminary tests revealed that applying 70 W to one reactor temperature raised to 95 ºC and MW irradiation to ten reactors simultaneously required a power of 700W to attain 95 ºC. The duration of experiments was 10 minutes. The temperature of solutions after the reaction raised to 95 ºC. Two samples were collected from each rector; one sample before microwave irradiation and one sample after reaction. The samples contained H_2O_2, quenched with methanol. Samples were immediately placed at refrigerator to cool down and avoid the reaction.

For each degradation processes, 24 samples were collected. Overall, 144 samples in HPLC vials were obtained.

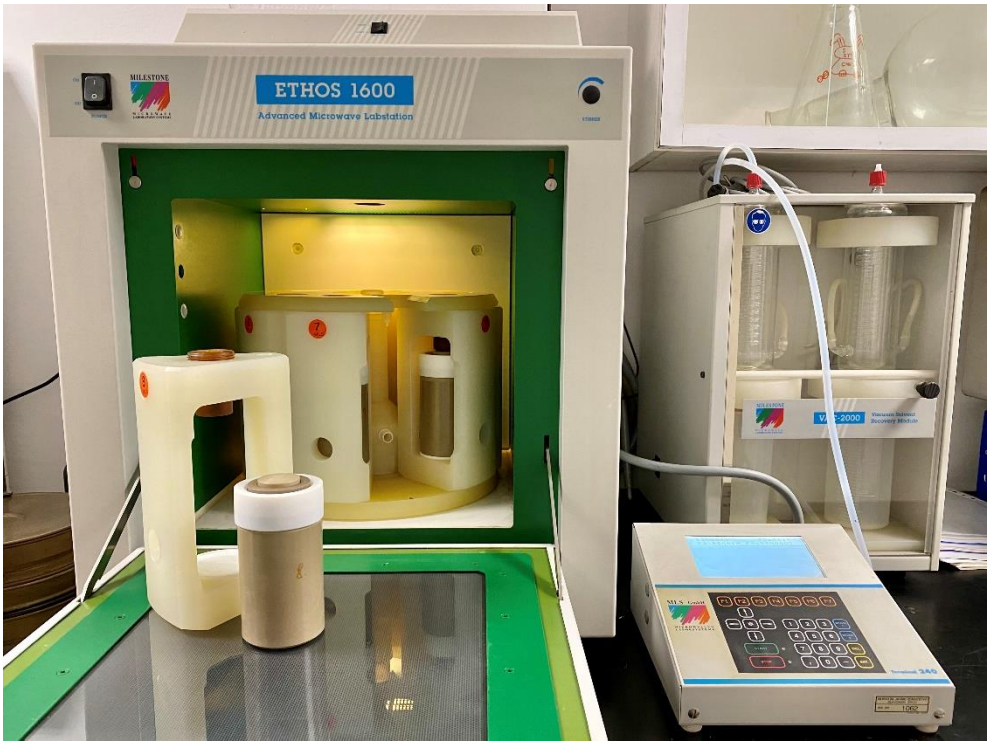

Figure 3.4. Microwave reactor.

3.11. Calculations

The percentage conversion of CBZ and IBP was calculated by following (Eq. (3.1)):

$$\text{Conversion (\%)} = \frac{(C_0 - C_t)}{C_0} \times 100 \qquad (3.1)$$

Where C_0 and C_t represent the CBZ or IBP concentration in the solution before and after the degradation process respectively. The degradation kinetic data of both studied pharmaceuticals were analyzed by the pseudo first-order kinetic model (Eq. (3.2)).

$$\ln\left(\frac{C_t}{C_0}\right) = -kt \qquad (3.2)$$

3.12. COD test

COD was determined by a colorimetric method following HACH COD analysis procedure. Briefly, 2 mL of samples were added to a COD test vial LCK 1414 (HACH) with a clean pipet, which was then digested in a preheated thermostat (HACH Co., USA) at 148 ℃ for 2 hr. COD of samples after 15 min cooling down was determined with a direct reading UV spectrophotometer (DR3900, HACH Co., USA) at a wavelength of 348 nm.

3.13. BOD test

First inoculation solution was made. One spoon of inoculation material and 10 mL BioKIT suspension were introduced to 20 ml vial and was mixed for 1 min and left for one hour at room temperature. After that 1 ml of inoculation solution was added to another vial with 9 ml of Milli-Q water. 500 µL of prepared inoculation solution and about 6 mL of samples were added to a BOD test vial LCK 554 (HACH) with a clean pipet, which was then digested in an incubator at 20 ℃ for 5 day. It should be noted that there shouldn’t be any oxygen bubble in BOD vials. After 5 day BOD tablets were added to the kit and after mixing was determined with a direct reading UV spectrophotometer (DR3900, HACH Co., USA) at a wavelength of 620 nm.

4. Results

4.1. Results obtained from UV-C based processes

4.1.1. Kinetics

In this chapter, all of the found results are shown with tables and graphs and the results are discussed in chapter 5.

The Taguchi design matrix for UV-C/H_2O_2 and UV-C/$S_2O_8^{2-}$ processes with eight factors (independent variables) expressed in coded units (1: maximum level and 2: minimum level) and experimentally determined first order degradation rates (k_{app}) for two studied pharmaceuticals is presented in Table 4.1.

Table 4.1. Taguchi design matrix for UV-C/H_2O_2 and UV-C/$S_2O_8^{2-}$ processes and experimentally determined first order degradation rates (k_{app}) for CBZ and IBP.

Experiment no.	Factors								First order degradation rates ($k_{app} \times 10^{-3}$, s^{-1})			
									UV-C/H_2O_2		UV-C/$S_2O_8^{2-}$	
	pH	Oxidant	HA	NO_2^-	NO_3^-	Cl^-	PO_4^{3-}	SO_4^{2-}	CBZ	IBP	CBZ	IBP
1	1	2	1	2	2	1	2	2	15.1	24.8	11.6	45.5
2	2	1	1	2	2	2	1	2	2.8	5.4	4.8	4.3
3	1	2	2	1	2	2	1	2	25.7	33.5	31.6	144.8
4	2	2	1	2	1	2	1	1	11.2	15.6	11.2	22.7
5	2	2	1	1	2	1	2	1	23.7	21.3	26.1	121.2
6	1	1	1	1	1	2	2	2	5.6	10.9	5	14.6
7	2	2	2	1	1	1	1	2	20.3	21.1	18.2	104
8	2	1	2	1	2	2	2	1	6	9.1	5.9	7.9
9	1	1	1	1	1	1	1	1	6.4	11	4.3	16.8
10	1	2	2	2	1	2	2	1	11	17.7	4.3	25.8
11	2	1	2	2	1	1	2	2	2.8	5.3	4.2	4.6
12	1	1	2	2	2	1	1	1	2.5	4.3	1.5	5.2

The Taguchi design matrix for UV-C process with seven factors (independent variables) expressed in coded units (1: maximum level and 2: minimum level) and experimentally determined first order degradation rates (k_{app}) for two studied pharmaceuticals is presented in Table 4.2.

Table 4.2. Taguchi design matrix for UV-C process and experimentally determined first order degradation rates (k_{app}) for CBZ and IBP.

Experiment no.	Factors							First order degradation rates ($k_{app} \times 10^{-3}$, s^{-1})	
								UV-C	
	pH	HA	NO_2^-	NO_3^-	Cl^-	PO_4^{3-}	SO_4^{2-}	CBZ	IBP
1	1	1	2	2	1	2	2	4.3	4
2	2	1	2	2	2	1	2	2.9	4.1
3	1	2	1	2	2	1	2	3.2	5.8
4	2	1	2	1	2	1	1	2.7	2.9
5	2	1	1	2	1	2	1	2.8	6
6	1	1	1	1	2	2	2	2.9	5.8
7	2	2	1	1	1	1	2	4.1	5.5
8	2	2	1	2	2	2	1	4.1	4.5
9	1	1	1	1	1	1	1	2.3	5.1
10	1	2	2	1	2	2	1	2.4	4.9
11	2	2	2	1	1	2	2	1.9	4.8
12	1	2	2	2	1	1	1	1.7	7.2

4.1.2. Influence of factors on degradation kinetics

4.1.2.1. CBZ degradation by UV-C based processes

Main effects plots for CBZ first order degradation rate by UV-C based processes are presented in Figure 4.1 – 4.3.

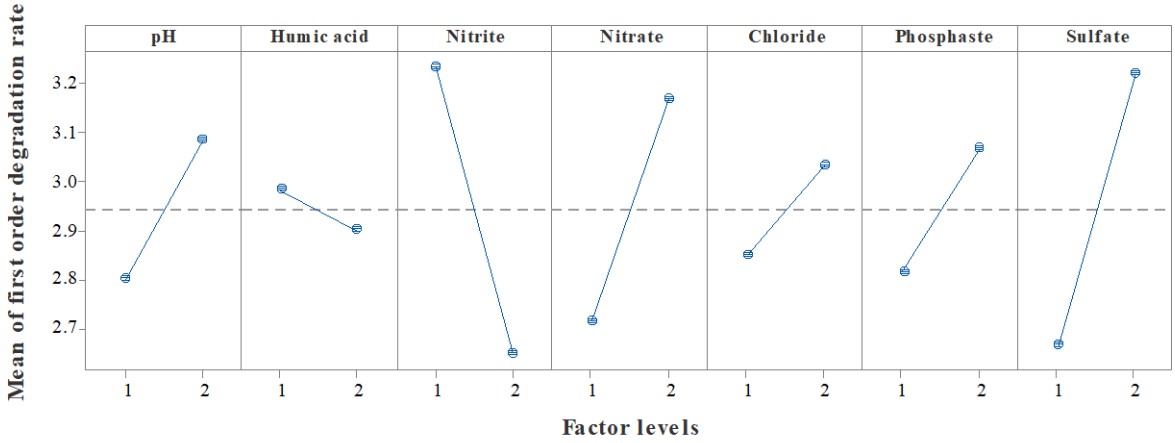

Figure 4.1. Main effects plot for first order degradation rate CBZ with UV-C process.

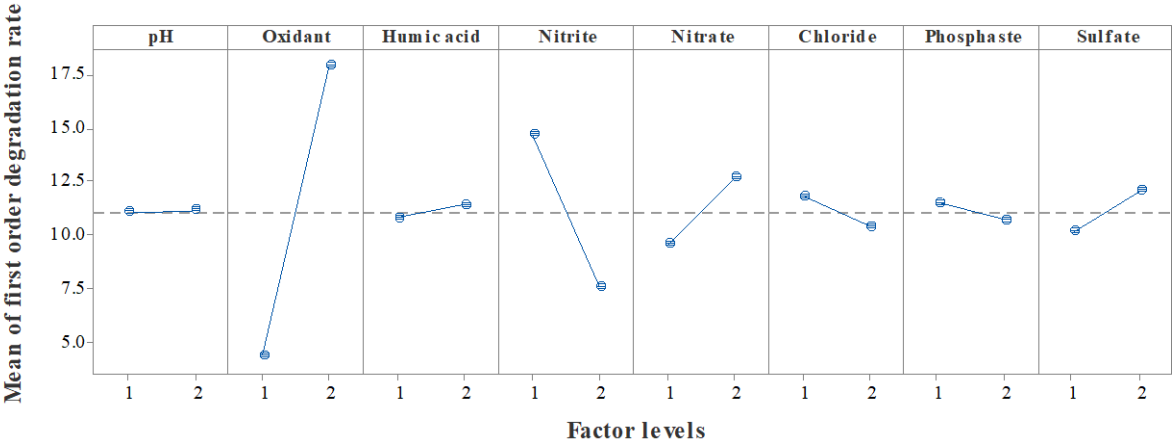

Figure 4.2. Main effects plot for first order degradation rate CBZ with UV-C/H_2O_2 process.

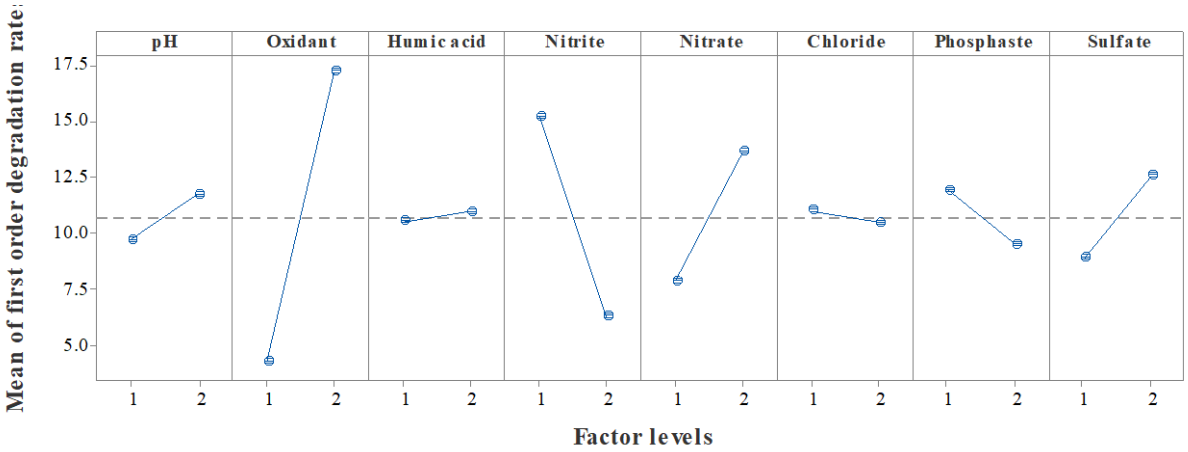

Figure 4.3. Main effects plot for first order degradation rate CBZ with UV-C/$S_2O_8^{2-}$ process.

4.1.2.2. IBP degradation by UV-C based processes

Main effects plots for IBP first order degradation rate by UV-C based processes are presented in Figures 4.4 – 4.6.

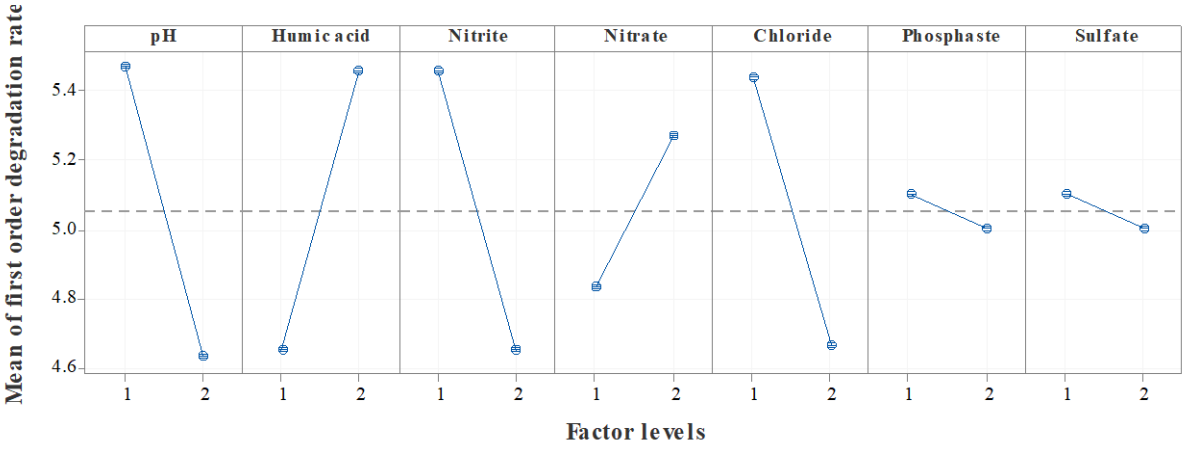

Figure 4.4. Main effects plot for first order degradation rate IBP with UV-C process.

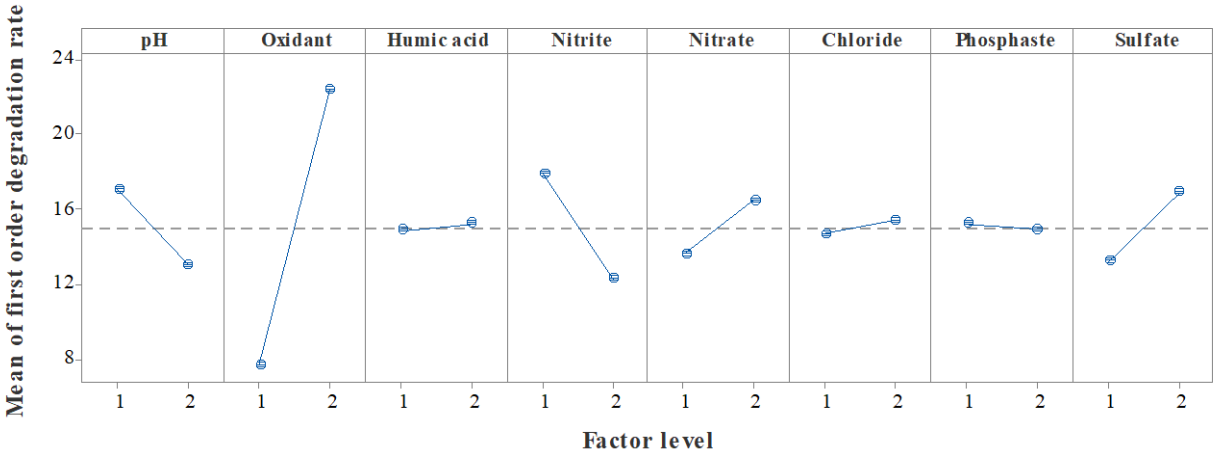

Figure 4.5. Main effects plot for first order degradation rate IBP with UV-C/H_2O_2 process.

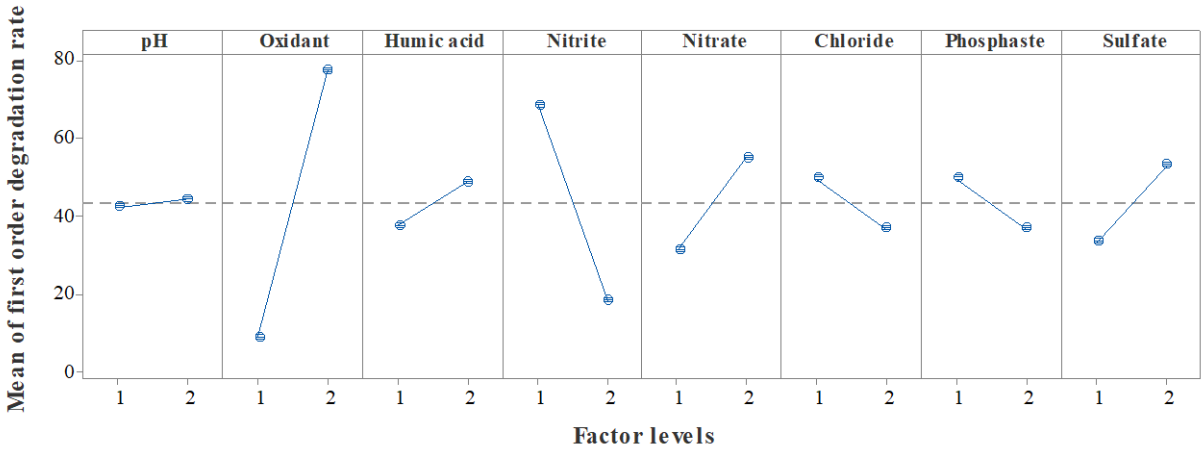

Figure 4.6. Main effects plot for first order degradation rate IBP with UV-C/$S_2O_8^{2-}$ process.

4.1.3. Optimal condition

First order degradation rates of UV-C based processes for two studied pharmaceuticals in optimal conditions are presented in Table 4.3. Optimal conditions of each process are the level of each factor that had synergistic effect on the degradation rate.

Table 4.3. First order degradation rates of UV-C based processes for two studied pharmaceuticals in optimal conditions.

Pharmaceutical	Process	First order degradation rates (k_{app}, $\times 10^{-3}$, s^{-1})	R^2
CBZ	UV-C	2.4	0.9989
	UV-C/H_2O_2	21.3	0.9988
	UV-C/$S_2O_8^{2-}$	29.9	0.9778
IBP	UV-C	3.8	0.9954
	UV-C/H_2O_2	27.4	0.9972
	UV-C/$S_2O_8^{2-}$	70.6	0.9613

Comparisons of conversion percentages of UV-based processes on CBZ and IBP in 30 min degradation process are presented in Figures 4.7 and 4.8.

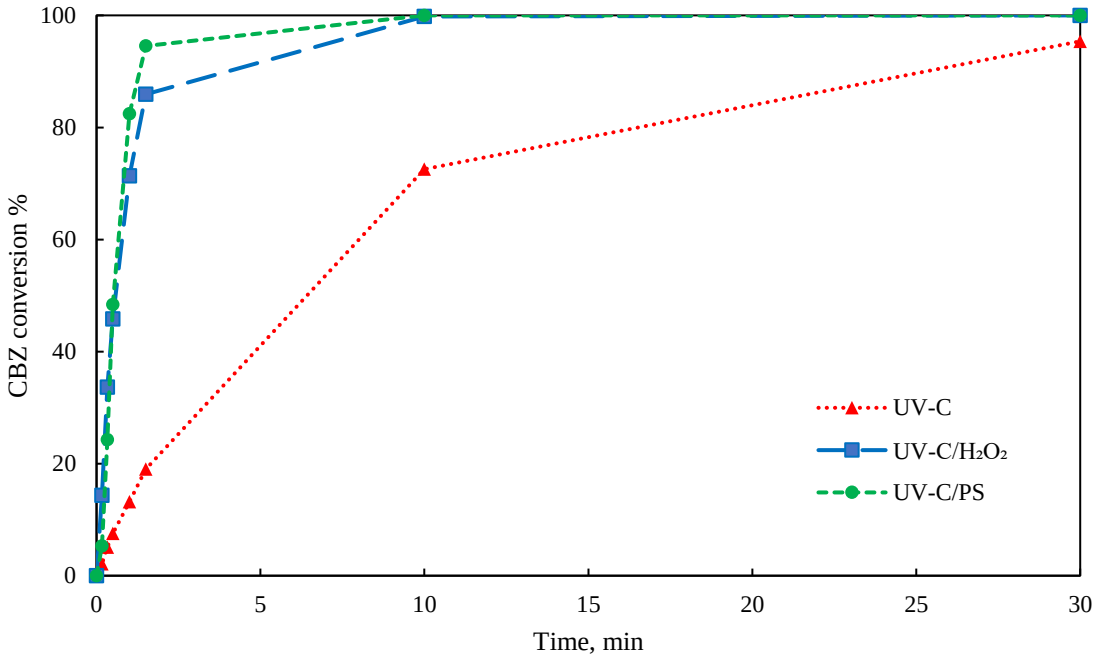

Figure 4.7. Comparison of CBZ conversion percentage by UV-based processes.

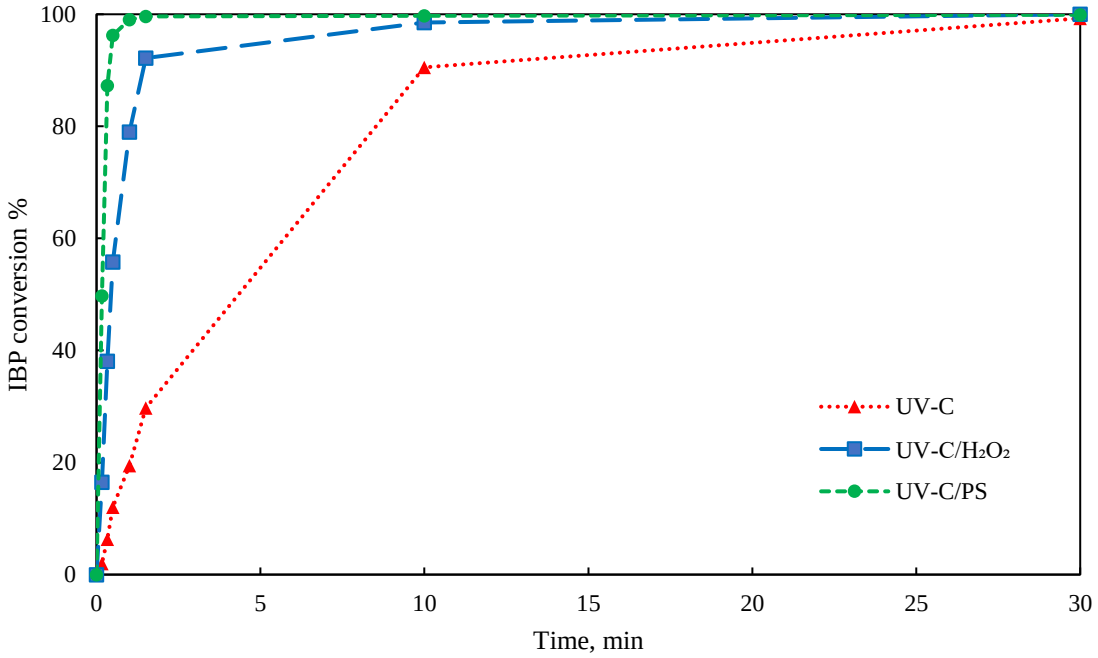

Figure 4.8. Comparison of IBP conversion percentage by UV-based processes.

4.2. Results obtained from ultrasound based processes

4.2.1. Kinetics

The Taguchi design matrix for US/H_2O_2 process with eight factors (independent variables) expressed in coded units (1: maximum level and 2: minimum level) and experimentally determined first order degradation rates (k_{app}) for two studied pharmaceuticals is presented in Table 4.4.

Table 4.4. Taguchi design matrix for US/H_2O_2 process and experimentally determined first order degradation rates (k_{app}) for CBZ and IBP.

Experiment no.	Factors								First order degradation rates ($k_{app} \times 10^{-3}$, s^{-1})	
									US/H_2O_2	
	pH	Oxidant	HA	NO_2^-	NO_3^-	Cl^-	PO_4^{3-}	SO_4^{2-}	CBZ	IBP
1	1	2	1	2	2	1	2	2	1.2	4.2
2	2	1	1	2	2	2	1	2	0.9	2.1
3	1	2	2	1	2	2	1	2	1.9	3
4	2	2	1	2	1	2	1	1	0.6	2.5
5	2	2	1	1	2	1	2	1	0.7	3.3
6	1	1	1	1	1	2	2	2	2.9	4.3
7	2	2	2	1	1	1	1	2	1	2.6
8	2	1	2	1	2	2	2	1	1.4	1.7
9	1	1	1	1	1	1	1	1	1.2	4.4
10	1	2	2	2	1	2	2	1	4.5	4.1
11	2	1	2	2	1	1	2	2	1.1	1.1
12	1	1	2	2	2	1	1	1	1.2	2.4

4.2.2. Influence of factors on degradation kinetics

4.2.2.1. CBZ degradation by US/H_2O_2 process

Main effects plot for CBZ first order degradation rate by US/H_2O_2 process is presented in Figure 4.9.

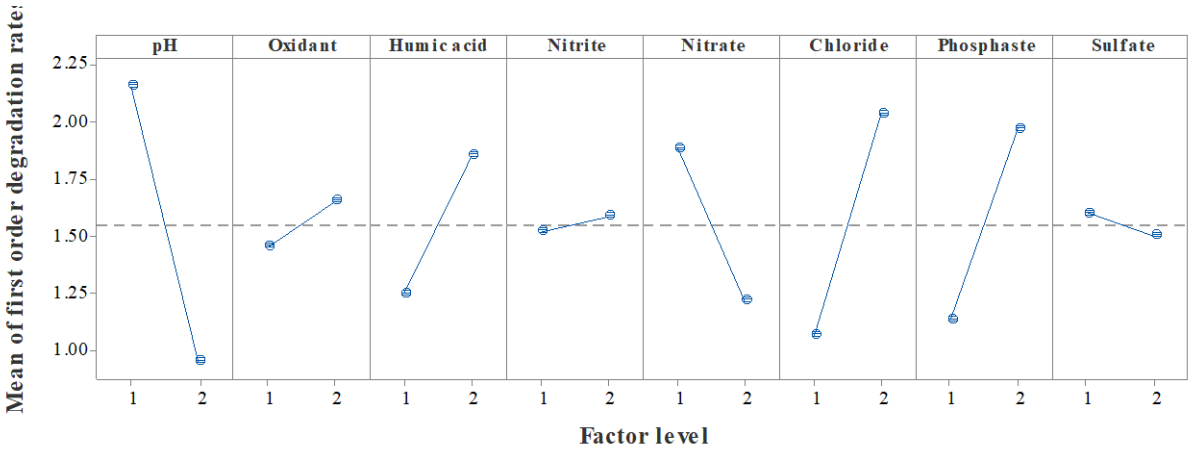

Figure 4.9. Main effects plot for first order degradation rate CBZ with US/H_2O_2 process.

4.2.2.2. IBP degradation by US/H_2O_2 process

Main effects plot for IBP first order degradation rate by US/H_2O_2 process is presented in Figure 4.10.

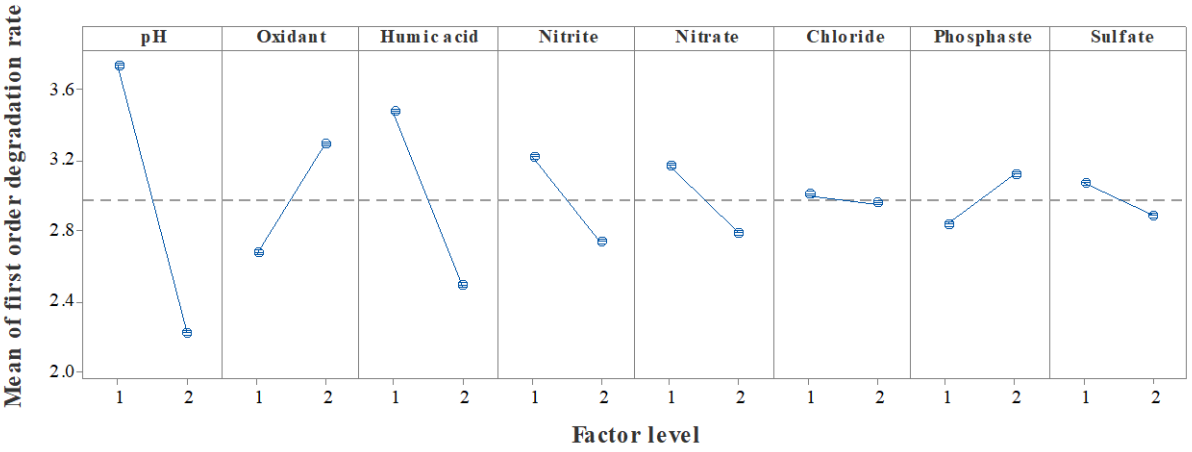

Figure 4.10. Main effects plot for first order degradation rate IBP with US/H_2O_2 process.

4.3. Results obtained from microwave based processes

4.3.1. Kinetics

The Taguchi design matrix for MW/H_2O_2 and MW/$S_2O_8^{2-}$ processes with eight factors (independent variables) expressed in coded units (1: maximum level and 2: minimum level) and experimentally determined first order degradation rates (k_{app}) for two studied pharmaceuticals is presented in Table 4.5.

Table 4.5. Taguchi design matrix for MW/H_2O_2 and MW/$S_2O_8^{2-}$ processes and experimentally determined first order degradation rates (k_{app}) for CBZ and IBP.

Experiment no.	Factors								First order degradation rates ($k_{app} \times 10^{-3}$, s^{-1})			
									MW/H_2O_2		MW/$S_2O_8^{2-}$	
	pH	Oxidant	HA	NO_2^-	NO_3^-	Cl^-	PO_4^{3-}	SO_4^{2-}	CBZ	IBP	CBZ	IBP
1	1	2	1	2	2	1	2	2	866	66.2	847	458.8
2	2	1	1	2	2	2	1	2	36.6	22.9	472	526
3	1	2	2	1	2	2	1	2	182.1	127.2	606.9	634.6
4	2	2	1	2	1	2	1	1	45.2	15.8	783.1	630.4
5	2	2	1	1	2	1	2	1	9.7	14.2	610.5	710.3
6	1	1	1	1	1	2	2	2	63.6	22.3	718	629.4
7	2	2	2	1	1	1	1	2	48.7	14.8	647.3	1248
8	2	1	2	1	2	2	2	1	24.3	20.4	674.8	1252.5
9	1	1	1	1	1	1	1	1	43.7	17.2	645.5	1250
10	1	2	2	2	1	2	2	1	282.2	159.7	674.1	805.6
11	2	1	2	2	1	1	2	2	7.7	10.3	469.8	751.6
12	1	1	2	2	2	1	1	1	135.6	79.1	474.5	581

The Taguchi design matrix for MW process with seven factors (independent variables) expressed in coded units (1: maximum level and 2: minimum level) and experimentally determined first order degradation rates (k_{app}) for two studied pharmaceuticals is presented in Table 4.6.

Table 4.6. Taguchi design matrix for MW process and experimentally determined first order degradation rates (k_{app}) for CBZ and IBP.

Experiment no.	Factors							First order degradation rates ($k_{app} \times 10^{-3}$, s^{-1})	
								MW	
	pH	HA	NO_2^-	NO_3^-	Cl^-	PO_4^{3-}	SO_4^{2-}	CBZ	IBP
1	1	1	2	2	1	2	2	8.2	10.4
2	2	1	2	2	2	1	2	3.8	8.6
3	1	2	1	2	2	1	2	0.6	11.8
4	2	1	2	1	2	1	1	0.4	7.2
5	2	1	1	2	1	2	1	16.9	10.2
6	1	1	1	1	2	2	2	1.6	7.2
7	2	2	1	1	1	1	2	8	10.6
8	2	2	1	2	2	2	1	9.9	5.3
9	1	1	1	1	1	1	1	2.8	16.5
10	1	2	2	1	2	2	1	0.4	4.7
11	2	2	2	1	1	2	2	1	11
12	1	2	2	2	1	1	1	8.2	3.8

4.3.2. Influence of factors on degradation kinetics

4.3.2.1. CBZ degradation by MW based processes

Main effects plots for CBZ first order degradation rate by MW based processes are presented in Figure 4.11 – 4.13.

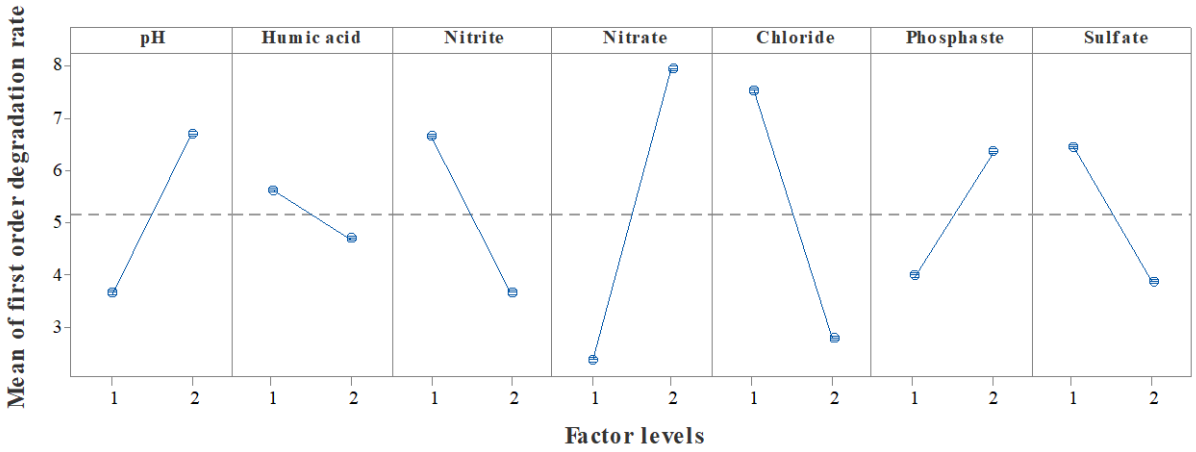

Figure 4.11. Main effects plot for first order degradation rate CBZ with MW process.

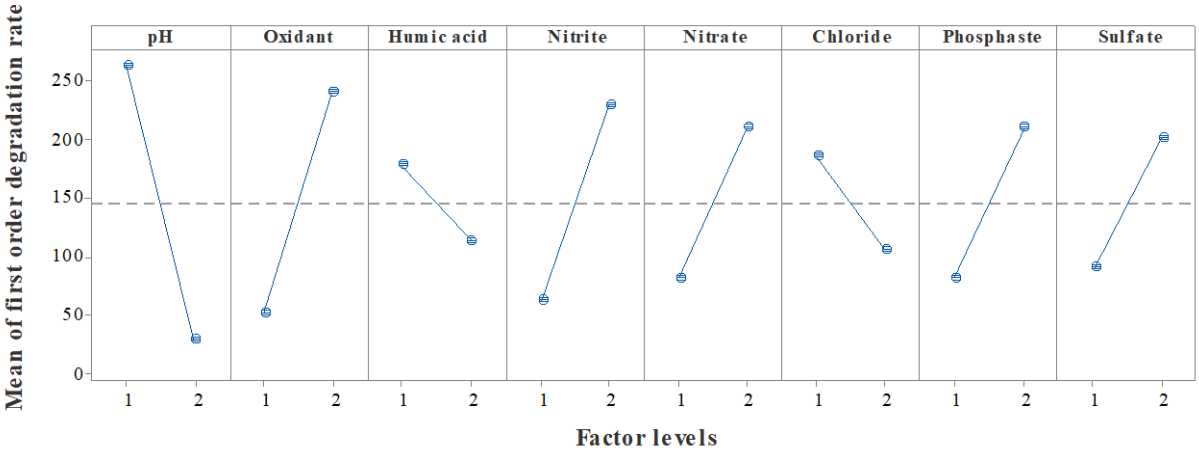

Figure 4.12. Main effects plot for first order degradation rate CBZ with MW/H_2O_2 process.

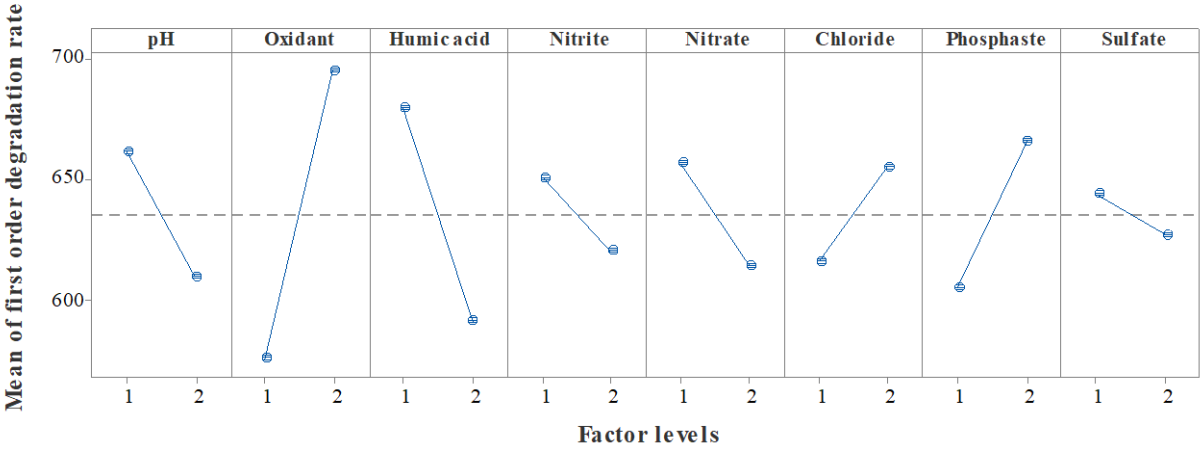

Figure 4.13. Main effects plot for first order degradation rate CBZ with MW/$S_2O_8^{2-}$ process.

4.3.2.2. IBP degradation by MW based processes

Main effects plots for IBP first order degradation rate by MW based processes are presented in Figure 4.14 – 4.16.

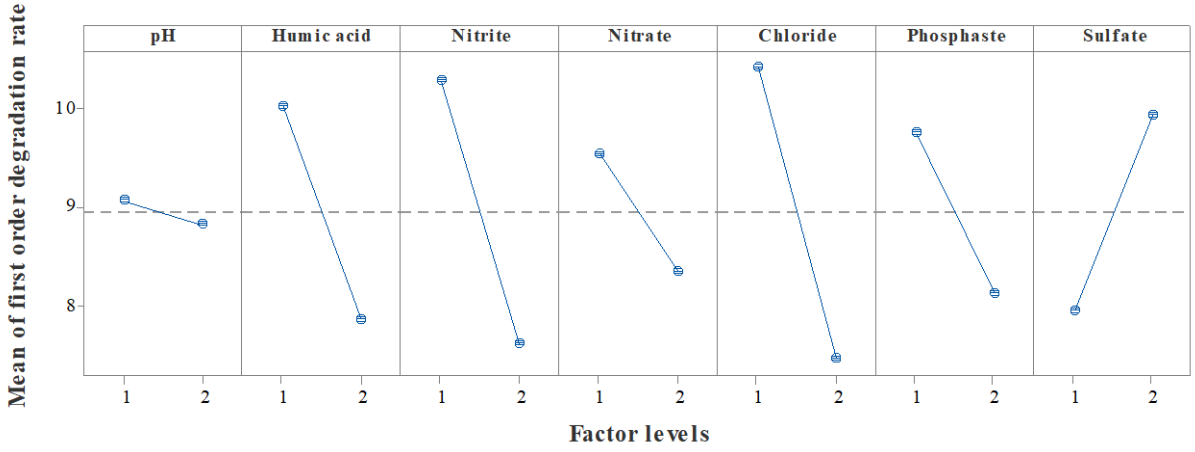

Figure 4.14. Main effects plot for first order degradation rate IBP with MW process.

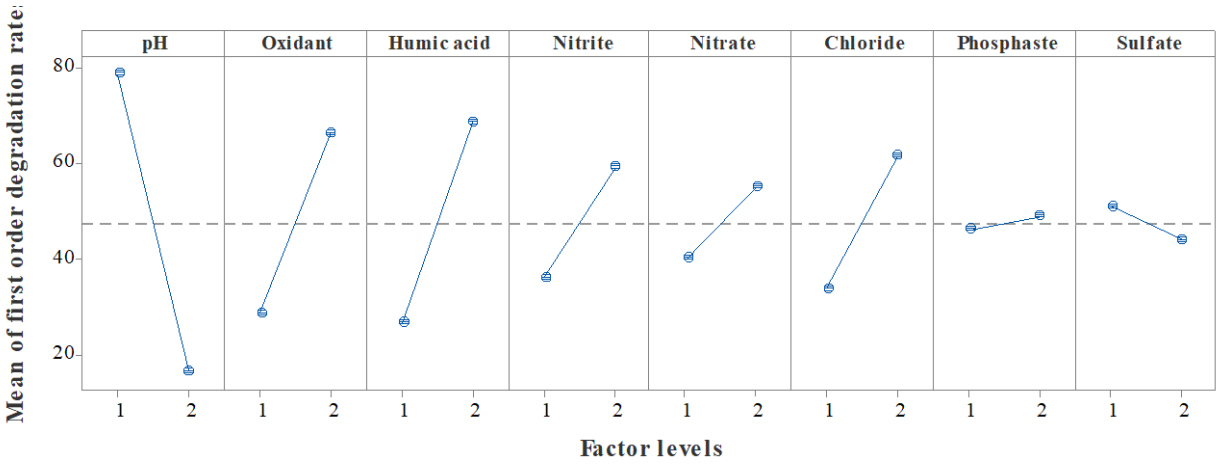

Figure 4.15. Main effects plot for first order degradation rate IBP with MW/H_2O_2 process.

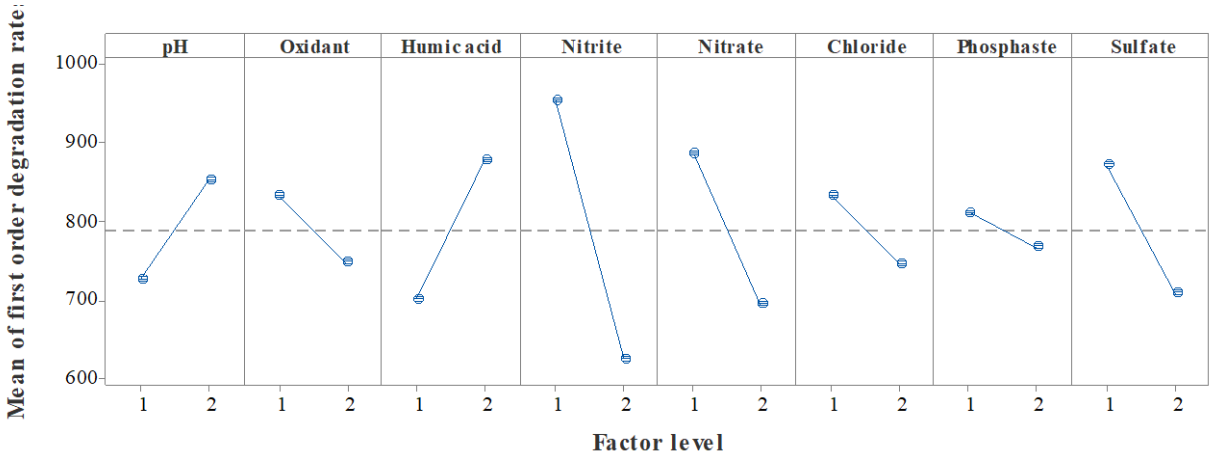

Figure 4.16. Main effects plot for first order degradation rate IBP with MW/$S_2O_8^{2-}$ process.

5. Discussion

5.1. Degradation kinetics and mechanism

Previous studies have found that kinetic regimes of pharmaceuticals with AOP based processes depend on experimental factors and parameters and structural features of the produced active radicals [125]. It is important to note that two studied pharmaceuticals degradation by all studied processes fitted pseudo first order kinetics (Eq. (3.2)). Approximately the same power value was utilized for each process in order to compare their degradation efficiency. In Table 5.1 the average of kinetic degradation rates was used for comparing the degradation processes. Because optimal values are not found in nature or in real life, average values were used instead. The UV-C, US, and MW instruments each had a power of 48.3W, 70W and 70W, respectively. IBP exhibited a greater degradation rate than CBZ in all procedures, which might be attributed to its more degradable physicochemical properties.

Table 5.1. Comparison of degradation processes by CBZ and IBP degradation rates.

Pharmaceutical	Process	First order degradation rates ($k_{app} \times 10^{-3}$, s^{-1})	R^2
CBZ	UV-C	2.9	0.99
	UV-C/H_2O_2	11.1	0.99
	UV-C/$S_2O_8^{2-}$	12.0	0.99
	US/H_2O_2	1.5	0.99
	MW	5.1	1.00
	MW/H_2O_2	145.4	1.00
	MW/$S_2O_8^{2-}$	635.2	1.00
IBP	UV-C	5.0	0.99
	UV-C/H_2O_2	15.0	0.99
	UV-C/$S_2O_8^{2-}$	43.11	0.99
	US/H_2O_2	2.9	0.99
	MW	8.9	1.00
	MW/H_2O_2	40.4	1.00
	MW/$S_2O_8^{2-}$	789.8	1.00

Among all degradation processes, US/H_2O_2 showed the lowest first order degradation rate (1.5×10^{-3} s^{-1} for CBZ and 2.9×10^{-3} s^{-1} for IBP), which might be attributed to the use of a low frequency (25 kHz) and low power ultrasound equipment (70W). After 2 hours of reaction, the maximum conversion of CBZ and IBP with US/H_2O_2 was 35.11 % and 42.75 %, respectively. IBP exhibited a greater conversion rate due to its physicochemical features, which might be more degradable. It should be noted that CBZ and IBP degradation by US/H_2O_2 process fitted ($R^2 > 0.98$) pseudo first order kinetics. To explain the degradation mechanism, Rao et al [84] examined CBZ degradation in the presence of 1.0 M methanol, an effective quencher for hydroxyl radicals. The addition of methanol remarkably diminished CBZ degradation by ultrasound both at 200 kHz and 400 kHz, implying hydroxyl radicals play a dominating role in CBZ sono-degradation. CBZ cannot be pyrolyzed inside the cavitation bubbles in view of the fact that its Henry's law constant was approximately 1.08×10^{-10} atm.m^3/mol, indicating low fugacity. In addition, due to its moderate water solubility (17.7 mg/L) and high Log P (2.45) which is octanol–water partition coefficient, CBZ may exist at the interface of bubble-bulk solution. Therefore, hydroxyl radical is the key player responsible for CBZ degradation by ultrasound. CBZ is also found within the bulk solution, allowing the protagonist of its degradation to be the HO•, which are immediately formed from the implosion both of the cavitation bubbles and the bubbles that travel within the solution.

Adityosulindro et al. [126] evaluated the degradation of ibuprofen (IBP) in order to ascertain the reaction zone in which the degradation of IBP was established, and whether it was due exclusively to HO•. For this purpose, they tested the sequestration of these radicals through two compounds, n-butanol, which is a short chain alcohol with partial solubility in water that is expected to react with the radicals housed in the bubble–liquid interface; and acetic acid, which should react with the free radicals in the bulk solution due to it is a completely miscible compound. The obtained results indicated that, indisputably, IBP reacted with the HO• recently formed during the implosion of the cavitation bubbles, which means that it is a compound housed in the interfacial zone. The same conclusion was reached by Méndez-Arriaga et al. [92], who attributed the degradation of IBP to the HO• recently produced, since IBP is considered to be housed at the bubble–water interface due to its Henry's constant (1.5×10^{-7} atm.m^3.mol^{-1}), low solubility in water (21 mg.L^{-1}) and octanol–water partition coefficient (3.9).

UV-C based AOPs provide CBZ and IBP degradation at a much faster rate than direct photolysis due to different degradation mechanisms occurring within the system. It should be noted that CBZ and IBP degradation by UV-C based processes fitted ($R^2 > 0.96$) pseudo first order kinetics. Because there are no photosensitive functional groups in CBZ, it is resistant to photodegradation [127]. In optimal conditions, degradation rate of CBZ is 2.4×10^{-3} s^{-1}, 21.3×10^{-3} s^{-1} and 29.9×10^{-3} s^{-1} for UV-C, UV-C/H_2O_2 and UV-C/$S_2O_8^{2-}$ respectively (Fig. 4.7). Degradation rate of IBP is 3.8×10^{-3} s^{-1}, 27.4×10^{-3} s^{-1} and 70.6×10^{-3} s^{-1} for UV-C, UV-C/H_2O_2 and UV-C/$S_2O_8^{2-}$ respectively (Fig. 4.8).

Interestingly, even considering the lower second-order rate constant of $SO_4^{-\bullet}$ with CBZ and IBP (5.57×10^9 and 1.32×10^9, respectively) than second-order rate constant of $HO^\bullet$ with CBZ and IBP (8.02×10^9 and 1.92×10^9, respectively), a higher removal rate was observed for the UV-C/$S_2O_8^{2-}$ process than for the UV-C/H_2O_2 process. Plausible explanations for this result might be the following: first, the production yield of $SO_4^{-\bullet}$ in the UV-C/$S_2O_8^{2-}$ process could be higher than the yield of $HO^\bullet$ in the UV-C/H_2O_2 process. This would be due to the higher radical formation quantum yield of $S_2O_8^{2-}$ ($\varepsilon_{S_2O_8^{2-}} = 47.45\ M^{-1}cm^{-1}$ and $\phi_{S_2O_8^{2-}} = 0.9$) as compared to the values for H_2O_2 ($\varepsilon_{H_2O_2} = 19.6\ M^{-1}cm^{-1}$ and $\phi_{H_2O_2} = 0.5$) [128], which would lead to a higher production of $SO_4^{-\bullet}$ in the UV-C/$S_2O_8^{2-}$ process compared to $HO^\bullet$ production in the UV-C/H_2O_2 process.

Second, the self-scavenging of $HO^\bullet$ by H_2O_2 in the UV-C/H_2O_2 process is much higher than the self-scavenging of $SO_4^{-\bullet}$ by $S_2O_8^{2-}$ in the UV-C/$S_2O_8^{2-}$ process. $HO^\bullet$ has higher reaction rate constants with H_2O_2 ($k_{HO^\bullet/H_2O_2} = 2.7 \times 10^7\ M^{-1}cm^{-1}$ and $k_{HO^\bullet/HO^\bullet} = 5.5 \times 10^9\ M^{-1}cm^{-1}$ [129]) than $SO_4^{-\bullet}$ with $S_2O_8^{2-}$ ($k_{SO_4^{-\bullet}/S_2O_8^{2-}} = 6.6 \times 10^9\ M^{-1}cm^{-1}$ and $k_{SO_4^{-\bullet}/SO_4^{-\bullet}} = 3.1 \times 10^8\ M^{-1}cm^{-1}$ [130]). According to previous studies [131-133], the main reaction mechanism for aromatic degradation by $HO^\bullet$ considers the addition to C–C, C–S and C–N double bonds and H-abstraction with subsequent hydroxylation, while in the case of $SO_4^{-\bullet}$, electron transfer is dominant.

Considering literature research in article databases, we can claim that this is the first study that worked on CBZ and IBP degradation using MW-based processes. MW based AOPs provide CBZ and IBP degradation at a much faster rate than only MW irradiaton due

to different degradation mechanisms occurring within the system. Degradation rate of CBZ is 5.1×10^{-3} s^{-1}, 145.4×10^{-3} s^{-1} and 635.2×10^{-3} s^{-1} for MW, MW/H_2O_2 and MW/$S_2O_8^{2-}$, respectively. Degradation rate of IBP is 8.9×10^{-3} s^{-1}, 40.4×10^{-3} s^{-1} and 789.8×10^{-3} s^{-1} for MW, MW/H_2O_2 and MW/$S_2O_8^{2-}$, respectively. MW irradiation alone did not degrade CBZ and IBP well due to a lack of oxidants. However, MW combined with PS or H_2O_2 achieved significantly greater removal efficiency than MW only. MW/$S_2O_8^{2-}$ process showed the highest degradation efficiency of CBZ and IBP comperade to other degradation processes.

Previous studies have shown that MW irradiation can reduce the activation energy of $S_2O_8^{2-}$ and H_2O_2, accelerate the decomposition rate of PS and H_2O_2 and the reaction rate, and thereby greatly increase the removal efficiency of organics [134, 135]. Qi et al. [135] also found that the decomposition rate of $S_2O_8^{2-}$ activated by MW radiation increased by 3–4 times compared to the rate achieved when $S_2O_8^{2-}$ was subjected to conventional thermal activation. Therefore, MW irradiation can effectively activate oxidants (H_2O_2 and $S_2O_8^{2-}$) and rapidly remove organics. $HO^{\bullet}$ and $SO_4^{-\bullet}$ coexisted in the MW/$S_2O_8^{2-}$ process, and $SO_4^{-\bullet}$ played a leading role in the degradation of organic matter, but in the MW/H_2O_2 process, only $HO^{\bullet}$ played an important role in the degradation of organic matter, which might be attributed to higher degradation efficiency with persulfate compered to H_2O_2 [136].

The dipolar polarization mechanism is responsible for enhancing the degradation of various pollutants in the systems combining MW and oxidants. This mechanism creates elevated temperature within a shorter span as compared to conventional heating methods, which provokes the increased decomposition of H_2O_2 into $HO^{\bullet}$ [120]. Subsequently, the $HO^{\bullet}$ generated in the system undergoes adduction reaction with the target pollutants and the resulting intermediates. As a result, rapid and improved degradation rates are observed [121].

Previous studies have shown that 140.2 and 195.4 $kJ.mol^{-1}$ of activation energy are needed to break the O-O bond in PS and H_2O_2 [78], respectively, for the generation of $SO_4^{-\bullet}$ and $HO^{\bullet}$. The lower activation energy indicates that $SO_4^{-\bullet}$ is more easily generated in the MW/PS system than is $HO^{\bullet}$ in the MW/H_2O_2 system. Not only that, owing to its instability, some H_2O_2 will decompose into H_2O and O_2, leading to a relatively low utilization efficiency [137]. From Table 5.1, we can observe very low degradation rate by MW/H_2O_2 process compered to MW/$S_2O_8^{2-}$. MW irradiation itself and its heating effect activated PS very well and generated a large amount of radicals to degrade organics. In contrast, H_2O_2 is highly

unstable at high temperature and decomposes into H_2O and O_2, leading to a poor utilization of H_2O_2 and a relatively low concentration of $HO^{\bullet}$ [137].

5.2. Influence of synthetic water matrix factors

Experiments were conducted to investigate the effects of oxidant dosage (H_2O_2 and $S_2O_8^{2-}$), solution pH, HA, NO_2^-, NO_3^-, Cl^-, PO_4^{3-} and SO_4^{2-} on CBZ and IBP degradation efficiencies by UV-C, UV-C/H_2O_2, UV-C/$S_2O_8^{2-}$, US/H_2O_2, MW, MW/H_2O_2 and MW/$S_2O_8^{2-}$ degradation systems. Inorganic anions are ubiquitous in water body, which has important influence on the types of reactive species [88]. The results of the effects were obtained from main effects plots (chapter 4) and response tables (appendix section). Contribution of each factors in the degradation processes also can be seen in ANOVA tables (appendix section). All the effects of the synthetic water matrix factors are summarized in Table 5.2.

Table 5.2. Summary of the synergistic (+) and inhibitory (-) effects of water matrix factors on the CBZ and IBP degradation processes.

Pharmaceutical	Process	HA	NO_2^-	NO_3^-	Cl^-	PO_4^{3-}	SO_4^{2-}
CBZ	UV-C	-	-	+	+	+	+
	UV-C/H_2O_2	+	-	+	-	-	+
	UV-C/$S_2O_8^{2-}$	+	-	+	-	-	+
	US/H_2O_2	+	+	-	+	+	-
	MW	-	-	+	-	+	-
	MW/H_2O_2	-	+	+	-	+	+
	MW/$S_2O_8^{2-}$	-	-	-	+	+	-
IBP	UV-C	+	-	+	-	-	-
	UV-C/H_2O_2	+	-	+	+	-	+
	UV-C/$S_2O_8^{2-}$	+	-	+	-	-	+
	US/H_2O_2	-	-	-	-	+	-
	MW	-	-	-	-	-	+
	MW/H_2O_2	+	+	+	+	+	-
	MW/$S_2O_8^{2-}$	+	-	-	-	-	-

In general terms, in studied AOPs, inorganic ions can: (i) absorb the incident radiation making the process less efficient because less radiation will be available for the activation of H_2O_2 or persulfate (ii) scavenge $HO^{\bullet}$ or $SO_4^{-\bullet}$ reducing the concentration of available radicals for the reaction with target contaminants (iii) produce new types of reactive species. However, the mechanism of each inorganic ion for the degradation of studied pharmaceuticals is not so clear, particularly in the case of microwave-based processes due to lack of literature.

It should be mentioned that each AOPs has its own mechanisms for the generation of active radicals from used oxidants. The presence of inorganic ions can both inhibit and enhance the degradation rate of pharmaceuticals and it depends on type of oxidant and degradation process. One thing to keep in mind is that this study focused on the influence of factors on the conversion of the investigated pharmaceuticals; nevertheless, the effect of factors on removal efficiency might be different, as Kovacic et al. stated [138].

5.2.1. Effect of solution pH

pH is one of the most important parameter that significantly affect the efficiency of AOPs and is always considered for optimization of the water treatment processes [132].

In the case of CBZ degradation by UV-C based processes, pH changes (range of 4–10) in UV-C/H_2O_2 and CBZ_UV-C/$S_2O_8^{2-}$ processes didn't have significant effect on the degradation of CBZ. Vogna et al. and Deng et al. and Liu et al. also observed that CBZ degradation by UV-C/H_2O_2 treatment was not affected by changing the solution pH in the range of 2–8 [30, 139, 140]. Alkaline conditions are favorable for the generation of hydroperoxide anion (HO_2^-) (Eq. (8)) in UV-C/H_2O_2 system. Although hydroperoxide anion can speed up the formation of hydroxyl radicals, it can also act as a scavenger of hydroxyl radicals and cause decomposition of H_2O_2 (Eqs. (5.1)–(5.4)). It is reported that the reaction of hydroxyl radicals with hydroperoxide anion is approximately 100 times faster than its reaction with H_2O_2 [32]. Furthermore, H_2O_2 becomes highly unstable and self-decomposition occurs under alkaline conditions, which makes the H_2O_2 molecules lose its characteristics as an oxidant (Eq. (5.5)).

$$H_2O_2 \longleftrightarrow HO_2^- + H^+ \quad pKa = 11.6 \tag{5.1}$$

$$HO_2^- + H^+ \xrightarrow{h\nu} 2HO^\bullet \tag{5.2}$$

$$HO_2^- + HO^\bullet \rightarrow HO_2^\bullet + OH^- \tag{5.3}$$

$$HO_2^- + H_2O_2 \rightarrow H_2O + O_2 + OH^- \tag{5.4}$$

$$2H_2O_2 \rightarrow 2H_2O + O_2 \tag{5.5}$$

CBZ was most susceptible to photolysis at slightly basic pH. The MW process also enhanced in basic pH condition. The absorbance of CBZ at 254 nm is relatively low. Thus, UV-C photolysis of this compound was expected to be relatively low. The slightly higher molar attenuation coefficients measured at pH 7 and 9, in comparison to that measured at pH 3, indicate that CBZ more readily absorbs photons in its dissociated form. Quantum yield value (0.06) obtained for CBZ confirm the stability of this compound under UV-C irradiation. Starling et al. observed the slightly higher decay of CBZ observed at pH 9 in comparison to that at pH 3 or 7 is also in agreement with the molar absorptivity values [141], which is consistent with our findings.

In the case of IBP, acidic condition enhanced most of the degradation processes, except with MW/PS. In the UV-C/PS pH didn't have significant effect on the IBP degradation. The pKa value of IBP is 4.9. Above this value ionic IBP is the predominant specie. On the other hand, at lower values, IBP is principally found in its molecular form [92]. Therefore, the IBP molecular species seem to be more affected by photodegradation than its ionic species.

Thus, for UV-C based processes, pH variation may exert its influence from the following two aspects: (1) changing the dissociation forms of peroxide and thus altering their photolysis quantum yields [142]; (2) affecting the existing species of organic molecules (protonated or deprotonated), which show different reactivity with radicals [143] and ability of light absorption [80].

It should be noted, that oxidant dosage was always the main and significant factor in most of the degradation processes, but, in the US/H_2O_2 process (Figure 4.9 and 4.10), CBZ and IBP degradation depends strongly on the pH more than on hydrogen peroxide dosage. In the US process, the pH indicates the hydrophobic or hydrophilic nature of the target compound behavior, depending on whether the structure in which the pollutant is found is ionic or molecular. This property will allow the position to be determined in which the contaminant is housed in the US process, i.e., in the bulk solution (hydrophilic, non-volatile compounds), in the bubble–water interface (semi-volatile hydrophobic compounds), or within the cavitation bubble (hydrophobic, volatile compounds) [84]. In the studied US/H_2O_2 process, both CBZ and IBP had higher degradation kinetics in acidic condition. As previously stated, CBZ and IBP degradation happen mostly at the interface of bubble-bulk solution due to their hydrophobicity and non-volatility. When the pH of the solution was below pKa, the hydrophobicity of the drugs and, therefore, their position in the bubble–water interface is improved, favoring a rapid reaction with the $HO^{\bullet}$ formed from H_2O_2 and also during the implosion of the cavitation bubbles [83]. Also, Thanekar et al. have also reported that maximum degradation of CBZ by US/H_2O_2 occurred at low pH [144]. They stated that degradation of CBZ with US/H_2O_2 processes enhanced in acidic pH due to generation of $HO^{\bullet}$ is favored as its oxidation potential is higher under the acidic conditions. In addition, Mendez-Arriaga et al. also stated that IBP is a non-volatile compound and the region of degradation would be at the exterior of the cavitation bubbles. Thus, the reaction between the radicals generated and IBP would be enhanced if its hydrophobicity is favored. IBP has a superior hydrophobic character when its structure is in the molecular state which occurs at a pH value lower than pKa. Under this condition, IBP is accumulated in the interface of the cavitation bubbles and highest degradation rate is reached [92].

Both CBZ and IBP degradation by MW/H_2O_2 enhanced in acidic condition. These results indicate that an alkaline environment is not beneficial to organics degradation in the MW/H_2O_2 system, which is because H_2O_2 is decomposed into HO_2^- in an alkaline environment, and such condition may decrease $HO^{\bullet}$ production, as mentioned before. CBZ degradation by MW/$S_2O_8^{2-}$ also was enhanced in acidic pH, but IBP is the opposite. This variation may be because $SO_4^{-\bullet}$ and $HO^{\bullet}$ are the main radicals in the MW/$S_2O_8^{2-}$ system, but $SO_4^{-\bullet}$ could react with HO^- and generate $HO^{\bullet}$ in alkaline conditions, thus starting a series of side reactions between $HO^{\bullet}$ and HO^-. Wang et al. stated that the MW/$S_2O_8^{2-}$ system

performed well in degrading organics in both acidic and alkaline conditions. However, the MW/H_2O_2 system degraded organics relatively well only in an acidic or neutral environment [137].

5.2.2. Effect of oxidant concentration

In this study, two oxidants, hydrogen peroxide and sodium persulfate, were used. The oxidants had concentrations of 0.5 mM and 10 mM. In all studied degradation processes, the highest level of oxidant was enhanced the degradation rate of the processes, except degradation of IBP with MW/$S_2O_8^{2-}$ process. This phenomena can be due to high temperature. Temperature plays a major role in MW-assisted degradation process with persulfate because at extremely high temperature the radical itself could act as a scavenger (Eqs. (5.6) and (5.7)) [112].

$$SO_4^{-\bullet} + S_2O_8^{2-} \rightarrow SO_4^{2-} + S_2O_8^{-\bullet} \quad (5.6)$$

$$SO_4^{-\bullet} + SO_4^{-\bullet} \rightarrow S_2O_8^{2-} \quad (5.7)$$

It should be emphasized that, with the exception of the US-based process, the contribution of the oxidant was the highest among the other factors. In US/H_2O_2 the observed trend is attributed to enhanced generation of hydroxyl radicals due to the dissociation of H_2O_2 in presence of US. Also, US generates turbulence leading to elimination of mass transfer resistances for the chemical oxidation of pollutant [145]. The effects of H_2O_2 were dependent on the properties of the target compounds. In particular, the addition of H_2O_2 had a significant influence on the degradation of non-volatile and hydrophilic compounds [146]. In our study both CBZ and IBP are non-volatile compound but they have hydrophobic character [92, 147] and due to this, as can be seen in table 4.17 and 4.19 the contribution of H_2O_2 for CBZ and IBP is low, just 0.88% and 8.60% respectively.

5.2.3. Effect of humic acid

Our findings suggest that humic acid presence may result in either inhibitory or synergistic effects on the degradation rate of pharmaceuticals. The presence of humic acid

may hinder the photodegradation of target compounds by either (i) absorbing the available light [148] or (ii) scavenging the free radicals produced [149]. Another explanation could be (iii) the reformation of the parent compounds. According to Canonica et al., the inhibitory effect of humic acid could be due to the mechanism below (Eqs. (5.8)-(5.9)) [150]:

$$\text{Step 1: } \text{radical}^{\bullet} + \text{MP} \rightarrow \text{radical}^{-} + \text{MP}^{+\bullet} \quad (5.8)$$

$$\text{Step 2: } \text{MP}^{+\bullet} + \text{HA} \rightarrow \text{MP} + \text{HA}^{+\bullet} \quad (5.9)$$

The apparent inhibition was caused by reforming the parent compound (from the radical cation form of the organic compound, $MP^{+\bullet}$) and producing an oxidised humic acid radical $HA^{+\bullet}$.

On the other hand, the synergistic effect of NOM might be due to the formation of radical species (of organic origin) that are capable to degrade targeted pollutants, and in such manner, to contribute to the overall degradation rate [52]. Humic acid, upon UV irradiation, produces chromophoric HA that further reacts with oxygen of the system and forms stable HA and singlet oxygen radicals. These singlet oxygen radicals react with hydride ion (H^{-}) to form hydrogen peroxide that split to generate hydroxyl radicals [68]. In the system containing HA, H_2O_2 was produced through the reduction of oxygen by intermediates formed from excited HA (Eqs. (5.10)–(5.12)) [151]. Hence, production of H_2O_2 via HA may be the reason of synergistic effect of HA.

$$\text{HA} \xrightarrow{h\nu} \text{HA}^{*} \quad (5.10)$$

$$\text{HA}^{*} + \text{O}_2 \rightarrow \text{Products} + \text{O}_2^{-\bullet} / \text{HO}_2^{\bullet} \quad (5.11)$$

$$\text{O}_2^{-\bullet} / \text{HO}_2^{\bullet} \rightarrow \text{H}_2\text{O}_2 \quad (5.12)$$

CBZ and IBP degradation by UV-C based processes was enhanced in presence of humic acid except degradation of CBZ by UV-C photolysis. Markic et al. investigated on influence of process parameters on the effectiveness of photooxidative treatment of pharmaceuticals and obtained that in the case of UV-C/H_2O_2, slight synergistic effects can be observed for CBZ in the presence of humic acid [125]. The presence of humic acid had inhibitory effect on CBZ degradation by UV-C photolysis. Canonica et al. and Wang et al.

also got same results [150, 152]. CBZ degradation by US/H_2O_2 was enhanced in presence of humic acid, but IBP is the opposite. Presence of humic acid had inhibitory effect on CBZ degradation by MW based processes, but in the case of IBP, only MW without oxidant had inhibitory effect.

5.2.4. Effect of nitrite (NO_2^-)

The presence of nitrite ions inhibited the constant rate of degradation in the majority of the studied degradation processes. Nitrite has high reactivity with active radicals to form nitrite radicals and scavenge the main radicals ($HO^\bullet$ or $SO_4^{-\bullet}$) (Eqs. (5.13)-(5.14)) [153]. No direct proof demonstrates the reaction between nitrite and sulfate radicals, but the occurrence of nitrite radicals during the degradation of phenolic compounds by sulfate radicals was suggested [154].

$$NO_2^- + OH^\bullet \rightarrow NO_2^\bullet + OH^- \quad (5.13)$$

$$NO_2^- + SO_4^{-\bullet} \rightarrow NO_2^\bullet + SO_4^{2-} \quad (5.14)$$

Due to the higher reaction rate of NO_2^- with hydroxyl radicals than other inorganic anions, NO_2^- usually exhibits stronger inhibition than other inorganic anions [155].

On the other hand, for both studied pharmaceuticals, the presence of nitrite ions showed a synergistic impact when using the MW/H_2O_2 process and also for CBZ in US/H_2O_2 process, which might be attributed to the ability of nitrite ions that can react with H_2O_2 to produce peroxynitrates (Eq. (5.15)), which can selectively degrade organic pollutants [156].

$$H_2O_2 + NO_2^- \rightarrow OONO^\bullet + H_2O \quad (5.15)$$

5.2.5. Effect of nitrate (NO_3^-)

In the most case of the studied degradation processes, nitrate ions had synergistic effect on degradation constant rate. Degradation of two studied pharmaceuticals by UV-C based processes was increased in the presence of nitrate ions. Some literature can be found

regarding the influence of the variation of NO_3^- concentration on photodegradation efficiency. Wang et al. investigated the effect of the variation of the NO_3^- concentration on the photocatalytic process applied to a secondary effluent of an urban wastewater treatment plant [157]. They showed that the higher the NO_3^- concentration, the higher will be the photocatalytic activity. The removal of IBP and others emerging pollutants by natural sunlight was studied by Koumaki et al. [158]. They observed that the removal efficiency improved due to the presence of NO_3^- and increased with increasing NO_3^- concentrations. Chianese et al. investigated on IBP degradation in aqueous solution by using UV light [159]. Nitrate was added as $NaNO_3$, a concentration of 10 mg L^{-1} was considered and after one hour of treatment, an increase in IBP removal was observed with the presence of NO_3^-, passing from 66%, without nitrate, to 75%, with nitrate. Koumaki et al. investigated on degradation of emerging contaminants (eight pharmaceuticals that IBP was included too) from water under natural sunlight, the removal of most of the compounds increased with the increase of NO_3^-. The removal percentage of IBP in the absence of nitrate was 12% and after 15 h of irradiation, it increased to 40%, which was observed in the presence of 10 mg L^{-1} of NO_3^- [158].

The most likely reason that nitrate enhanced the degradation kinetics is that nitrate acts as a sensitizer to promote the photoreaction. Nitrate photolysis produces $HO^\bullet$ radicals according to Equations (5.16) and (5.17) [160]. Thus, the obtained results were mainly due to the hydroxyl radicals generated through the irradiation of nitrate in the solution.

It is interesting to note that recently the UV/nitrate process has received significant attention for degradation of different trace organic contaminants as an AOP process [161].

$$NO_3^- \xrightarrow{h\nu} NO_2^\bullet + O^{-\bullet} \quad (5.16)$$

$$O^{-\bullet} + H_2O \rightarrow OH^\bullet + OH^- \quad (5.17)$$

Interestingly, previous study showed that high concentration of nitrate ions increased the removal efficiency of organic pollutant, but did not affect the degradation rate of organic pollutant [162]. The reason needs to be further investigated.

The presence of nitrate in US/H_2O_2 process decreased the degradation rate of both studied pharmaceuticals. The scavenging of $HO^{\bullet}$ radicals with nitrate ions could be the reason (Eq. (5.18)). This is in agreement with Nikitenko et al. study that discovered scavenging of $HO^{\bullet}$ radicals formed during H_2O sonolysis with nitrate-ions was studied in HNO_3/$NaNO_3$ mixture [163]. It also should be mentioned that the reduction potential of nitrate radicals was slightly lower than hydroxyl radicals [164].

$$NO_3^- + H^+ + HO^{\bullet} \rightarrow NO_3^{\bullet} + H_2O \quad (5.18)$$

In addition, in the case of MW/$S_2O_8^{2-}$ degradation process for both pharmaceuticals and MW process for IBP degradation, the presence of nitrate had inhibitory effect on degradation rate. The mechanism is not clear, but it might be attributed to ability of nitrate ions that can react with persulfate radicals to form nitrate radicals that have lower degradation potential (Eq. (5.19)).

$$SO_4^{-\bullet} + NO_3^- \rightarrow NO_3^{\bullet} + SO_4^{2-} \quad (5.19)$$

Nitrate ions cannot react with H_2O_2 and $S_2O_8^{2-}$. Moreover, nitrate ions cannot cause the variation of solution pH. It has thus no effect on the stability of oxidants [165].

5.2.6. Effect of chloride (Cl^-)

Another ion that plays a significant role is chloride, which can absorb radiation at 254 nm and can be photolyzed forming $HO^{\bullet}$ radicals [166]. Also, it can scavenge photons and $HO^{\bullet}$ radicals making the AOP less efficient [167]. In addition, since $Cl^{\bullet}$ is formed it can react with the organic substrate forming toxic chlorinated byproducts. Figure 5.1 shows the effect of chloride ion on the reactive species produced during AOPs [165].

In the case of CBZ, presence of Cl^- had different effects on CBZ degradation by the studied degradation processes. The presence of Cl^- can both inhibit and enhance the CBZ degradation rate and it depends on type of oxidant and degradation process. In the case of UV-C based processes, CBZ degradation by both UV-C/H_2O_2 and UV-C/$S_2O_8^{2-}$ will be decreased in presence of Cl^-. However, the decrease in UV-C/H_2O_2 is significant, but the decrease in UV-C/$S_2O_8^{2-}$ is minor and negligible (0.08% contribution), in agreement with the

findings of Deng et al. and Liu et al.[30, 140]. Deng et al. discovered that, adding 50 mM Cl^- into the oxidation system, the degradation rate decreases from 0.0363 to 0.0233 min^{-1} and from 0.0483 to 0.0443 min^{-1} in UV-C/H_2O_2 and UV-C/$S_2O_8^{2-}$ system, respectively [30].

Hydroxyl radicals could react with Cl^- to initially form hypochlorous acid radicals ($ClOH^{-\bullet}$) (Eq. (5.20)), which can be quickly decomposed to hydroxyl radicals and chloride ion (Eq. (5.21)) [168]. Moreover, under acid conditions, $ClOH^{-\bullet}$ can further react with hydrogen ions to form $Cl^\bullet$ (Eq. (5.22)). Of note, the pKa value for deprotonation is 7.2, which is a critical value in affecting the concentrations of hydroxyl radicals in the solution [166]. When the pH is greater than 7.2, $ClOH^{-\bullet}$ becomes the main species, and conversely $Cl^\bullet$ and $Cl_2^{-\bullet}$ become the dominant ones when the pH is less than 7.2. A similar situation occurs in UV-C/$S_2O_8^{2-}$ system. A part of sulfate radicals can also react with Cl^- to generate $Cl^\bullet$ and $Cl_2^{-\bullet}$ (Eqs. (5.23)–(5.26)). It is noted that the redox potentials of the Cl^- containing radicals are much lower than sulfate radicals [169], which causes the slowdown of degradation rate in UV-C/$S_2O_8^{2-}$ and UV/H_2O_2 systems. Compared with UV-C/H_2O_2 system, the degradation rate of CBZ does not decline with addition of the lower dosage of Cl^- (<10 mM) in UV-C/$S_2O_8^{2-}$ system. Hydroxyl radicals possess one order of magnitude higher reaction rate than sulfate radicals when reaction with chlorides (Eqs. (5.20) and (5.23)). Hence, the low chloride concentration will not have influence on CBZ decomposition at the lower Cl^- dosage. Sulfate radical has lower reaction rate with chloride ion, compared to hydroxyl radicals.

$$HO^\bullet + Cl^- \rightarrow ClOH^{-\bullet} \qquad k = 4.3 \times 10^9\ M^{-1}s^{-1} \qquad (5.20)$$

$$ClOH^{-\bullet} \rightarrow HO^\bullet + Cl^- \qquad k = 6.1 \times 10^9\ M^{-1}s^{-1} \qquad (5.21)$$

$$ClOH^{-\bullet} + H^+ \rightarrow Cl^\bullet + H_2O \qquad k = 2.6 \times 10^{10}\ M^{-1}s^{-1} \qquad (5.22)$$

$$SO_4^{-\bullet} + Cl^- \rightarrow Cl^\bullet + SO_4^{2-} \qquad k = 3.1 \times 10^8\ M^{-1}s^{-1} \qquad (5.23)$$

$$Cl^\bullet + Cl^- \rightarrow Cl_2^{-\bullet} \qquad k = 7.8 \times 10^9\ M^{-1}s^{-1} \qquad (5.24)$$

$$Cl_2^{-\bullet} + Cl_2^{-\bullet} \rightarrow Cl_2 + 2Cl^- \qquad k = 9 \times 10^8\ M^{-1}s^{-1} \qquad (5.25)$$

$$Cl^\bullet + Cl^\bullet \rightarrow Cl_2 \qquad k = 1 \times 10^8\ M^{-1}s^{-1} \qquad (5.26)$$

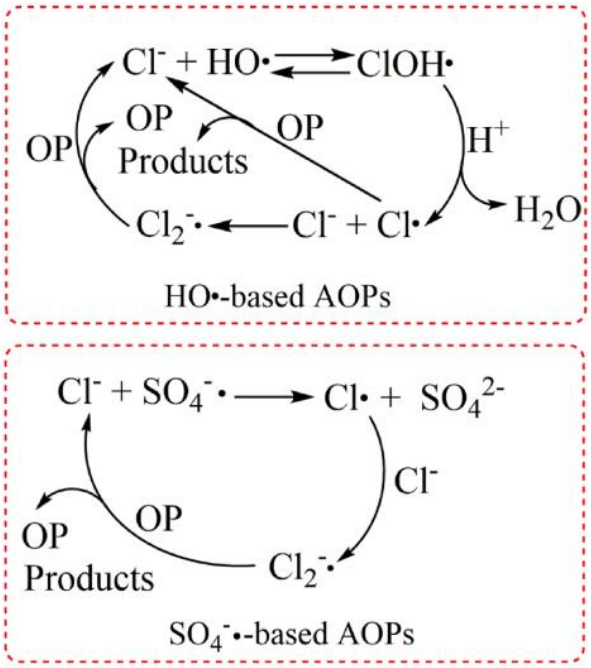

Figure 5.1. Effect of chloride ion on the reactive species produced during AOPs. OP means organic pollutants. (taken from [165])

In contrast, degradation rate of IBP by UV-C/H_2O_2 minor enhancement (0.18% contribution) in the presence of chloride ions which might be attributed to the formation of chloride radicals that helped in the degradation. We observed different effects in CBZ and IBP degradation by UV-C/H_2O_2 in the presence of chloride. It might be attributed to higher constant rate between IBP and chloride radical than CBZ and chloride radical. On the other hand, degradation of IBP by UV-C/$S_2O_8^{2-}$ decreased due to reasons that already are mentioned for CBZ degradation by UV-C/$S_2O_8^{2-}$. The scavenging of $SO_4^{-\bullet}$ by Cl^- has already been studied by George et al, $Cl_2^{-\bullet}$ was found to be the main secondary radical in UV-C/$S_2O_8^{2-}$ process [170]. UV-C photolysis of CBZ and IBP in presence of chloride ions had positive and negative effects, respectively.

In degradation of CBZ by US/H_2O_2, chloride had the highest effect among other inorganic ions and the presence of it significantly promoted CBZ degradation due to generation of additional radicals such as $Cl^\bullet$ and $Cl_2^{-\bullet}$ (Eqs. (5.20), (5.22) and (5.24)). Our finding are in agreement with Rao et al. [84]. On the other hand, degradation of IBP by US/H_2O_2 in presence of chloride was negligible (0.06% contribution).

In MW based processes, the presence of chloride mostly had inhibitory effect and the mechanism and reason for that are not clear yet.

Chloride ion cannot react with H_2O_2 and $S_2O_8^{2-}$. Thus, the presence of chloride ion has no effect on the stability of H_2O_2 and $S_2O_8^{2-}$ [165].

5.2.7. Effect of phosphate (PO_4^{3-})

Phosphate ions had either inhibitory or synergistic effects on the degradation rate of CBZ and IBP by the studied degradation processes. The exact mechanism is not clear, but the possible mechanism of phosphate ion presence in AOPs is discussed below.

Phosphate ions can react with hydroxyl radicals. The formed radicals varied with the existing form of phosphate ions in solution [165]. Phosphate ions can change the solution pH. The existence form of phosphate ions depends on the solution pH. Hydrogen phosphate ions are the main form with pH lower than 11. Phosphate ions dominant when pH is higher than 12 [171]. In our study the studied pH rang was 4-10. Hydrogen phosphate ions can react with hydroxyl radicals to form hydrogen phosphate ions radicals (Eq. (5.27)) [172]. Due to the lower reaction rate of phosphate derived radicals with organic compounds, compared to hydroxyl radicals, phosphate ions usually presented inhibition phenomenon [165].

$$HPO_4^{2-} + OH^{\bullet} \rightarrow HPO_4^{-\bullet} + OH^- \qquad k = 8 \times 10^5\ M^{-1}s^{-1} \qquad (5.27)$$

Hydrogen phosphate can also react with sulfate radicals to produce hydrogen phosphate radicals (Eq. (5.28)) [172]. Nevertheless, the presence of phosphate ions can lead to the change of reactive species. Phosphate ions and hydrogen phosphate ions have no effect on the stability of H_2O_2 and $S_2O_8^{2-}$ [165]. Effects of different form of phosphate ions on the reactive species produced during AOPs are presented in Figure 5.2.

$$HPO_4^{2-} + SO_4^{-\bullet} \rightarrow SO_4^{2-} + HPO_4^{-\bullet} \qquad k = 1.2 \times 10^6\ M^{-1}s^{-1} \qquad (5.28)$$

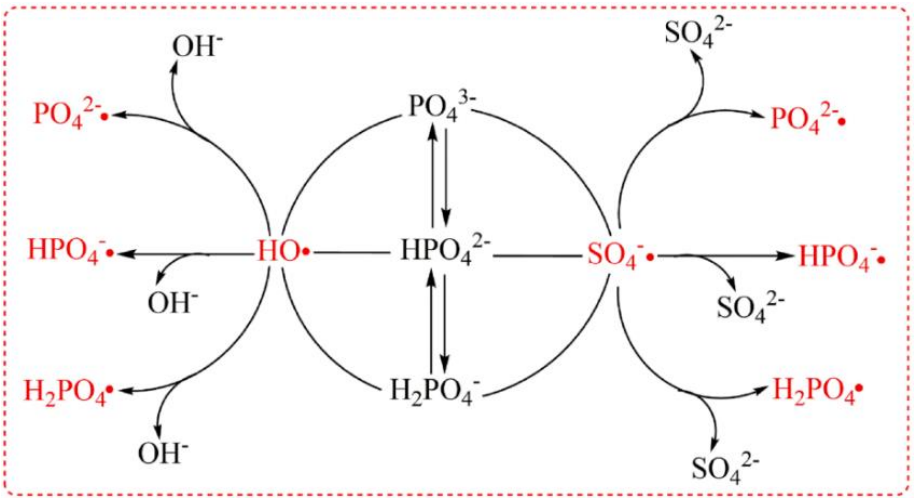

Figure 5.2. Effects of phosphate, hydrogen phosphate and dihydrogen phosphate on the reactive species produced during AOPs (taken from [165]).

5.2.8. Effect of sulfate (SO_4^{2-})

Sulfate ions had either inhibitory or synergistic effects on the degradation rate of CBZ and IBP by the studied degradation processes. The exact mechanism is not clear, but the possible mechanism of sulfate ion presence in AOPs is discussed below.

Sulfate ions can react with hydroxyl radicals to produce sulfate radicals (Eq. (5.29)) [173]. Sulfate radicals have similar or even higher reduction potential (2.5 ~ 3.1 V) than hydroxyl radicals [78]. But for some organic pollutants, hydroxyl radicals showed higher reaction rate than sulfate radicals [174], which explained the slight inhibition phenomenon in the presence of sulfate ions.

$$SO_4^{2-} + HO^{\bullet} \rightarrow HO^{-} + SO_4^{-\bullet} \qquad (5.29)$$

Sulfate ions cannot react with sulfate radicals, but the inhibition phenomenon on the degradation of organic pollutants can be found in the presence of sulfate radicals [175]. This was due to the effect of sulfate ions on the reduction potential of sulfate radicals [175]. The high concentration of sulfate ions can result in the decrease of sulfate radicals' reduction potential based on the Nernst Equation [165].

It is important to mention that sulfate ions have no effect on the stability of oxidant because sulfate ions cannot react with H_2O_2 and $S_2O_8^{2-}$, and change the solution pH [165].

Kwon et al discovered that sulfate has no significant inhibitory effect on the IBP removal in either the UV/PS or the UV/H_2O_2 process [176].

In contrast, Duca et al. stated another theory, i.e. sulfate does not react with HO radicals, and for this reason, it cannot interfere with the degradation rate of pharmaceuticals as an HO scavenger. In addition, the molar absorption coefficient is negligible at 254 nm, and this is why the addition of sulfate has no effect on the UV-C based processes because it cannot act as an $HO^{\bullet}$ scavenger or as an inner filter [177].

5.3. Biodegradability of UV-C based processes

The biodegradability of the solution prior to and during the treatments was expressed as the BOD_5/COD ratio. It is commonly accepted that wastewater with BOD_5/COD < 0.3 are not biodegradable; those with 0.3 < BOD_5/COD < 0.4 are partially biodegradable; and those with BOD_5/COD > 0.4 are biodegradable [64].

The initial BOD_5 and COD values of the CBZ solution were 5.15 and 24.4 mg O_2 /L, respectively, giving a BOD_5/COD of 0.21. In the case of IBP solution, the initial BOD_5 and COD values were 7.24 and 27.8 mg O_2 /L, respectively, giving a BOD_5/COD of 0.26. These values indicating that CBZ and IBP are non-biodegradable and therefore not suited for biological treatment.

The biodegradability profile of CBZ and IBP recorded during 90 min UV-C treatment presented in Figures 5.3 and 5.4, respectively. In the case of IBP degradation by UV-C process, an increase in the BOD_5/COD ratio from 0.12 to 0.44 was achieved and it seems to become biodegradable and as a result, formation of its byproducts is more susceptible to biodegradation. However, in the rest of the processes, oxidation intermediates were less readily biodegradable than the pharmaceutical itself as shown by the decreased BOD_5/COD values. Taking into account that CBZ and IBP was continuously removed during studied period of treatment, the trend of their biodegradability can be assigned to the nature of formed intermediates. BOD_5/COD values of UV-C based processes for CBZ and IBP are presented in Table 5.3.

Table 5.3. BOD_5/COD values of UV-C based processes for CBZ and IBP

Process	UV-C					UV-C/H_2O_2					UV-C/$S_2O_8^{2-}$				
Time, min	0	15	30	60	90	0	15	30	60	90	0	15	30	60	90
CBZ	0.16	0.12	0.09	0.06	0.09	0.13	0.12	0.11	0.12	0.13	0.04	0.04	0.03	0.04	0
IBP	0.12	0.20	0.22	0.23	0.44	0.11	0.11	0.1	0.12	0.12	0.02	0	0.01	0	0

It is important to note that the use of a synthetic water matrix resulted in lower BOD_5/COD levels than the original values obtained with only pharmaceutical solutions in Milli-Q water, by increasing the COD values, due to the fact that different reactive species formed from inorganic ions have different degradation mechanisms for organic pollutants [178].

In the case of CBZ degradation by UV-C, in period from t = 0 min to t = 60 min presumably quite non-biodegradable intermediates are formed, which were then transformed to more biodegradable, as reflected in the increase in BOD_5/COD ratio in period between t = 60 min to t = 90 min (Fig. 5.3). In the case of CBZ degradation by UV-C/$S_2O_8^{2-}$, in period from t = 0 min to t = 60 min biodegradability was almost invariant. However, biodegradability again decreased in further treatment period, presumably as a consequence of increase of organic content (Fig. 5.3). As can be seen, the biodegradability of IBP by UV-C AOPs was almost invariant and hardly changed (Fig. 5.4).

In the hydroxyl radicals-induced system, chloride ion can react with hydroxyl radicals to produce chlorine radicals that have higher selectivity than hydroxyl radicals [179]. Chlorine radicals can degrade organic compounds by hydrogen abstraction, one-electron oxidation and chlorine adduct [168, 180], which could result in the production of chlorinated products. Similar phenomenon was observed in the sulfate radicals-dominated system. Sulfate radicals can also react with chloride ion to produce chlorine radicals that react with organic pollutant to result in the formation of several chlorinated products via the above-described ways [181, 182]. The presence of inorganic anions could induce the variation of degradation products. Due to the different properties of degradation intermediate products, their biodegradability may vary and furthermore may be the cause of a decrease in biodegradability.

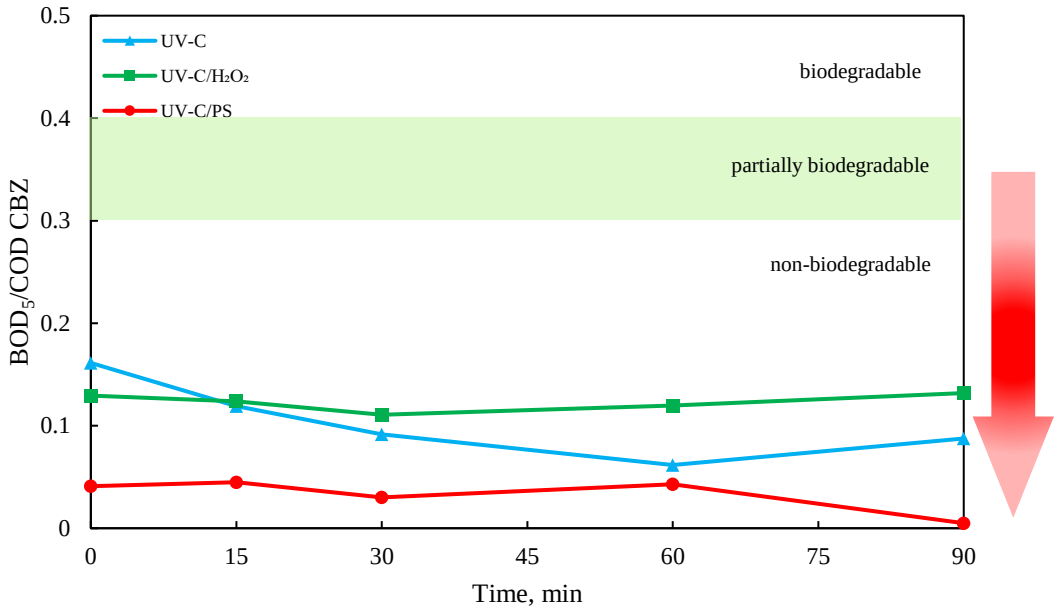

Figure 5.3. Changes in CBZ biodegradability during the performed UV-C-based processes.

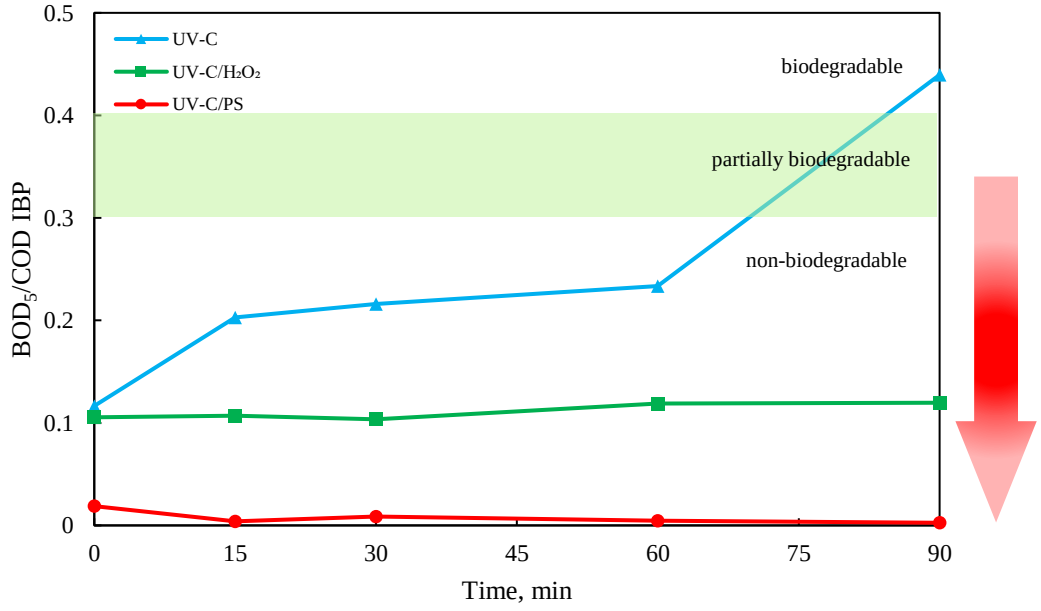

Figure 5.4. Changes in IBP biodegradability during the performed UV-C-based processes.

5.4. Degradation products of UV-C based processes

For identifying byproducts, samples from kinetic experiments with a reaction duration of 60 seconds were analyzed to identify the byproducts. Intermediates were identified by comparing their MS data with those previously reported in the literature.

One CBZ byproduct for UV-C, two for UV-C/H_2O_2, and five for UV-C/$S_2O_8^{2-}$ has been found. The number of discovered byproducts might be related to the kinetics of each process. The accurate mass spectrum of CBZ showed a protonated molecular ion $[M + H]^+$ at m/z 237, which is attributed to the parent compound of CBZ with the formula of $C_{15}H_{12}N_2O$ (M = 236.27). The one CBZ byproduct with UV-C process had the $[M - 56]^+$ signal at m/z 181 with the detection time of 2.1 min corresponds to the intermediate Acridine that is in agreement with literature findings [183, 184]. The following are the CBZ intermediates identified by the UV-C/H_2O_2 process. The $[M + 16]^+$ signal at m/z 253 with the detection time of 2.8 min corresponds to the intermediate 10, 11-epoxycarbamazepine. The $[M + 14]^+$ signal at m/z 251 with the detection time of 2.3 min were detected. These two byproducts were also discovered during the UV-C/$S_2O_8^{2-}$ process. The following are the CBZ intermediates identified by the UV-C/$S_2O_8^{2-}$ process. The $[M + 16]^+$ signal at m/z 253 with the detection time of 2.1 min corresponds to the intermediate 10, 11-epoxycarbamazepine arising from $SO_4^{-\bullet}$ directly attacked at the olefinic double bond on the heterocyclic ring [185]. During UV-C/$S_2O_8^{2-}$ process, $SO_4^{-\bullet}$ attack of CBZ is the predominant pathway and CBZ electron-transfer is the major oxidation mechanism. Thus, under the attack of $SO_4^{-\bullet}$, CBZ was preferentially transformed to CBZ radical ($CBZ^{+\bullet}$), which reacts quickly with H_2O by way of hydroxyl abstraction or addition reaction to generate (hydroxyl)CBZ radical ((OH)CBZ) with m/z 253 [135]. The $[M - 56]^+$ signal at m/z 181 with the detection time of 2.6 min corresponds to the intermediate Acridine. The $[M + 14]^+$ signal at m/z 251 with the detection time of 2.8 min were detected. The $[M - 44]^+$ signal at m/z 193 with the detection time of 7.8 min corresponds to the intermediate Iminostilbene with chemical formula $C_{14}H_{11}N$. All identified byproducts are consistent with previous studies [28, 183, 185, 186]. New signal was detected from CBZ degradation by UV-C/$S_2O_8^{2-}$, the $[M + 34]^+$ signal at m/z 271 with the detection time of 2.12 min. There are two possibility, (i) from Cl attack (atomic mass Cl=35 u) or attaching 2 of -HO molecules (35 u).

Acridine is noted as an air and water pollutant with mutagenic and carcinogenic activity [187]. The formation of recalcitrant by-products of higher toxicity suggests that direct UV photolysis is not a suitable method for treatment of CBZ [184]. We also discovered acridine as a byproduct of UV/PS, suggesting that UV/PS is not a promising treatment option for CBZ. It should be noted that these byproducts were discovered after only 60 seconds of UV-C exposure. Proposed degradation byproducts of CBZ with UV-C based processes are presented in Figure 5.5.

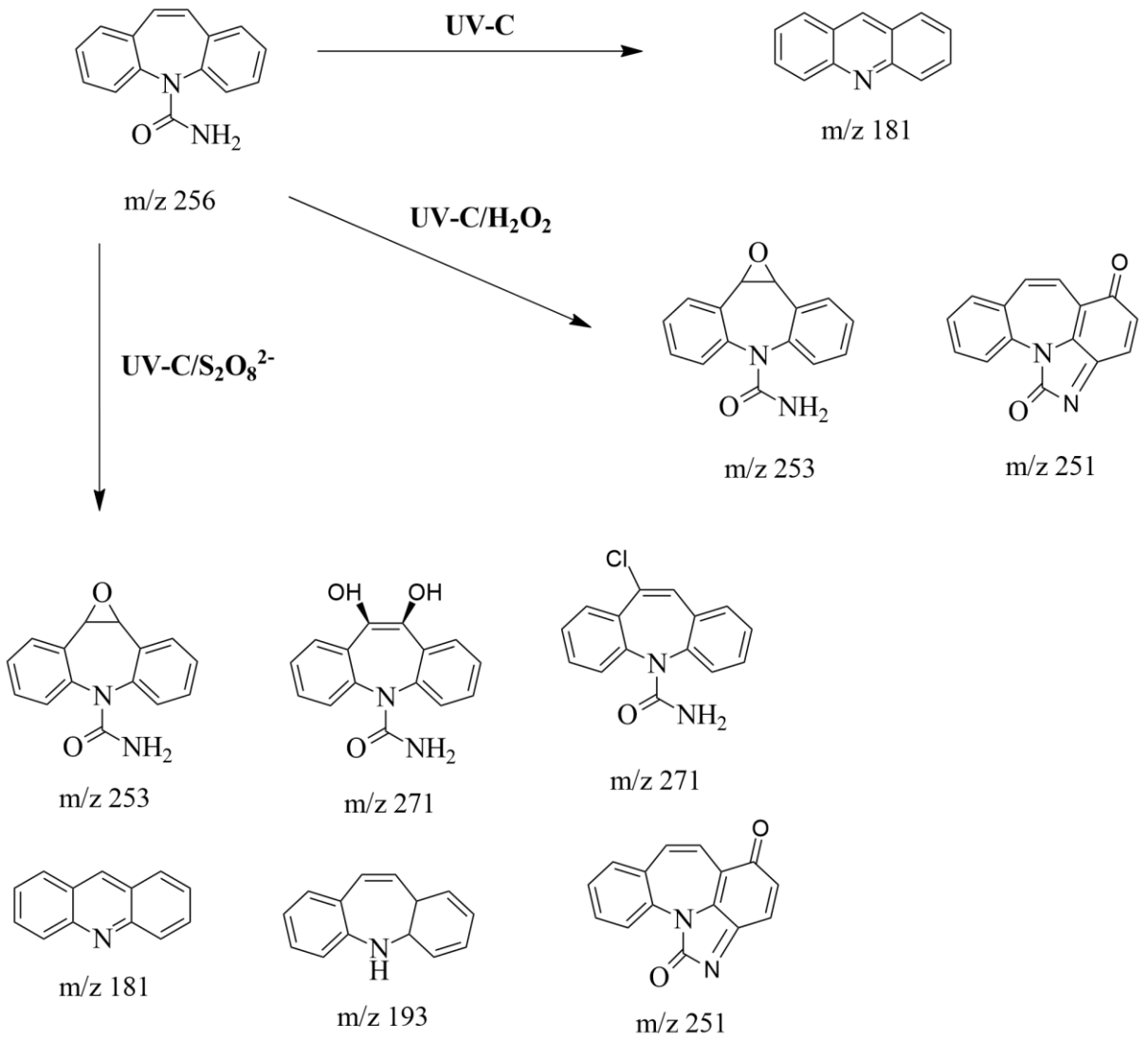

Figure 5.5. Proposed degradation byproducts of CBZ with UV-C based processes.

6. Conclusion

The kinetic degradation of CBZ by studied AOPs was compered and the order is: MW/$S_2O_8^{2-}$ > MW/H_2O_2 > UV-C/$S_2O_8^{2-}$ > UV-C/H_2O_2 > MW > UV-C > US/H_2O_2 and for IBP the order is: MW/$S_2O_8^{2-}$ > UV-C/$S_2O_8^{2-}$ > MW/H_2O_2 > UV-C/H_2O_2 > MW > UV-C > US/H_2O_2. MW/$S_2O_8^{2-}$ process had the highest conversion of both CBZ and IBP after 10 min of reaction.

The used Taguchi method had great and significant results and indicated the effect of studied factors on degradation processes that, in most cases, were in agreement with previous literature findings, as well as required fewer experiments, time, and costs. Since H_2O_2 is more effective under acidic pH levels, combining AOPs with persulfate could be a wise option for water treatment around neutral pH. In all studied degradation processes, the highest level of oxidant (10 mM) enhanced the degradation rate of the processes, except degradation of IBP with MW/$S_2O_8^{2-}$ process due to scavenging effect at extremely high temperatures. Humic acid and inorganic ions could result in either inhibitory or synergistic effects on the degradation rate of pharmaceuticals. However, the presence of nitrite ions inhibited the constant rate of degradation in the majority of the studied degradation processes and on the other hand, in the majority of the studied degradation processes, nitrate ions had synergistic effect.

Furthermore, the biodegradability of CBZ and IBP through UV-C based processes was investigated and only IBP degradation by UV-C process had an increase in the BOD_5/COD ratio and it became biodegradable and as a result, the formation of its byproducts was more susceptible to biodegradation. The rest of the degradation processes had non-biodegradable byproducts and the BOD_5/COD ratio was almost invariant and hardly changed.

References

1. Supply, W.U.J.W. and S.M. Programme, *Progress on drinking water and sanitation: 2014 update*. 2014: World Health Organization.

2. Luo, Y., et al., *A review on the occurrence of micropollutants in the aquatic environment and their fate and removal during wastewater treatment.* Science of The Total Environment, 2014. 473-474: p. 619-641.

3. Oller, I., S. Malato, and J.A. Sánchez-Pérez, *Combination of Advanced Oxidation Processes and biological treatments for wastewater decontamination--a review.* Sci Total Environ, 2011. 409(20): p. 4141-66.

4. Santos, L.H.M.L.M., et al., *Ecotoxicological aspects related to the presence of pharmaceuticals in the aquatic environment.* Journal of Hazardous Materials, 2010. 175(1): p. 45-95.

5. Gros, M., et al., *Removal of pharmaceuticals during wastewater treatment and environmental risk assessment using hazard indexes.* Environment International, 2010. 36(1): p. 15-26.

6. Jelic, A., et al., *Occurrence, partition and removal of pharmaceuticals in sewage water and sludge during wastewater treatment.* Water Research, 2011. 45(3): p. 1165-1176.

7. de Witte, B., et al., *Advanced Oxidation of Pharmaceuticals: Chemical Analysis and Biological Assessment of Degradation Products.* Critical Reviews in Environmental Science and Technology, 2011. 41(3): p. 215-242.

8. Zhang, N., et al., *Photodegradation of diclofenac in seawater by simulated sunlight irradiation: The comprehensive effect of nitrate, Fe (III) and chloride.* Marine pollution bulletin, 2017. 117(1-2): p. 386-391.

9. Zúñiga-Benítez, H., J. Soltan, and G. Peñuela, *Application of ultrasound for degradation of benzophenone-3 in aqueous solutions.* International journal of environmental science and technology, 2016. 13(1): p. 77-86.

10. Miklos, D.B., et al., *Evaluation of advanced oxidation processes for water and wastewater treatment–A critical review.* Water research, 2018. 139: p. 118-131.

11. Kilic, M.Y., et al., *Photochemical treatment of tyrosol, a model phenolic compound present in olive mill wastewater, by hydroxyl and sulfate radical-based advanced oxidation processes (AOPs).* Journal of hazardous materials, 2019. 367: p. 734-742.

12. Wang, S. and J. Wang, *Radiation-induced degradation of sulfamethoxazole in the presence of various inorganic anions.* Chemical Engineering Journal, 2018. 351: p. 688-696.

13. aus der Beek, T., et al., *Pharmaceuticals in the environment—Global occurrences and perspectives.* Environmental toxicology and chemistry, 2016. 35(4): p. 823-835.

14. Kolpin, D.W., et al., *Pharmaceuticals, hormones, and other organic wastewater contaminants in US streams, 1999− 2000: A national reconnaissance.* Environmental science & technology, 2002. 36(6): p. 1202-1211.

15. Kümmerer, K., *Antibiotics in the aquatic environment–a review–part I.* Chemosphere, 2009. 75(4): p. 417-434.

16. Jiang, J.-Q., Z. Zhou, and V. Sharma, *Occurrence, transportation, monitoring and treatment of emerging micro-pollutants in waste water—A review from global views.* Microchemical Journal, 2013. 110: p. 292-300.

17. Sirés, I. and E. Brillas, *Remediation of water pollution caused by pharmaceutical residues based on electrochemical separation and degradation technologies: a review.* Environment international, 2012. 40: p. 212-229.

18. Verlicchi, P., M. Al Aukidy, and E. Zambello, *Occurrence of pharmaceutical compounds in urban wastewater: removal, mass load and environmental risk after a secondary treatment—a review.* Science of the total environment, 2012. 429: p. 123-155.

19. Larsson, D.J., C. de Pedro, and N. Paxeus, *Effluent from drug manufactures contains extremely high levels of pharmaceuticals.* Journal of hazardous materials, 2007. 148(3): p. 751-755.

20. Fatta-Kassinos, D., S. Meric, and A. Nikolaou, *Pharmaceutical residues in environmental waters and wastewater: current state of knowledge and future research.* Analytical and bioanalytical chemistry, 2011. 399(1): p. 251-275.

21. Deblonde, T., C. Cossu-Leguille, and P. Hartemann, *Emerging pollutants in wastewater: a review of the literature.* International journal of hygiene and environmental health, 2011. 214(6): p. 442-448.

22. Jongbloed, A. and N. Lenis, *Environmental concerns about animal manure.* Journal of Animal Science, 1998. 76(10): p. 2641-2648.

23. Orias, F. and Y. Perrodin, *Characterisation of the ecotoxicity of hospital effluents: a review.* Science of the Total Environment, 2013. 454: p. 250-276.

24. aus der Beek, T., et al., *Pharmaceuticals in the environment: Global occurrence and potential cooperative action under the Strategic Approach to International Chemicals Management.* Ger. Fed. Environ. Agency, 2016. 94.

25. Enick, O.V. and M.M. Moore, *Assessing the assessments: pharmaceuticals in the environment.* Environmental Impact Assessment Review, 2007. 27(8): p. 707-729.

26. Fent, K., A.A. Weston, and D. Caminada, *Ecotoxicology of human pharmaceuticals.* Aquatic toxicology, 2006. 76(2): p. 122-159.

27. Gomez Cortes, L., Marinov, D., Sanseverino, I., Navarro Cuenca, A., Niegowska, M., Porcel Rodriguez, E. and Lettieri, T., *Selection of substances for the 3rd Watch List under the Water Framework Directive, EUR 30297 EN*. 2020: Publications Office of the European Union, Luxembourg.

28. Kosjek, T., et al., *Fate of carbamazepine during water treatment.* Environmental science & technology, 2009. 43(16): p. 6256-6261.

29. Dai, C.-m., et al., *Comparative study of the degradation of carbamazepine in water by advanced oxidation processes.* Environmental technology, 2012. 33(10): p. 1101-1109.

30. Deng, J., et al., *Degradation of the antiepileptic drug carbamazepine upon different UV-based advanced oxidation processes in water.* Chemical Engineering Journal, 2013. 222: p. 150-158.

31. Kudlek, E., J. Bohdziewicz, and M. Dudziak, *Photocatalytic oxidation OF carbamazepine IN the aquatic environment.* 2015.

32. Tixier, C., et al., *Occurrence and fate of carbamazepine, clofibric acid, diclofenac, ibuprofen, ketoprofen, and naproxen in surface waters.* Environmental science & technology, 2003. 37(6): p. 1061-1068.

33. Zhang, Y., S.-U. Geißen, and C. Gal, *Carbamazepine and diclofenac: removal in wastewater treatment plants and occurrence in water bodies.* Chemosphere, 2008. 73(8): p. 1151-1161.

34. Pomati, F., et al., *Effects of a complex mixture of therapeutic drugs at environmental levels on human embryonic cells.* Environmental science & technology, 2006. 40(7): p. 2442-2447.

35. Galus, M., et al., *Chronic, low concentration exposure to pharmaceuticals impacts multiple organ systems in zebrafish.* Aquatic toxicology, 2013. 132: p. 200-211.

36. Estevez, E., et al., *Ibuprofen adsorption in four agricultural volcanic soils.* Science of the total environment, 2014. 468: p. 406-414.

37. Zwiener, C. and F. Frimmel, *Oxidative treatment of pharmaceuticals in water.* Water Research, 2000. 34(6): p. 1881-1885.

38. Jacobs, L.E., et al., *Fulvic acid mediated photolysis of ibuprofen in water.* Water research, 2011. 45(15): p. 4449-4458.

39. Farré, M., et al., *Assessment of the acute toxicity of triclosan and methyl triclosan in wastewater based on the bioluminescence inhibition of Vibrio fischeri.* Analytical and Bioanalytical Chemistry, 2008. 390(8): p. 1999-2007.

40. Marković, M., et al., *Application of non-thermal plasma reactor and Fenton reaction for degradation of ibuprofen.* Science of the Total Environment, 2015. 505: p. 1148-1155.

41. Buser, H.-R., T. Poiger, and M.D. Müller, *Occurrence and environmental behavior of the chiral pharmaceutical drug ibuprofen in surface waters and in wastewater.* Environmental science & technology, 1999. 33(15): p. 2529-2535.

42. Han, S., et al., *Endocrine disruption and consequences of chronic exposure to ibuprofen in Japanese medaka (Oryzias latipes) and freshwater cladocerans Daphnia magna and Moina macrocopa.* Aquatic toxicology, 2010. 98(3): p. 256-264.

43. Illés, E., et al., *Hydroxyl radical induced degradation of ibuprofen.* Science of the total environment, 2013. 447: p. 286-292.

44. Richards, S.M. and S.E. Cole, *A toxicity and hazard assessment of fourteen pharmaceuticals to Xenopus laevis larvae.* Ecotoxicology, 2006. 15(8): p. 647-656.

45. Nallani, G.C., et al., *Bioconcentration of ibuprofen in fathead minnow (Pimephales promelas) and channel catfish (Ictalurus punctatus).* Chemosphere, 2011. 84(10): p. 1371-1377.

46. Bennett Jr, W., Y.P. Turmelle, and R.W. Shepherd, *Ibuprofen-induced liver injury in an adolescent athlete.* Clinical pediatrics, 2009. 48(1): p. 84-86.

47. Cleuvers, M., *Mixture toxicity of the anti-inflammatory drugs diclofenac, ibuprofen, naproxen, and acetylsalicylic acid.* Ecotoxicology and environmental safety, 2004. 59(3): p. 309-315.

48. Matamoros, V., M. Hijosa, and J.M. Bayona, *Assessment of the pharmaceutical active compounds removal in wastewater treatment systems at enantiomeric level. Ibuprofen and naproxen.* Chemosphere, 2009. 75(2): p. 200-205.

49. Dehghani, M., S. Behzadi, and M.S. Sekhavatjou, *Optimizing Fenton process for the removal of amoxicillin from the aqueous phase using Taguchi method.* Desalination and Water Treatment, 2016. 57(14): p. 6604-6613.

50. Gökkuş, Ö., Y.Ş. Yıldız, and B. Yavuz, *Optimization of chemical coagulation of real textile wastewater using Taguchi experimental design method.* Desalination and Water Treatment, 2012. 49(1-3): p. 263-271.

51. Madaeni, S.S. and S. Koocheki, *Application of taguchi method in the optimization of wastewater treatment using spiral-wound reverse osmosis element.* Chemical Engineering Journal, 2006. 119(1): p. 37-44.

52. Thomas, M., et al., *Synthetic Textile Wastewater Treatment using Potassium Ferrate (VI)–Application of Taguchi Method for Optimisation of Experiment.* Fibres & Textiles in Eastern Europe, 2018.

53. Yousefi, Z., A. Zafarzadeh, and A. Ghezel, *Application of Taguchi's experimental design method for optimization of Acid Red 18 removal by electrochemical oxidation process.* ehemj, 2018. 5(4): p. 241-248.

54. Bendell, A. *Introduction to Taguchi methodology*. in *Taguchi Methods: Proceedings of the 1988 European Conference 1988*. 1988.

55. Park, S.H. and J.J. Kim, *Quality engineering using robust design and analysis*, in *Industrial statistics*. 1997, Springer. p. 3-15.

56. Madaeni, S. and S. Koocheki, *Application of taguchi method in the optimization of wastewater treatment using spiral-wound reverse osmosis element.* Chemical Engineering Journal, 2006. 119(1): p. 37-44.

57. Roy, R.K., *A primer on the Taguchi method*. 2010: Society of Manufacturing Engineers.

58. Sirtori, C., et al., *Effect of water-matrix composition on Trimethoprim solar photodegradation kinetics and pathways.* Water Research, 2010. 44(9): p. 2735-2744.

59. Alam, T., *Estimation of Chemical Oxygen Demand in WasteWater using UV-VIS Spectroscopy*. 2015, Applied Sciences: School of Mechatronic Systems Engineering.

60. Boyles, W., *Chemical oxygen demand.* Technical information series, Booklet,(9), 1997. 24.

61. LaPara, T.M., J.E. Alleman, and P.G. Pope, *Miniaturized closed reflux, colorimetric method for the determination of chemical oxygen demand.* Waste management, 2000. 20(4): p. 295-298.

62. Yang, X., R. Foley, and G.-C. Low, *A modified digestion procedure for analysing silver in environmental water samples.* Analyst, 2002. 127(2): p. 315-318.

63. Schwartz, J., R. Levin, and R. Goldstein, *Drinking water turbidity and gastrointestinal illness in the elderly of Philadelphia.* Journal of Epidemiology & Community Health, 2000. 54(1): p. 45-51.

64. Farré, M.J., et al., *Biodegradability of treated aqueous solutions of biorecalcitrant pesticides by means of photocatalytic ozonation.* Desalination, 2007. 211(1-3): p. 22-33.

65. Huang, C.P., C. Dong, and Z. Tang, *Advanced chemical oxidation: Its present role and potential future in hazardous waste treatment.* Waste Management, 1993. 13(5): p. 361-377.

66. Glaze, W.H., J.-W. Kang, and D.H. Chapin, *The chemistry of water treatment processes involving ozone, hydrogen peroxide and ultraviolet radiation.* 1987.

67. Yang, S., et al., *Understanding the factors controlling the removal of trace organic contaminants by white-rot fungi and their lignin modifying enzymes: a critical review.* Bioresource technology, 2013. 141: p. 97-108.

68. Tufail, A., W.E. Price, and F.I. Hai, *A critical review on advanced oxidation processes for the removal of trace organic contaminants: A voyage from individual to integrated processes.* Chemosphere, 2020. 260: p. 127460.

69. Oppenländer, T., *Photochemical purification of water and air: advanced oxidation processes (AOPs)-principles, reaction mechanisms, reactor concepts*. 2007: John Wiley & Sons.

70. Wols, B. and C. Hofman-Caris, *Review of photochemical reaction constants of organic micropollutants required for UV advanced oxidation processes in water.* Water research, 2012. 46(9): p. 2815-2827.

71. Schwarzenbach, R.P., P.M. Gschwend, and D.M. Imboden, *Environmental organic chemistry*. 2016: John Wiley & Sons.

72. Liao, C.-H. and M.D. Gurol, *Chemical oxidation by photolytic decomposition of hydrogen peroxide.* Environmental science & technology, 1995. 29(12): p. 3007-3014.

73. Morgan, M.S., et al., *Ultraviolet molar absorptivities of aqueous hydrogen peroxide and hydroperoxyl ion.* Analytica chimica acta, 1988. 215: p. 325-329.

74. Oturan, M.A. and J.-J. Aaron, *Advanced oxidation processes in water/wastewater treatment: principles and applications. A review.* Critical Reviews in Environmental Science and Technology, 2014. 44(23): p. 2577-2641.

75. Guo, K., et al., *Comparison of the UV/chlorine and UV/H2O2 processes in the degradation of PPCPs in simulated drinking water and wastewater: kinetics, radical mechanism and energy requirements.* Water research, 2018. 147: p. 184-194.

76. Afzal, A., et al., *Decomposition of cyclohexanoic acid by the UV/H2O2 process under various conditions.* Science of the total environment, 2012. 426: p. 387-392.

77. Ghanbari, F. and M. Moradi, *Application of peroxymonosulfate and its activation methods for degradation of environmental organic pollutants.* Chemical Engineering Journal, 2017. 310: p. 41-62.

78. Wang, J. and S. Wang, *Activation of persulfate (PS) and peroxymonosulfate (PMS) and application for the degradation of emerging contaminants.* Chemical Engineering Journal, 2018. 334: p. 1502-1517.

79. Hou, S., et al., *Degradation kinetics and pathways of haloacetonitriles by the UV/persulfate process.* Chemical Engineering Journal, 2017. 320: p. 478-484.

80. Criquet, J. and N.K.V. Leitner, *Degradation of acetic acid with sulfate radical generated by persulfate ions photolysis.* Chemosphere, 2009. 77(2): p. 194-200.

81. Norman, R., P. Storey, and P. West, *Electron spin resonance studies. Part XXV. Reactions of the sulphate radical anion with organic compounds.* Journal of the Chemical Society B: Physical Organic, 1970: p. 1087-1095.

82. Madhavan, V., H. Levanon, and P. Neta, *Decarboxylation by $SO_4^{\cdot-}$ radicals.* Radiation Research, 1978. 76(1): p. 15-22.

83. Camargo-Perea, A.L., A. Rubio-Clemente, and G.A. Peñuela, *Use of ultrasound as an advanced oxidation process for the degradation of emerging pollutants in water.* Water, 2020. 12(4): p. 1068.

84. Rao, Y., et al., *Sonolytic and sonophotolytic degradation of Carbamazepine: Kinetic and mechanisms.* Ultrasonics Sonochemistry, 2016. 32: p. 371-379.

85. Nie, E., et al., *Degradation of diclofenac by ultrasonic irradiation: Kinetic studies and degradation pathways.* Chemosphere, 2014. 113: p. 165-170.

86. Tufail, A., et al., *A critical review of advanced oxidation processes for emerging trace organic contaminant degradation: Mechanisms, factors, degradation products, and effluent toxicity.* Journal of Water Process Engineering, 2020: p. 101778.

87. Mahamuni, N.N. and Y.G. Adewuyi, *Advanced oxidation processes (AOPs) involving ultrasound for waste water treatment: A review with emphasis on cost estimation.* Ultrasonics Sonochemistry, 2010. 17(6): p. 990-1003.

88. Wang, J. and S. Wang, *Reactive species in advanced oxidation processes: Formation, identification and reaction mechanism.* Chemical Engineering Journal, 2020. 401.

89. Zúñiga-Benítez, H., J. Soltan, and G.A. Peñuela, *Application of ultrasound for degradation of benzophenone-3 in aqueous solutions.* International Journal of Environmental Science and Technology, 2016. 13(1): p. 77-86.

90. Nasseri, S., et al., *Degradation kinetics of tetracycline in aqueous solutions using peroxydisulfate activated by ultrasound irradiation: Effect of radical scavenger and water matrix.* Journal of Molecular Liquids, 2017. 241: p. 704-714.

91. Chiha, M., et al., *Modeling of ultrasonic degradation of non-volatile organic compounds by Langmuir-type kinetics.* Ultrasonics Sonochemistry, 2010. 17(5): p. 773-782.

92. Méndez-Arriaga, F., et al., *Ultrasonic treatment of water contaminated with ibuprofen.* Water Research, 2008. 42(16): p. 4243-4248.

93. Jiang, Y., C. Pétrier, and T. David Waite, *Kinetics and mechanisms of ultrasonic degradation of volatile chlorinated aromatics in aqueous solutions.* Ultrasonics Sonochemistry, 2002. 9(6): p. 317-323.

94. I Litter, M. and N. Quici, *Photochemical advanced oxidation processes for water and wastewater treatment.* Recent Patents on Engineering, 2010. 4(3): p. 217-241.

95. Ivanova, I.P., et al., *Mechanism of chemiluminescence in Fenton reaction.* Journal of Biophysical Chemistry, 2012. 3(01): p. 88.

96. Naddeo, V., et al., *Ultrasonic degradation, mineralization and detoxification of diclofenac in water: Optimization of operating parameters.* Ultrasonics Sonochemistry, 2010. 17(1): p. 179-185.

97. Huang, T., et al., *Effects and mechanism of diclofenac degradation in aqueous solution by US/Zn0.* Ultrasonics Sonochemistry, 2017. 37: p. 676-685.

98. Hartmann, J., et al., *Degradation of the drug diclofenac in water by sonolysis in presence of catalysts.* Chemosphere, 2008. 70(3): p. 453-461.

99. Torres-Palma, R.A. and E.A. Serna-Galvis, *Sonolysis*, in *Advanced Oxidation Processes for Waste Water Treatment*. 2018, Elsevier. p. 177-213.

100. Beckett, M.A. and I. Hua, *Impact of ultrasonic frequency on aqueous sonoluminescence and sonochemistry.* The Journal of Physical Chemistry A, 2001. 105(15): p. 3796-3802.

101. Pétrier, C. and A. Francony, *Ultrasonic waste-water treatment: incidence of ultrasonic frequency on the rate of phenol and carbon tetrachloride degradation.* Ultrasonics Sonochemistry, 1997. 4(4): p. 295-300.

102. Naddeo, V., et al., *Degradation of diclofenac during sonolysis, ozonation and their simultaneous application.* Ultrasonics Sonochemistry, 2009. 16(6): p. 790-794.

103. Petrier, C., B. David, and S. Laguian, *Ultrasonic degradation at 20 kHz and 500 kHz of atrazine and pentachlorophenol in aqueous solution: Preliminary results.* Chemosphere, 1996. 32(9): p. 1709-1718.

104. Ziylan, A., et al., *More on sonolytic and sonocatalytic decomposition of Diclofenac using zero-valent iron.* Ultrasonics Sonochemistry, 2013. 20(1): p. 580-586.

105. Kidak, R. and S. Dogan, *Degradation of trace concentrations of alachlor by medium frequency ultrasound.* Chemical Engineering and Processing: Process Intensification, 2015. 89: p. 19-27.

106. Jacob, J., L. Chia, and F. Boey, *Thermal and non-thermal interaction of microwave radiation with materials.* Journal of materials science, 1995. 30(21): p. 5321-5327.

107. Liao, W., et al., *Microwave-enhanced photolysis of norfloxacin: kinetics, matrix effects, and degradation pathways.* International journal of environmental research and public health, 2017. 14(12): p. 1564.

108. Kim, Y.-B. and J.-H. Ahn, *Changes of absorption spectra, SUVA 254, and color in treating landfill leachate using microwave-assisted persulfate oxidation.* Korean Journal of Chemical Engineering, 2017. 34(7): p. 1980-1984.

109. Liao, Y., W.C. Chen, and R. Borsali, *Carbohydrate-Based Block Copolymer Thin Films: Ultrafast Nano-Organization with 7 nm Resolution Using Microwave Energy.* Advanced Materials, 2017. 29(35): p. 1701645.

110. Wang, N. and P. Wang, *Study and application status of microwave in organic wastewater treatment–a review.* Chemical Engineering Journal, 2016. 283: p. 193-214.

111. Wacławek, S., et al., *Chemistry of persulfates in water and wastewater treatment: a review.* Chemical Engineering Journal, 2017. 330: p. 44-62.

112. Remya, N. and J.-G. Lin, *Current status of microwave application in wastewater treatment—a review.* Chemical Engineering Journal, 2011. 166(3): p. 797-813.

113. Remya, N. and J.-G. Lin, *Microwave-assisted carbofuran degradation in the presence of GAC, ZVI and H2O2: Influence of reaction temperature and pH.* Separation and purification technology, 2011. 76(3): p. 244-252.

114. Gayathri, P., Y. Suguna, and E. Yesodharan, *Purification of water contaminated with traces of Rhodamine B dye by microwave-assisted, oxidant-induced and zinc oxide catalyzed advanced oxidation process.* Desalination and Water Treatment, 2017. 85: p. 161-174.

115. Chou, Y.-C., et al., *Microwave-enhanced persulfate oxidation to treat mature landfill leachate.* Journal of hazardous materials, 2015. 284: p. 83-91.

116. Cravotto, G., et al., *Oxidative degradation of chlorophenol derivatives promoted by microwaves or power ultrasound: a mechanism investigation.* Environmental Science and Pollution Research, 2010. 17(3): p. 674-687.

117. Lin, L., et al., *Removal of ammonia nitrogen in wastewater by microwave radiation.* Journal of hazardous materials, 2009. 161(2-3): p. 1063-1068.

118. Anwar, J., et al., *Microwave chemistry: Effect of ions on dielectric heating in microwave ovens.* Arabian Journal of Chemistry, 2015. 8(1): p. 100-104.

119. Zhang, L., et al., *Study of the degradation behaviour of dimethoate under microwave irradiation.* Journal of hazardous materials, 2007. 149(3): p. 675-679.

120. Eskicioglu, C., et al., *Synergetic pretreatment of sewage sludge by microwave irradiation in presence of H2O2 for enhanced anaerobic digestion.* Water research, 2008. 42(18): p. 4674-4682.

121. Ravera, M., et al., *Oxidative degradation of 1, 5-naphthalenedisulfonic acid in aqueous solutions by microwave irradiation in the presence of H2O2.* Chemosphere, 2009. 74(10): p. 1309-1314.

122. Shiying, Y., et al., *A novel advanced oxidation process to degrade organic pollutants in wastewater: Microwave-activated persulfate oxidation.* Journal of Environmental Sciences, 2009. 21(9): p. 1175-1180.

123. Jou, C.-J., *Degradation of pentachlorophenol with zero-valence iron coupled with microwave energy.* Journal of hazardous materials, 2008. 152(2): p. 699-702.

124. Quan, X., et al., *Generation of hydroxyl radical in aqueous solution by microwave energy using activated carbon as catalyst and its potential in removal of persistent organic substances.* Journal of Molecular Catalysis A: Chemical, 2007. 263(1-2): p. 216-222.

125. Markic, M., et al., *Influence of process parameters on the effectiveness of photooxidative treatment of pharmaceuticals.* Journal of Environmental Science and Health, Part A, 2018. 53(4): p. 338-351.

126. Adityosulindro, S., et al., *Sonolysis and sono-Fenton oxidation for removal of ibuprofen in (waste)water.* Ultrasonics Sonochemistry, 2017. 39: p. 889-896.

127. Lekkerkerker-Teunissen, K., et al., *Transformation of atrazine, carbamazepine, diclofenac and sulfamethoxazole by low and medium pressure UV and UV/H2O2 treatment.* Separation and Purification Technology, 2012. 96: p. 33-43.

128. Mark, G., et al., *The photolysis of potassium peroxodisulphate in aqueous solution in the presence of tert-butanol: a simple actinometer for 254 nm radiation.* Journal of Photochemistry and Photobiology A: Chemistry, 1990. 55(2): p. 157-168.

129. Buxton, G.V., et al., *Critical review of rate constants for reactions of hydrated electrons, hydrogen atoms and hydroxyl radicals (· OH/· O− in aqueous solution.* Journal of physical and chemical reference data, 1988. 17(2): p. 513-886.

130. Løgager, T., K. Sehested, and J. Holcman, *Rate constants of the equilibrium reactions SO⨪ 4+ HNO3⇄ HSO-4+ NO. 3 and SO⨪ 4+ NO-3⇄ SO2-4+ NO. 3.* Radiation Physics and Chemistry, 1993. 41(3): p. 539-543.

131. Cvetnić, M., et al., *Key structural features promoting radical driven degradation of emerging contaminants in water.* Environment international, 2019. 124: p. 38-48.

132. Khan, J.A., et al., *Kinetic and mechanism investigation on the photochemical degradation of atrazine with activated H2O2, S2O82− and HSO5−.* Chemical Engineering Journal, 2014. 252: p. 393-403.

133. He, X., et al., *Degradation kinetics and mechanism of β-lactam antibiotics by the activation of H2O2 and Na2S2O8 under UV-254 nm irradiation.* Journal of hazardous materials, 2014. 279: p. 375-383.

134. Gu, Z., et al., *Kinetics study of dinitrodiazophenol industrial wastewater treatment by a microwave-coupled ferrous-activated persulfate process.* Chemosphere, 2019. 215: p. 82-91.

135. Qi, C., et al., *Degradation of sulfamethoxazole by microwave-activated persulfate: Kinetics, mechanism and acute toxicity.* Chemical Engineering Journal, 2014. 249: p. 6-14.

136. Chen, W., et al., *Molecular-level comparison study on microwave irradiation-activated persulfate and hydrogen peroxide processes for the treatment of refractory organics in mature landfill leachate.* Journal of hazardous materials, 2020. 397: p. 122785.

137. Wang, Y., et al., *Comparison study on microwave irradiation-activated persulfate and hydrogen peroxide systems in the treatment of dinitrodiazophenol industrial wastewater.* Chemosphere, 2020. 242: p. 125139.

138. Kovacic, M., et al., *Degradation of polar and non-polar pharmaceutical pollutants in water by solar assisted photocatalysis using hydrothermal TiO2-SnS2.* Chemical Engineering Journal, 2020. 382: p. 122826.

139. Vogna, D., et al., *Kinetic and chemical assessment of the UV/H2O2 treatment of antiepileptic drug carbamazepine.* Chemosphere, 2004. 54(4): p. 497-505.

140. Liu, N., et al., *Aquatic photolysis of carbamazepine by UV/H 2 O 2 and UV/Fe (II) processes.* Research on Chemical Intermediates, 2015. 41(10): p. 7015-7028.

141. Starling, M.C.V., et al., *Intensification of UV-C treatment to remove emerging contaminants by UV-C/H2O2 and UV-C/S2O82−: Susceptibility to photolysis and investigation of acute toxicity.* Chemical Engineering Journal, 2019. 376: p. 120856.

142. Guan, Y.-H., et al., *Influence of pH on the formation of sulfate and hydroxyl radicals in the UV/peroxymonosulfate system.* Environmental Science & Technology, 2011. 45(21): p. 9308-9314.

143. Ji, Y., et al., *Nitrate-induced photodegradation of atenolol in aqueous solution: kinetics, toxicity and degradation pathways.* Chemosphere, 2012. 88(5): p. 644-649.

144. Thanekar, P., M. Panda, and P.R. Gogate, *Degradation of carbamazepine using hydrodynamic cavitation combined with advanced oxidation processes.* Ultrasonics sonochemistry, 2018. 40: p. 567-576.

145. Raut-Jadhav, S., et al., *Synergetic effect of combination of AOP's (hydrodynamic cavitation and H2O2) on the degradation of neonicotinoid class of insecticide.* Journal of Hazardous Materials, 2013. 261: p. 139-147.

146. Lim, M., Y. Son, and J. Khim, *The effects of hydrogen peroxide on the sonochemical degradation of phenol and bisphenol A.* Ultrasonics Sonochemistry, 2014. 21(6): p. 1976-1981.

147. Hai, F.I., et al., *Carbamazepine as a Possible Anthropogenic Marker in Water: Occurrences, Toxicological Effects, Regulations and Removal by Wastewater Treatment Technologies.* Water, 2018. 10(2): p. 107.

148. Andreozzi, R., M. Raffaele, and P. Nicklas, *Pharmaceuticals in STP effluents and their solar photodegradation in aquatic environment.* Chemosphere, 2003. 50(10): p. 1319-1330.

149. Ma, J. and N.J. Graham, *Degradation of atrazine by manganese-catalysed ozonation: Influence of humic substances.* Water Research, 1999. 33(3): p. 785-793.

150. Canonica, S. and H.-U. Laubscher, *Inhibitory effect of dissolved organic matter on triplet-induced oxidation of aquatic contaminants.* Photochemical & Photobiological Sciences, 2008. 7(5): p. 547-551.

151. Ou, X., et al., *Atrazine photodegradation in aqueous solution induced by interaction of humic acids and iron: photoformation of iron (II) and hydrogen peroxide.* Journal of agricultural and food chemistry, 2007. 55(21): p. 8650-8656.

152. Wang, Y., F.A. Roddick, and L. Fan, *Direct and indirect photolysis of seven micropollutants in secondary effluent from a wastewater lagoon.* Chemosphere, 2017. 185: p. 297-308.

153. Neta, P., R.E. Huie, and A.B. Ross, *Rate constants for reactions of inorganic radicals in aqueous solution.* Journal of Physical and Chemical Reference Data, 1988. 17(3): p. 1027-1284.

154. Ji, Y., et al., *The role of nitrite in sulfate radical-based degradation of phenolic compounds: An unexpected nitration process relevant to groundwater remediation by in-situ chemical oxidation (ISCO).* Water research, 2017. 123: p. 249-257.

155. Rehman, F., et al., *Oxidative removal of brilliant green by UV/S2O82–, UV/HSO5– and UV/H2O2 processes in aqueous media: A comparative study.* Journal of Hazardous Materials, 2018. 357: p. 506-514.

156. Lukes, P., et al., *Aqueous-phase chemistry and bactericidal effects from an air discharge plasma in contact with water: evidence for the formation of peroxynitrite through a pseudo-second-order post-discharge reaction of H2O2 and HNO2.* Plasma Sources Science and Technology, 2014. 23(1): p. 015019.

157. Wang, D., et al., *Mechanism and experimental study on the photocatalytic performance of Ag/AgCl@ chiral TiO2 nanofibers photocatalyst: The impact of wastewater components.* Journal of hazardous materials, 2015. 285: p. 277-284.

158. Koumaki, E., et al., *Degradation of emerging contaminants from water under natural sunlight: The effect of season, pH, humic acids and nitrate and identification of photodegradation by-products.* Chemosphere, 2015. 138: p. 675-681.

159. Chianese, S., et al., *Ibuprofen degradation in aqueous solution by using UV light.* Desalination and Water Treatment, 2016. 57(48-49): p. 22878-22886.

160. Calza, P., et al., *The role of nitrite and nitrate ions as photosensitizers in the phototransformation of phenolic compounds in seawater.* Science of the total environment, 2012. 439: p. 67-75.

161. Li, A., et al., *Nitrogen dioxide radicals mediated mineralization of perfluorooctanoic acid in aqueous nitrate solution with UV irradiation.* Chemosphere, 2017. 188: p. 367-374.

162. Sbardella, L., et al., *The impact of wastewater matrix on the degradation of pharmaceutically active compounds by oxidation processes including ultraviolet radiation and sulfate radicals.* Journal of Hazardous Materials, 2019. 380: p. 120869.

163. Nikitenko, S.I., L. Venault, and P. Moisy, *Scavenging of OH radicals produced from H2O sonolysis with nitrate ions.* Ultrasonics Sonochemistry, 2004. 11(3): p. 139-142.

164. Thomas, K., et al., *On the exchange of NO 3 radicals with aqueous solutions: Solubility and sticking coefficient.* Journal of atmospheric chemistry, 1998. 29(1): p. 17-43.

165. Wang, J. and S. Wang, *Effect of inorganic anions on the performance of advanced oxidation processes for degradation of organic contaminants.* Chemical Engineering Journal, 2021. 411: p. 128392.

166. Liao, C.-H., S.-F. Kang, and F.-A. Wu, *Hydroxyl radical scavenging role of chloride and bicarbonate ions in the H2O2/UV process.* Chemosphere, 2001. 44(5): p. 1193-1200.

167. Kashif, N. and F. Ouyang, *Parameters effect on heterogeneous photocatalysed degradation of phenol in aqueous dispersion of TiO2.* Journal of Environmental Sciences, 2009. 21(4): p. 527-533.

168. Minakata, D., D. Kamath, and S. Maetzold, *Mechanistic insight into the reactivity of chlorine-derived radicals in the aqueous-phase UV–chlorine advanced oxidation process: Quantum mechanical calculations.* Environmental science & technology, 2017. 51(12): p. 6918-6926.

169. Tan, C., et al., *Heat-activated persulfate oxidation of diuron in water.* Chemical Engineering Journal, 2012. 203: p. 294-300.

170. George, C. and J.-M. Chovelon, *A laser flash photolysis study of the decay of SO4− and Cl2− radical anions in the presence of Cl− in aqueous solutions.* Chemosphere, 2002. 47(4): p. 385-393.

171. Lampre, I., et al., *Oxidation of bromide ions by hydroxyl radicals: Spectral characterization of the intermediate BrOH•.* Journal of Physical Chemistry A, 2013. 117(5): p. 877-887.

172. Black, E.D. and E. Hayon, *Pulse radiolysis of phosphate anions H2PO4-, HPO42-, PO43-, and P2O74- in aqueous solutions.* Journal of Physical Chemistry, 1970. 74(17): p. 3199-3203.

173. Ghanbari, F., M. Moradi, and F. Gohari, *Degradation of 2,4,6-trichlorophenol in aqueous solutions using peroxymonosulfate/activated carbon/UV process via sulfate and hydroxyl radicals.* Journal of Water Process Engineering, 2016. 9: p. 22-28.

174. Yang, Z., et al., *Comparison of the reactivity of ibuprofen with sulfate and hydroxyl radicals: An experimental and theoretical study.* Science of The Total Environment, 2017. 590-591: p. 751-760.

175. Wu, X., et al., *Strong enhancement of trichloroethylene degradation in ferrous ion activated persulfate system by promoting ferric and ferrous ion cycles with hydroxylamine.* Separation and Purification Technology, 2015. 147: p. 186-193.

176. Kwon, M., et al., *Comparative evaluation of ibuprofen removal by UV/H2O2 and UV/S2O82− processes for wastewater treatment.* Chemical Engineering Journal, 2015. 269: p. 379-390.

177. Duca, C., G. Imoberdorf, and M. Mohseni, *Effects of inorganics on the degradation of micropollutants with vacuum UV (VUV) advanced oxidation.* Journal of Environmental Science and Health, Part A, 2017. 52(6): p. 524-532.

178. Wang, J. and S. Wang, *Reactive species in advanced oxidation processes: Formation, identification and reaction A.* Chemical Engineering Journal, 2020: p. 126158.

179. Hirakawa, T. and Y. Nosaka, *Properties of O2•-and OH• formed in TiO2 aqueous suspensions by photocatalytic reaction and the influence of H2O2 and some ions.* Langmuir, 2002. 18(8): p. 3247-3254.

180. Grebel, J.E., J.J. Pignatello, and W.A. Mitch, *Effect of halide ions and carbonates on organic contaminant degradation by hydroxyl radical-based advanced oxidation processes in saline waters.* Environmental science & technology, 2010. 44(17): p. 6822-6828.

181. Xu, L., et al., *Sulfate radical-induced degradation of 2, 4, 6-trichlorophenol: a de novo formation of chlorinated compounds.* Chemical engineering journal, 2013. 217: p. 169-173.

182. Yuan, R., et al., *Effects of chloride ion on degradation of Acid Orange 7 by sulfate radical-based advanced oxidation process: implications for formation of chlorinated aromatic compounds.* Journal of hazardous materials, 2011. 196: p. 173-179.

183. De Laurentiis, E., et al., *Photochemical fate of carbamazepine in surface freshwaters: laboratory measures and modeling.* Environmental science & technology, 2012. 46(15): p. 8164-8173.

184. Somathilake, P., et al., *Influence of UV dose on the UV/H2O2 process for the degradation of carbamazepine in wastewater.* Environmental technology, 2019. 40(23): p. 3031-3039.

185. Zhang, Q., et al., *Degradation of carbamazepine and toxicity evaluation using the UV/persulfate process in aqueous solution.* Journal of Chemical Technology & Biotechnology, 2015. 90(4): p. 701-708.

186. Matta, R., et al., *Removal of carbamazepine from urban wastewater by sulfate radical oxidation.* Environmental chemistry letters, 2011. 9(3): p. 347-353.

187. Chiron, S., C. Minero, and D. Vione, *Photodegradation processes of the antiepileptic drug carbamazepine, relevant to estuarine waters.* Environmental science & technology, 2006. 40(19): p. 5977-5983.

Appendix

Table A.1. ANOVA table for CBZ degradation by UV-C process.

Source	DF	Seq SS	Contribution	Adj SS	Adj MS	F-Value	P-Value
pH	1	0.24083	3.01%	0.24083	0.24083	0.20	0.681
Humic acid	1	0.02083	0.26%	0.02083	0.02083	0.02	0.903
Nitrite	1	1.02083	12.75%	1.02083	1.02083	0.83	0.414
Nitrate	1	0.60750	7.59%	0.60750	0.60750	0.49	0.521
Chloride	1	0.10083	1.26%	0.10083	0.10083	0.08	0.789
Phosphaste	1	0.18750	2.34%	0.18750	0.18750	0.15	0.716
Sulfate	1	0.90750	11.33%	0.90750	0.90750	0.74	0.439
Error	4	4.92333	61.47%	4.92333	1.23083		
Total	11	8.00917	100.00%				

Table A.2. Response table for mean of first order degradation rate CBZ by UV-C process.

Level	pH	HA	NO_2^-	NO_3^-	Cl^-	PO_4^{3-}	SO_4^{2-}
1	2.800	2.983	3.233	2.717	2.850	2.817	2.667
2	3.083	2.900	2.650	3.167	3.033	3.067	3.217
Delta	0.283	0.083	0.583	0.450	0.183	0.250	0.550
Rank	4	7	1	3	6	5	2

Table A.3. ANOVA table for CBZ degradation by UV-C/H_2O_2 process.

Source	DF	Seq SS	Contribution	Adj SS	Adj MS	F-Value	P-Value
pH	1	0.021	0.00%	0.021	0.021	0.00	0.959
Oxidant	1	545.401	71.51%	545.401	545.401	82.99	0.003
Humic acid	1	1.021	0.13%	1.021	1.021	0.16	0.720
Nitrite	1	149.107	19.55%	149.107	149.107	22.69	0.018
Nitrate	1	28.521	3.74%	28.521	28.521	4.34	0.129
Chloride	1	6.021	0.79%	6.021	6.021	0.92	0.409
Phosphaste	1	1.841	0.24%	1.841	1.841	0.28	0.633
Sulfate	1	11.021	1.45%	11.021	11.021	1.68	0.286
Error	3	19.716	2.59%	19.716	6.572		
Total	11	762.669	100.00%				

Table A.4. Response table for mean of first order degradation rate CBZ by UV-C/H_2O_2 process.

Level	pH	Oxidant	HA	NO_2^-	NO_3^-	Cl^-	PO_4^{3-}	SO_4^{2-}
1	11.050	4.350	10.800	14.617	9.550	11.800	11.483	10.133
2	11.133	17.833	11.383	7.567	12.633	10.383	10.700	12.050
Delta	0.083	13.483	0.583	7.050	3.083	1.417	0.783	1.917
Rank	8	1	7	2	3	5	6	4

Table A.5. ANOVA table for CBZ degradation by UV-C/$S_2O_8^{2-}$ process.

Source	DF	Seq SS	Contribution	Adj SS	Adj MS	F-Value	P-Value
pH	1	12.20	1.18%	12.201	12.201	0.29	0.625
Oxidant	1	497.94	48.32%	497.941	497.941	12.04	0.040
Humic acid	1	0.61	0.06%	0.608	0.608	0.01	0.911
Nitrite	1	238.52	23.15%	238.521	238.521	5.77	0.096
Nitrate	1	98.04	9.51%	98.041	98.041	2.37	0.221
Chloride	1	0.80	0.08%	0.801	0.801	0.02	0.898
Phosphaste	1	17.52	1.70%	17.521	17.521	0.42	0.562
Sulfate	1	40.70	3.95%	40.701	40.701	0.98	0.394
Error	3	124.09	12.04%	124.089	41.363		
Total	11	1030.42	100.00%				

Table A.6. Response table for mean of first order degradation rate CBZ by UV-C/$S_2O_8^{2-}$ process.

Level	pH	Oxidant	HA	NO_2^-	NO_3^-	Cl^-	PO_4^{3-}	SO_4^{2-}
1	9.717	4.283	10.500	15.183	7.867	10.983	11.933	8.883
2	11.733	17.167	10.950	6.267	13.583	10.467	9.517	12.567
Delta	2.017	12.883	0.450	8.917	5.717	0.517	2.417	3.683
Rank	6	1	8	2	3	7	5	4

Table A.7. ANOVA table for IBP degradation by UV-C process.

Source	DF	Seq SS	Contribution	Adj SS	Adj MS	F-Value	P-Value
pH	1	2.0833	15.02%	2.08333	2.08333	1.50	0.288
Humic acid	1	1.9200	13.84%	1.92000	1.92000	1.38	0.305
Nitrite	1	1.9200	13.84%	1.92000	1.92000	1.38	0.305
Nitrate	1	0.5633	4.06%	0.56333	0.56333	0.41	0.559
Chloride	1	1.7633	12.71%	1.76333	1.76333	1.27	0.323
Phosphaste	1	0.0300	0.22%	0.03000	0.03000	0.02	0.890
Sulfate	1	0.0300	0.22%	0.03000	0.03000	0.02	0.890
Error	4	5.5600	40.09%	5.56000	1.39000		
Total	11	13.8700	100.00%				

Table A.8. Response table for mean of first order degradation rate IBP by UV-C process.

Level	pH	HA	NO_2^-	NO_3^-	Cl^-	PO_4^{3-}	SO_4^{2-}
1	5.467	4.650	5.450	4.833	5.433	5.100	5.100
2	4.633	5.450	4.650	5.267	4.667	5.000	5.000
Delta	0.833	0.800	0.800	0.433	0.767	0.100	0.100
Rank	1	2.5	2.5	5	4	7	6

Table A.9. ANOVA table for IBP degradation by UV-C/H_2O_2 process.

Source	DF	Seq SS	Contribution	Adj SS	Adj MS	F-Value	P-Value
pH	1	49.613	5.57%	49.613	49.613	4.26	0.131
Oxidant	1	645.333	72.41%	645.333	645.333	55.35	0.005
Humic acid	1	0.333	0.04%	0.333	0.333	0.03	0.876
Nitrite	1	95.203	10.68%	95.203	95.203	8.16	0.065
Nitrate	1	23.520	2.64%	23.520	23.520	2.02	0.251
Chloride	1	1.613	0.18%	1.613	1.613	0.14	0.735
Phosphaste	1	0.270	0.03%	0.270	0.270	0.02	0.889
Sulfate	1	40.333	4.53%	40.333	40.333	3.46	0.160
Error	3	34.980	3.93%	34.980	11.660		
Total	11	891.200	100.00%				

Table A.10. Response table for mean of first order degradation rate IBP by UV-C/H_2O_2 process.

Level	pH	Oxidant	HA	NO_2^-	NO_3^-	Cl^-	PO_4^{3-}	SO_4^{2-}
1	17.033	7.667	14.833	17.817	13.600	14.633	15.150	13.167
2	12.967	22.333	15.167	12.183	16.400	15.367	14.850	16.833
Delta	4.067	14.667	0.333	5.633	2.800	0.733	0.300	3.667
Rank	3	1	7	2	5	6	8	4

Table A.11. ANOVA table for IBP degradation by UV-C/$S_2O_8^{2-}$ process.

Source	DF	Seq SS	Contribution	Adj SS	Adj MS	F-Value	P-Value
pH	1	12.0	0.04%	12.0	12.0	0.02	0.907
Oxidant	1	14049.4	50.11%	14049.4	14049.4	18.91	0.022
Humic acid	1	376.3	1.34%	376.3	376.3	0.51	0.528
Nitrite	1	7560.1	26.96%	7560.1	7560.1	10.18	0.050
Nitrate	1	1642.7	5.86%	1642.7	1642.7	2.21	0.234
Chloride	1	496.7	1.77%	496.7	496.7	0.67	0.473
Phosphaste	1	509.6	1.82%	509.6	509.6	0.69	0.468
Sulfate	1	1164.3	4.15%	1164.3	1164.3	1.57	0.299
Error	3	2228.6	7.95%	2228.6	742.9		
Total	11	28039.6	100.00%				

Table A.12. Response table for mean of first order degradation rate IBP by UV-C/$S_2O_8^{2-}$ process.

Level	pH	Oxidant	HA	NO_2^-	NO_3^-	Cl^-	PO_4^{3-}	SO_4^{2-}
1	42.117	8.900	37.517	68.217	31.417	49.550	49.633	33.267
2	44.117	77.333	48.717	18.017	54.817	36.683	36.600	52.967
Delta	2.000	68.433	11.200	50.200	23.400	12.867	13.033	19.700
Rank	8	1	7	2	3	6	5	4

Table A.13. ANOVA table for CBZ degradation by US/H_2O_2 process.

Source	DF	Seq SS	Contribution	Adj SS	Adj MS	F-Value	P-Value
pH	1	4.3200	31.79%	4.32000	4.32000	7.17	0.075
Oxidant	1	0.1200	0.88%	0.12000	0.12000	0.20	0.686
Humic acid	1	1.0800	7.95%	1.08000	1.08000	1.79	0.273
Nitrite	1	0.0133	0.10%	0.01333	0.01333	0.02	0.891
Nitrate	1	1.3333	9.81%	1.33333	1.33333	2.21	0.233
Chloride	1	2.8033	20.63%	2.80333	2.80333	4.65	0.120
Phosphaste	1	2.0833	15.33%	2.08333	2.08333	3.46	0.160
Sulfate	1	0.0300	0.22%	0.03000	0.03000	0.05	0.838
Error	3	1.8067	13.29%	1.80667	0.60222		
Total	11	13.5900	100.00%				

Table A.14. Response table for mean of first order degradation rate CBZ by US/H_2O_2 process.

Level	pH	Oxidant	HA	NO_2^-	NO_3^-	Cl^-	PO_4^{3-}	SO_4^{2-}
1	2.1500	1.4500	1.2500	1.5167	1.8833	1.0667	1.1333	1.6000
2	0.9500	1.6500	1.8500	1.5833	1.2167	2.0333	1.9667	1.5000
Delta	1.2000	0.2000	0.6000	0.0667	0.6667	0.9667	0.8333	0.1000
Rank	1	6	5	8	4	2	3	7

Table A.15. ANOVA table for IBP degradation by US/H_2O_2 process.

Source	DF	Seq SS	Contribution	Adj SS	Adj MS	F-Value	P-Value
pH	1	6.9008	52.03%	6.90083	6.90083	24.97	0.015
Oxidant	1	1.1408	8.60%	1.14083	1.14083	4.13	0.135
Humic acid	1	2.9008	21.87%	2.90083	2.90083	10.50	0.048
Nitrite	1	0.7008	5.28%	0.70083	0.70083	2.54	0.210
Nitrate	1	0.4408	3.32%	0.44083	0.44083	1.59	0.296
Chloride	1	0.0075	0.06%	0.00750	0.00750	0.03	0.880
Phosphaste	1	0.2408	1.82%	0.24083	0.24083	0.87	0.419
Sulfate	1	0.1008	0.76%	0.10083	0.10083	0.36	0.588
Error	3	0.8292	6.25%	0.82917	0.27639		
Total	11	13.2625	100.00%				

Table A.16. Response table for mean of first order degradation rate IBP by US/H_2O_2 process.

Level	pH	Oxidant	HA	NO_2^-	NO_3^-	Cl^-	PO_4^{3-}	SO_4^{2-}
1	3.733	2.667	3.467	3.217	3.167	3.000	2.833	3.067
2	2.217	3.283	2.483	2.733	2.783	2.950	3.117	2.883
Delta	1.517	0.617	0.983	0.483	0.383	0.050	0.283	0.183
Rank	1	3	2	4	5	8	6	7

Table A.17. ANOVA table for CBZ degradation by MW process.

Source	DF	Seq SS	Contribution	Adj SS	Adj MS	F-Value	P-Value
pH	1	27.603	9.51%	27.603	27.603	2.99	0.159
Humic acid	1	2.613	0.90%	2.613	2.613	0.28	0.623
Nitrite	1	26.403	9.09%	26.403	26.403	2.86	0.166
Nitrate	1	92.963	32.02%	92.963	92.963	10.05	0.034
Chloride	1	67.213	23.15%	67.213	67.213	7.27	0.054
Phosphaste	1	16.803	5.79%	16.803	16.803	1.82	0.249
Sulfate	1	19.763	6.81%	19.763	19.763	2.14	0.218
Error	4	36.987	12.74%	36.987	9.247		
Total	11	290.350	100.00%				

Table A.18. Response table for mean of first order degradation rate CBZ by MW process.

Level	pH	HA	NO_2^-	NO_3^-	Cl^-	PO_4^{3-}	SO_4^{2-}
1	3.633	5.617	6.633	2.367	7.517	3.967	6.433
2	6.667	4.683	3.667	7.933	2.783	6.333	3.867
Delta	3.033	0.933	2.967	5.567	4.733	2.367	2.567
Rank	3	7	4	1	2	6	5

Table A.19. ANOVA table for CBZ degradation by MW/H_2O_2 process.

Source	DF	Seq SS	Contribution	Adj SS	Adj MS	F-Value	P-Value
pH	1	163567	25.57%	163567	163567	4.00	0.139
Oxidant	1	104982	16.41%	104982	104982	2.57	0.207
Humic acid	1	12301	1.92%	12301	12301	0.30	0.622
Nitrite	1	83533	13.06%	83533	83533	2.04	0.248
Nitrate	1	48540	7.59%	48540	48540	1.19	0.356
Chloride	1	18993	2.97%	18993	18993	0.46	0.545
Phosphaste	1	48336	7.56%	48336	48336	1.18	0.357
Sulfate	1	36741	5.74%	36741	36741	0.90	0.413
Error	3	122733	19.19%	122733	40911		
Total	11	639725	100.00%				

Table A.20. Response table for mean of first order degradation rate CBZ by MW/H_2O_2 process.

Level	pH	Oxidant	HA	NO_2^-	NO_3^-	Cl^-	PO_4^{3-}	SO_4^{2-}
1	262.20	51.92	177.47	62.02	81.85	185.23	81.98	90.12
2	28.70	238.98	113.43	228.88	209.05	105.67	208.92	200.78
Delta	233.50	187.07	64.03	166.87	127.20	79.57	126.93	110.67
Rank	1	2	8	3	4	7	5	6

Table A.21. ANOVA table for CBZ degradation by MW/$S_2O_8^{2-}$ process.

Source	DF	Seq SS	Contribution	Adj SS	Adj MS	F-Value	P-Value
pH	1	7931	5.01%	7931.0	7931.0	0.40	0.573
Oxidant	1	42519	26.89%	42518.7	42518.7	2.13	0.240
Humic acid	1	23294	14.73%	23293.6	23293.6	1.17	0.359
Nitrite	1	2776	1.75%	2775.5	2775.5	0.14	0.734
Nitrate	1	5296	3.35%	5296.2	5296.2	0.27	0.642
Chloride	1	4575	2.89%	4574.7	4574.7	0.23	0.665
Phosphaste	1	11096	7.02%	11096.0	11096.0	0.56	0.510
Sulfate	1	859	0.54%	858.5	858.5	0.04	0.849
Error	3	59806	37.82%	59805.8	19935.3		
Total	11	158150	100.00%				

Table A.22. Response table for mean of first order degradation rate CBZ by MW/$S_2O_8^{2-}$ process.

Level	pH	Oxidant	HA	NO_2^-	NO_3^-	Cl^-	PO_4^{3-}	SO_4^{2-}
1	661.0	575.8	679.4	650.5	656.3	615.8	604.9	643.7
2	609.6	694.8	591.2	620.1	614.3	654.8	665.7	626.8
Delta	51.4	119.0	88.1	30.4	42.0	39.0	60.8	16.9
Rank	4	1	2	7	5	6	3	8

Table A.23. ANOVA table for IBP degradation by MW process.

Source	DF	Seq SS	Contribution	Adj SS	Adj MS	F-Value	P-Value
pH	1	0.188	0.13%	0.1875	0.1875	0.01	0.913
Humic acid	1	13.868	9.91%	13.8675	13.8675	1.01	0.371
Nitrite	1	21.067	15.06%	21.0675	21.0675	1.54	0.283
Nitrate	1	4.201	3.00%	4.2008	4.2008	0.31	0.609
Chloride	1	26.108	18.67%	26.1075	26.1075	1.91	0.240
Phosphaste	1	7.841	5.61%	7.8408	7.8408	0.57	0.491
Sulfate	1	11.801	8.44%	11.8008	11.8008	0.86	0.406
Error	4	54.797	39.18%	54.7967	13.6992		
Total	11	139.869	100.00%				

Table A.24. Response table for mean of first order degradation rate IBP by MW process.

Level	pH	HA	NO_2^-	NO_3^-	Cl^-	PO_4^{3-}	SO_4^{2-}
1	9.067	10.017	10.267	9.533	10.417	9.750	7.950
2	8.817	7.867	7.617	8.350	7.467	8.133	9.933
Delta	0.250	2.150	2.650	1.183	2.950	1.617	1.983
Rank	7	3	2	6	1	5	4

Table A.25. ANOVA table for IBP degradation by MW/H_2O_2 process.

Source	DF	Seq SS	Contribution	Adj SS	Adj MS	F-Value	P-Value
pH	1	11612.7	41.85%	11612.7	11612.7	19.15	0.022
Oxidant	1	4245.0	15.30%	4245.0	4245.0	7.00	0.077
Humic acid	1	5329.9	19.21%	5329.9	5329.9	8.79	0.059
Nitrite	1	1584.7	5.71%	1584.7	1584.7	2.61	0.204
Nitrate	1	673.5	2.43%	673.5	673.5	1.11	0.369
Chloride	1	2310.2	8.33%	2310.2	2310.2	3.81	0.146
Phosphaste	1	21.6	0.08%	21.6	21.6	0.04	0.862
Sulfate	1	151.9	0.55%	151.9	151.9	0.25	0.651
Error	3	1819.2	6.56%	1819.2	606.4		
Total	11	27748.8	100.00%				

Table A.26. Response table for mean of first order degradation rate IBP by MW/H_2O_2 process.

Level	pH	Oxidant	HA	NO_2^-	NO_3^-	Cl^-	PO_4^{3-}	SO_4^{2-}
1	78.62	28.70	26.43	36.02	40.02	33.63	46.17	51.07
2	16.40	66.32	68.58	59.00	55.00	61.38	48.85	43.95
Delta	62.22	37.62	42.15	22.98	14.98	27.75	2.68	7.12
Rank	1	3	2	5	6	4	8	7

Table A.27. ANOVA table for IBP degradation by MW/$S_2O_8^{2-}$ process.

Source	DF	Seq SS	Contribution	Adj SS	Adj MS	F-Value	P-Value
pH	1	48057	5.10%	48057	48057	0.61	0.490
Oxidant	1	21067	2.24%	21067	21067	0.27	0.640
Humic acid	1	95123	10.10%	95123	95123	1.22	0.351
Nitrite	1	323868	34.39%	323868	323868	4.14	0.135
Nitrate	1	110554	11.74%	110554	110554	1.41	0.320
Chloride	1	22637	2.40%	22637	22637	0.29	0.628
Phosphaste	1	5712	0.61%	5712	5712	0.07	0.804
Sulfate	1	80262	8.52%	80262	80262	1.03	0.386
Error	3	234543	24.90%	234543	78181		
Total	11	941824	100.00%				

Table A.28. Response table for mean of first order degradation rate IBP by MW/$S_2O_8^{2-}$ process.

Level	pH	Oxidant	HA	NO_2^-	NO_3^-	Cl^-	PO_4^{3-}	SO_4^{2-}
1	726.6	831.8	700.8	954.1	885.8	833.3	811.7	871.6
2	853.1	748.0	878.9	625.6	693.9	746.4	768.0	708.1
Delta	126.6	83.8	178.1	328.6	192.0	86.9	43.6	163.6
Rank	5	7	3	1	2	6	8	4